UNIVERSITÀ
DEGLI STUDI
DI BRESCIA

Dottorato di Ricerca in Technology for Health

Ciclo XXXVI

ING-IND/12 MISURE MECCANICHE E TERMICHE

Augmented reality and instrumented crutches to generate visual feedback during assisted walking

Marco Ghidelli

Supervisori:
Prof. Emilio Sardini
Prof. Matteo Lancini

Università degli Studi di Brescia
2023

Sommario

Le tecnologie assistive, come ad esempio le stampelle, sono fondamentali per le persone con difficoltà di mobilità, promuovendo la loro indipendenza e benessere. Imparare ad utilizzare efficacemente i dispositivi per il supporto della camminata richiede tempo e la riabilitazione si basa spesso su valutazioni soggettive da parte dei terapisti. Nell'ottica di fornire valutazioni oggettive, diverse tecnologie assistive sono state equipaggiate da sensori per il monitoraggio delle prestazioni dell'utilizzatore durante la deambulazione. Negli ultimi anni, l'integrazione della realtà aumentata nelle procedure cliniche ha suscitato un forte interesse. Questo studio presenta un approccio per combinare la realtà aumentata e le stampelle strumentate per fornire al personale clinico un nuovo strumento per migliore la valutazione della camminata assistita. Per garantire l'efficacia del sistema, i terapisti in qualità di utenti finali, sono stati coinvolti attivamente alla progettazione e al perfezionamento dell'interfaccia in realtà aumentata mediante riunioni, interviste, attività di brainstorming e sessioni collaborative. L'interfaccia è stata ottimizzata in base ai suggerimenti dei terapisti e alle attuali capacità tecnologiche presenti sul mercato. Le stampelle strumentate sono state migliorate per aumentare l'affidabilità delle misurazioni di forza adottando una nuova configurazione a ponte intero di estensimetri e dimezzandone l'incertezza. Una telecamera di profondità è stata fissata sulle stampelle per rilevare le fasi della deambulazione del paziente senza richiedere sistemi di analisi del movimento aggiuntivi. Inoltre, è stato convalidato uno stimatore del carico applicato sulle gambe dall'utilizzatore delle stampelle basato sulle misurazioni delle stampelle stesse. La stima, che anch'essa può essere ottenuta in tempo reale, fornisce informazioni aggiuntive da fornire al terapista durante la valutazione del paziente. Per valutare l'usabilità dell'interfaccia basata sulla realtà aumentata, è stata condotta una campagna di test in un contesto reale coinvolgendo terapisti e pazienti, e confrontando due condizioni di lavoro: la modalità "display" con ologrammi posizionati su uno schermo virtuale sempre frontale al terapista e la modalità "in-place" con ologrammi posizionati vicino al paziente. I risultati suggeriscono una risposta positiva in termini di qualità delle informazioni e dell'interfaccia. Gli utenti hanno reputato la soluzione utile per compiere la loro attività ed il carico cognitivo/fisico non viene fortemente influenzato. Inoltre, lo studio esamina anche

i potenziali effetti collaterali dovuti all’utilizzo di tecnologie immersive. Dal tracciamento oculare del terapista sono state riscontrate due strategie distinte ponendo un maggiore interesse sui carichi delle stampelle oppure sul carico applicato sulle gambe. Si è riscontrato che il comportamento dei terapisti è influenzato da fattori soggettivi, tra cui le condizioni di salute e sicurezza dei pazienti. Complessivamente, la ricerca sottolinea l'importanza di un approccio orientato all'utente nello sviluppo e nell'implementazione della tecnologia per la valutazione della deambulazione nella riabilitazione. I risultati dello studio contribuiscono al miglioramento del processo di riabilitazione, rendendolo più coinvolgente, efficace e personalizzato in base alle esigenze e agli obiettivi individuali del paziente.

Abstract

Assistive technologies, such as crutches, are vital for individuals with mobility challenges, promoting independence and well-being. Learning to use crutches effectively is often time-consuming, with rehabilitation relying on subjective therapist evaluations. To address this, instrumented assistive devices have been developed to objectively assess and improve walking performance, reducing the reliance on subjective assessments. In recent years, the integration of augmented reality (AR) into clinical procedures has gained interest. This study presents a user-focused approach to combine AR technology and instrumented crutches for improved gait assessment. To ensure the system's effectiveness, therapists, as end-users, actively participated in designing and refining of the AR interface through meetings, interviews, and collaborative sessions. The interface was optimized based on therapists' input and the capabilities of AR technology. The instrumented crutches were upgraded to enhance the reliability of force measurements, adopting a new full-bridge configuration of strain gauges, halving the uncertainty. A depth camera was integrated into the crutches to detect the patient's gait phases without requiring additional motion capture systems. Moreover, a weight-bearing estimator based on the crutches' measurements was validated, augmenting the information provided during crutch-assisted gait. To assess the usability of the AR interface, a test campaign was conducted in a real-world setting, comparing the "display mode" with holograms on a virtual screen to the "in-place mode" with holograms positioned near the patient. Results indicate a positive response in terms of information and interface quality, as well as perceived system usefulness among users and the required workload. The study also examines potential side effects such as sickness when using immersive technologies. The study identifies two distinct gaze strategies employed by therapists when using the AR interface. One focuses on the left and right crutches' loads, while the other emphasizes the patient's legs' weight-bearing. The therapists' behaviour was found to be influenced by subjective factors, including therapist preferences, patient health conditions, and safety. Overall, the research underscores the significance of a user-oriented approach in the development of AR technology for gait assessment in rehabilitation. The study's

findings contribute to the ongoing efforts to enhance the rehabilitation process, making it more engaging, effective, and tailored to individual needs and goals.

Contents

Introduction

The human physiological walking is a complex pattern of movements, which requires the simultaneous activity of different body systems. Neurological injuries and diseases often result in physical impairments that interfere with a person's ability to walk. Common neurological causes of immobility in the adult population include stroke, spinal cord injury and other progressive neurological diseases such as Parkinson's [1]. The World Health Organization (WHO) estimates that globally, the prevalence of Parkinson disease has doubled in the past 25 years with global estimates in 2019 showing over 8.5 million individuals living with Parkinson [2]. Not only neurological disease can reduce walking ability but also anxiety and fear of falling, especially in the elderly [3], or orthopaedic impairment and amputation [4]. Prevalence of gait disorders increases with age, and almost 60% of elderlies above the 80 years old manifest gait problem, often due neurological pathologies and associated with higher risk of falling [5]. The loss of physical mobility reduces the desire to participate in activities or prevents the possibility [6], facilitates the mood of depression, causes cognitive dysfunction, and compromises the quality of life [5].

According to the WHO, an assistive device is any hardware or software produced or designed to help people with disabilities maintain or rehabilitate their functionality and independence, with the aim of promoting their well-being. Assistive technologies for mobility are all the tools and devices that allow people with mobility difficulties to mobilize freely in indoor or outdoor environments [7].

Assistive devices such as canes, crutches and walkers can help to maintain balance, reduce pain, and improve mobility, confidence and autonomy [8], [9], [10].

Crutches are among the most used devices for assisting walking. They help users maintain an upright posture, remain active and improve their independence, bringing long-term health benefits [11]. Special attention is required during rehabilitation both by the patient and the therapist to not introduce incorrect habits and to avoid falls and injury during the walking with crutches [12]. Learning how to use crutches correctly is a time-consuming process. From the patient's perspective, rehabilitation of walking with crutches can present several challenges. Firstly, there may be physical difficulties related to the use of crutches, such as maintaining balance, coordinating movements, and distributing weight effectively. Patients may experience discomfort or fatigue in their upper body due to the increased reliance on their arms and shoulders for support. Additionally, adapting to the altered gait pattern required with crutches can be challenging. Depending on the injury or disability there are many walking patterns, such as two, three or four-step walking sequences [13]. Patients may struggle with maintaining a steady and coordinated walking rhythm, resulting in a slower and more cautious pace [3], [13]. They may also face difficulties navigating uneven or challenging terrains, which can further impact their confidence and mobility. Furthermore, psychological factors can come into play during crutch-assisted walking rehabilitation. Patients may experience frustration, decreased self-esteem, or a sense of dependency due to their temporary reliance on crutches. These emotional challenges can affect motivation and overall engagement in the rehabilitation process.

There are several strategies that healthcare professionals can employ to assist patients in crutch-assisted rehabilitation: providing comprehensive instruction on the proper use of crutches, including techniques for weight distribution, balance, and safe walking patterns [14], [15], [16]; designing tailored exercise programs to improve strength, balance, and coordination; addressing the emotional aspects by providing counselling, encouragement, and motivation [17]; implementing a step-by-step approach to gradually increase the patient's walking distances, speed, and complexity of movements. Since the access to assistive technology is as low as 3% in some countries [18], the World Health Organization (WHO) has also developed an online platform called Training in Assistive Production [19] to improve access to assistive technologies and build competencies.

In the field of rehabilitation, many researchers have developed systems to analyse and enhance walking: instrumented assistive devices, biofeedback, robotics, VR, AR, games and much more. The design and development of assistive devices is a highly active field related, but not limited, to robotics, electrical engineering, mechanical engineering, mathematical modelling and analysis, control, vision systems, neural networks, artificial intelligence, and data analysis [7]. Instrumented assistive devices are advanced technological tools that are designed to aid individuals in their rehabilitation process, and it is a highly active field related, but not limited, to robotics, electrical engineering, mechanical engineering, mathematical modelling and analysis, control, vision systems, neural networks, artificial intelligence, and data analysis [7]. Commonly used instrumented assistive devices include parallel bars [20], walkers [21], [22], [23], crutches [24], [25], [26], [27], [28], [29], [30], [31], and canes [32], [33]. These devices are typically equipped with sensors that capture parameters such as step length, step width, walking speed, ground reaction forces and orientation. By measuring these variables, healthcare professionals can obtain quantitative data about a patient's walking patterns and biomechanical characteristics. The collected data from instrumented assistive devices helps in the assessment of a patient's functional abilities and gait abnormalities. The objective measurements obtained through these devices provide a more accurate representation of a person's movement patterns, enabling healthcare professionals to identify specific areas of difficulty or asymmetry, and an effective evaluation of interventions by comparing pre- and post-rehabilitation measurements. This information is crucial for making evidence-based decisions regarding the modification of treatment plans and adjusting rehabilitation strategies as needed. Furthermore, instrumented assistive devices facilitate the personalization of rehabilitation programs. By analysing the objective data obtained through these devices, healthcare professionals can tailor treatment plans to address specific weaknesses or imbalances in a patient's gait. This personalized approach ensures that the rehabilitation process is targeted and optimized for each individual, leading to improved outcomes and a more efficient recovery.

However, observational gait analysis is usually assessed during the therapy and the therapist’s experience and perception are therefore fundamental during the rehabilitation process and influence the results [34], [35]. Most therapists feel confident about their ability to assess gait and usually prefer observational to instrumented gait assessments, mostly because gait assessment tools used in clinical

practice lacked information concerning their validity and repeatability [36]. Moreover, the information provided by the instrumented device is not often directly comparable with the common parameters evaluated during observational gait assessments [37].

In recent years, there has been a growing interest in utilizing immersive technologies such as AR, virtual reality (VR), and mixed reality (MR) in various fields, including healthcare and rehabilitation. AR refers to the integration of digital information or virtual objects into the real-world environment, augmenting the user's perception of reality. VR immerses the user in a completely virtual environment, typically using a head-mounted display, while MR combines elements of both AR and VR. Immersive technologies hold great potential for transforming the way rehabilitation is delivered, enhancing patient engagement, improving outcomes, and providing a more effective and enjoyable rehabilitation experience. By creating realistic and interactive virtual environments, patients can be transported to different settings, scenarios, or activities that are specifically designed to target their rehabilitation goals. Moreover, the ability to track and analyse real-time data during rehabilitation sessions is a significant advantage of immersive technologies. Sensors and tracking devices integrated into AR, VR, and MR systems can capture and measure various parameters, such as joint movements, range of motion, and force exertion. This objective data can be used to monitor progress, provide immediate feedback, and adjust treatment plans accordingly.

The applications of AR, VR, and MR in rehabilitation are diverse and cover various domains. For example, in physical therapy, these technologies can be utilized to simulate real-life activities and exercises, providing patients with a safe and controlled environment to practice functional movements [38], [39], [40], [41]. In cognitive rehabilitation, immersive technologies can be employed to enhance cognitive training through interactive tasks and simulations that target attention, memory, and problem-solving skills [42], [43], [44]. Additionally, immersive technologies can be utilized in phobia and pain management, providing distraction techniques and immersive experiences [45], [46].

(a) (b)

Figure 1: AUSILIA project [47]**: example of information in AR from the therapist's point of view on the (a) patient's lower and (b) upper body.**

To our knowledge, only a few works have been conducted on using immersive technologies to support the therapist during observational assessment of the patient. The AUSILIA project [47], [48], [49], [50] has developed an advanced demotics environment that captures an individual's movements and actions, their interactions with the surroundings (such as forces, contact pressure maps, and motion parameters related to object manipulation), as well as their physiological parameters (such as heart rate, blood pressure, respiratory rate, and sweating) while engaging in self-selected activities of daily living. This data is then presented to clinicians through immersive AR, as in Figure 1, and this system offers a clearer understanding of the individual's performance and provides an additional quantitative means for assessment and classification.

According to the current literature, most instrumented assistive devices primarily focus on monitoring, and if feedback is provided, it is typically intended for the patient alone [24], [51], [52]. However, the study conducted by Chamorro-Moriana et al. [26] takes a different approach by displaying real-time data from instrumented crutches on a PC or through a projector, allowing the information to be viewed by both the patient and the physiotherapist. Despite the therapist having access to the information, the use of a fixed monitor or projection prevents the simultaneous observation of both the loads and the patient's movements.

The integration of AR with crutches rehabilitation has been explored in the study conducted by Peres et al. [53]. In their work, a wearable projector is used to display the desired walking pattern to be performed by the patient. The device provides timed cues to patients with Parkinson's disease, and it has shown effectiveness in improving their cadence and rhythm. It is important to note that this

approach facilitates data visualization for patients, but it should not be considered as a biofeedback or monitoring solution since it does not provide any objective measurements [54].

Gait Analysis

This chapter describes the activities related to gait analysis using assistive devices. The focus is primarily on the development of an upgraded version of instrumented crutches, which were part of the EUROBENCH project aimed at benchmarking exoskeletons. The upgraded crutches offer improved reliability in force measurement, and they are equipped with depth cameras to assess the patient's gait phases. This solution enables the analysis of forces involved in different gait phases without the need for motion capture devices. Additionally, a synchronizer has been developed to simplify data synchronization in gait laboratories and ensure compatibility with existing motion capture and other technologies available on the market. The chapter also discusses the validation of an estimator for assessing weight-bearing in the legs and reaction forces in the shoulders. Furthermore, field tests with the instrumented crutches and exoskeletons are described, followed by the introduction of an instrumented walker.

5.1 The BULLET project

The Eurobench project is a European initiative aimed at creating a benchmarking framework for robotic systems, with a specific focus on bipedal robotics. The motivation behind this initiative is the increasing relevance of human-centred robots, such as prostheses, exoskeletons, and humanoids, in various market

domains. However, several roadblocks exist, including the lack of reliable performance and safety indicators for these devices to meet international certifications and standardization requirements. A consolidated benchmarking methodology for Robotics has not been reached yet. Firstly, current benchmarking approaches in bipedal robotics focus on generic performance indicators and lack detailed measurements of technical causes of performance. Secondly, the reproducibility of results in scientific publications is challenging due to insufficiently specified experimental protocols and methods. Finally, current measurement systems and procedures used to evaluate robotic performance are heterogeneous and lack standardization, hindering their widespread adoption. Eurobench aims to address these gaps by creating a European framework for applying benchmarking methodology to robotic systems, specifically in the domain of bipedal robotics. The Eurobench committee has issued an Open Call to commission projects to proposers for the development of the facility in two stages. The first stage is dedicated to the realization of the proposed solution, while the second stage focuses on its validation.

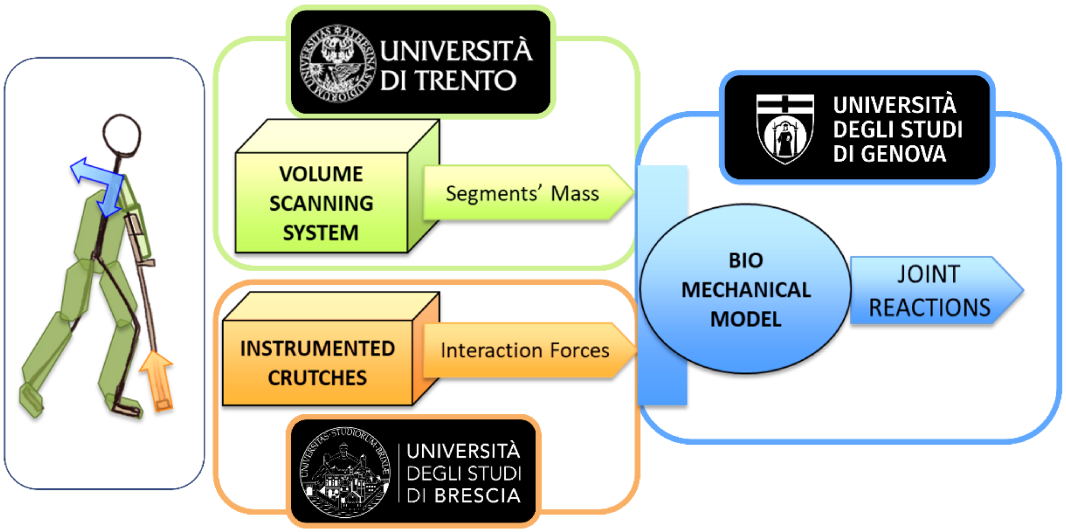

Figure 2: The BULLET testbed for Eurobench project.

The BULLET project is one of the Eurobench's testbeds developed by the University of Brescia in collaboration with the universities of Genoa and Trento and aims to properly assess the shoulder joints' reaction forces during assisted walking.

Most wearable robots for locomotion require the usage of crutches changing the gait patterns and the internal forces and moments acting on the articulations of the exoskeleton pilot. Measuring articulations' reactions is critical to correctly compare robotic solutions since repetitive overloading could lead to pain and chronic pathologies. While performing the benchmarking scenarios we require:

- a biomechanical model of the pilot and exoskeleton.
- mass and inertial data of both.
- kinematic data.
- force data, both at the feet and on the crutches.

All these information could be obtained by three different systems, as represented in Figure 2, integrated into the benchmark environment:

- instrumented crutches, equipped with a wireless system able to measure the load applied by the user on each crutch, the crutch orientation, and the gait phases.
- a volume scanning system, based on depth cameras, to measure the body segments' centre of mass, inertia and mass using the volumetric information acquired.
- a biomechanical model, to compute inverse dynamic analysis using the measured data, and the uncertainty associated with the joints' reaction forces.

5.2 Instrumented Crutches – A New Version

5.2.1 Framework

The Eurobench project imposed some data format and exchange requirements to simplify the integration and communication between devices with several origins. The Robot Operating System (ROS) protocol [55] has been selected to propagate information on the network in a standardized manner, and since it is one of the most used protocols in the robotic field, it also enhances the distribution of the developed solutions. Thus, the instrumented crutches, an upgraded version of the previously developed crutches [29], [30], [31], [56], must satisfy the following requirements:

- Measure the axial force.
- Measure the acceleration and orientation.
- Measure the gait phases.
- Be implemented in ROS to send data in the Eurobench network.

The board selected is the Raspberry Pi 3 B+ because it allows integration with ROS libraries, as well as provides digital I/O and allows management via the USB port of the camera recordings used for the gait phase detection. A shield was designed to equip the raspberry with an IMU to measure the crutch orientation and a load cell amplifier, as shown in Figure 3, to acquire the voltage of a Wheatstone bridge of strain gauges.

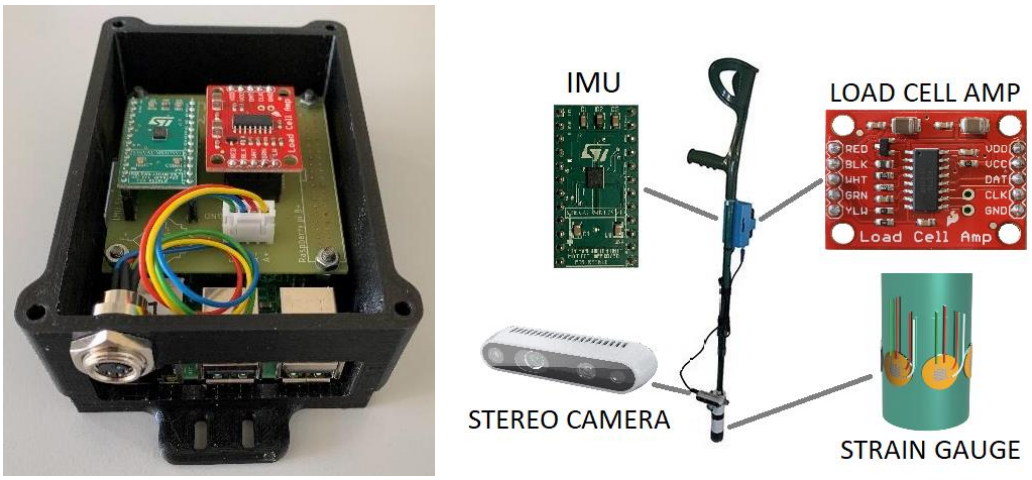

Figure 3: Acquisition board of the instrumented crutches.

The IMU selected is the LSM9DS1 with 9DoF and it supports the I2C communication protocol. The choice for the load cell amplifier falls on the 24-bit ADC HX711 which offers high resolution, signal pre-amplification and filtering. The HX711 measures the voltage from the strain gauges with a sampling rate of up to 80 Hz that it's enough if compared with the dynamic of the crutch forces due to human usage.

The acquisition board is supplied by a 10Ah power bank, and each crutch can be controlled remotely via Wi-Fi. All the data are directly sent to the computer connected to the same network via ROS, apart from the depth images that are pre-saved onboard and sent offline. The user interface shown in Figure 4 allows the instrumented crutches to connect and launch all the equipped devices, or part of them. The acquisition from the loadcell involves a phase of zeroing the force offset usually performed by asking to lift the crutches from the floor. The computer saves

data following the Eurobench data format, which stipulates that pre-processed data must adhere to the following contextualized pattern:

$$subject\_X\_cond\_Y\_run\_Z\_[type].csv$$

- **Z = Run number.** A set of runs consists of repeating the same actions (and recording) in the same conditions (for enabling statistics for instance).
- **Y = Condition number.** A setting is changed. It can be a configuration of the testbed or environmental settings or an indication to the user. For each condition, we can have a set of runs.
- **X = Subject number**. Each subject undergoes the same execution, which may involve multiple conditions. Additionally, each condition can have several repetitions or runs.

Even other information as crutch height and patient height and weight can be set and saved in an information file of the test.

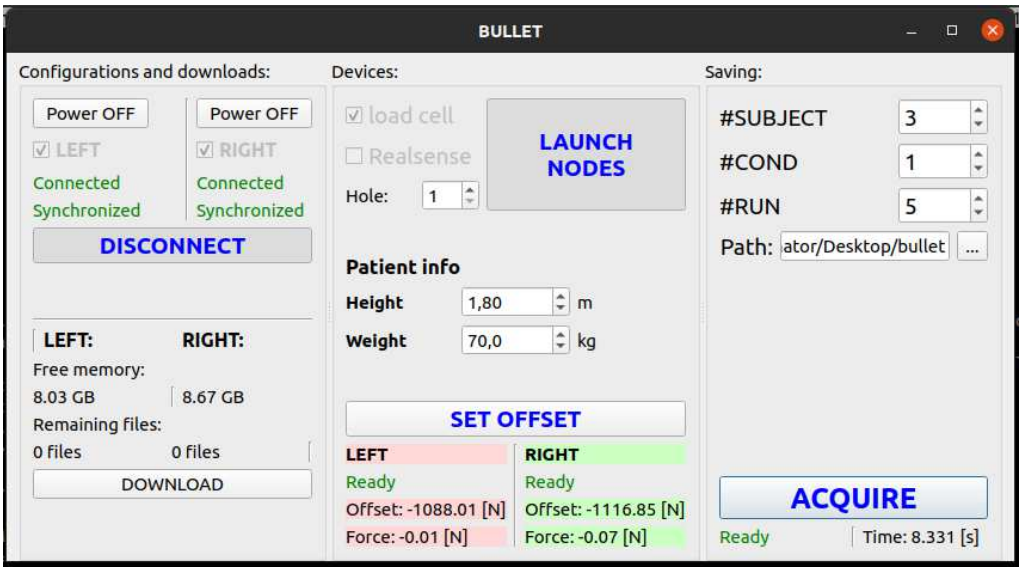

Figure 4: Instrumented crutches' user interface.

Using the Eurobench protocol, receiving the current test numbers, the crutches acquisitions could be controlled from another device by just sending a specific start and stop command through the ROS network. The date and time synchronization are performed via NTP after every boot and the data are aligned in time with other devices.

5.2.2 Force measurements

The University of Brescia has previously developed a version of instrumented crutches that allow measuring the axial and shear forces exerted by the user during assisted walking [29], [30], [31], [56]. Each crutch is equipped with 12 strain gauges connected in Wheatstone Bridge configurations to form three full bridges, as shown in Figure 5. The calibration was performed by applying a known load in a static condition, but despite we can assume the walk is a quasi-static process, the bending of the crutch in contact with the ground is not negligible and it worsens the load measurement. Furthermore, the strain gauges are manually placed on the crutch rod and misalignments could lead to higher uncertainty since some general assumptions are no longer completely respected.

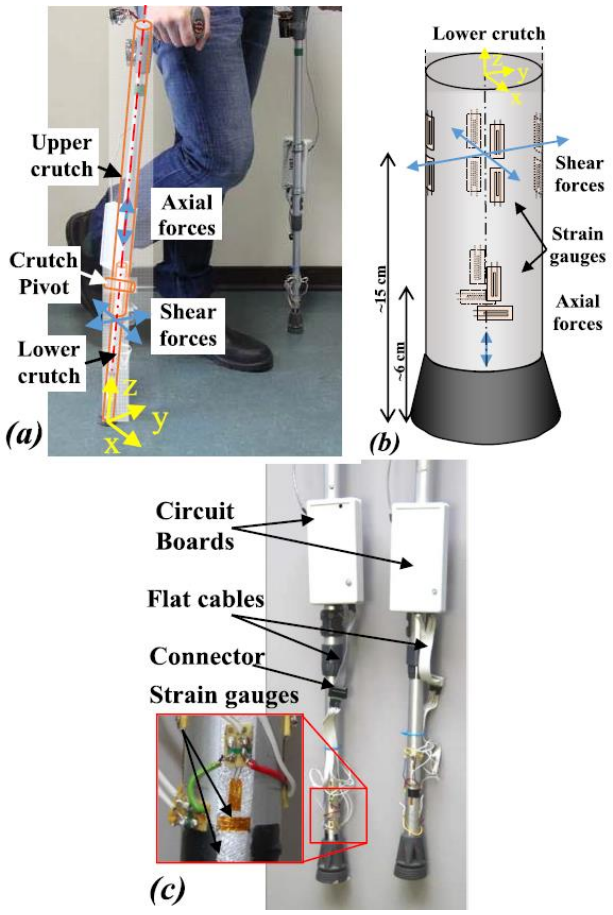

Figure 5: Instrumented crutches of [29]**. a) Crutch constitutional elements and forces; b) Image of the strain gauge positions; c) View of mounting solution.**

In order to quantify the uncertainty an instrumented crutch has been tested walking on force platforms, while the crutch pose is recorded by marker-based optical tracker, as in Figure 6. The reference value of the axial load is computed as the force component along the crutch's axis, that passes through the medium position of the markers on the tip and the medium position of the marker on the back of the handle. The calibration and test procedure has been conducted in two conditions, shown in Figure 6: pushing on the handle with the crutch perpendicular to the force plate (Perpendicular Calibration); and pushing on the crutch handle while walking (Walking Test). In each condition, the loading/unloading cycle is repeated at least 10 times. The error obtained from the linear regression in the Perpendicular Calibration, shown in Figure 7, is 7 N while for the Walking Test is 14 N. With the full-bridge configuration described in [29], the force is typically overestimated during the first half of the crutch stance phase and underestimated in the second half, as displayed in Figure 8. It is plausible, therefore, that the contact point of the crutch tip with the ground due to the inclination of the crutch is an influencing factor in the measurement.

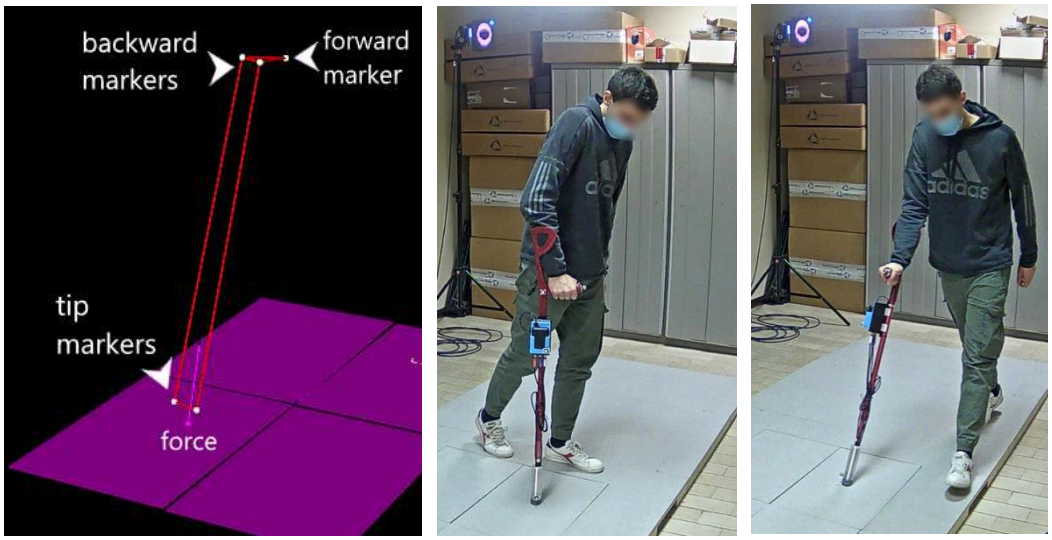

a) **b)** **c)**

Figure 6: Instrumented crutches calibration setup: a) View from the optical tracker's analysis software; b) calibration on the force platform with the crutch in the vertical pose; c) test on the force platform walking with crutches.

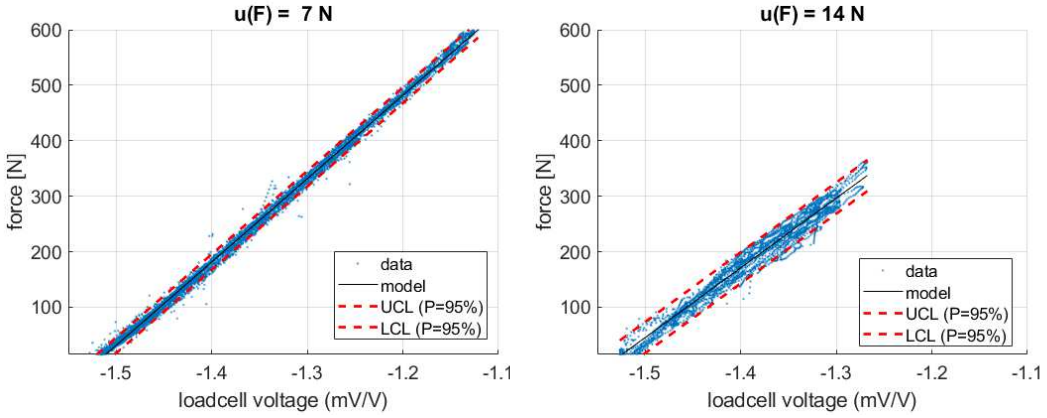

a) b)

Figure 7: Comparison between linear regressions. a) Load applied along the crutch's axis in the vertical position; b) Load applied on the crutch while walking.

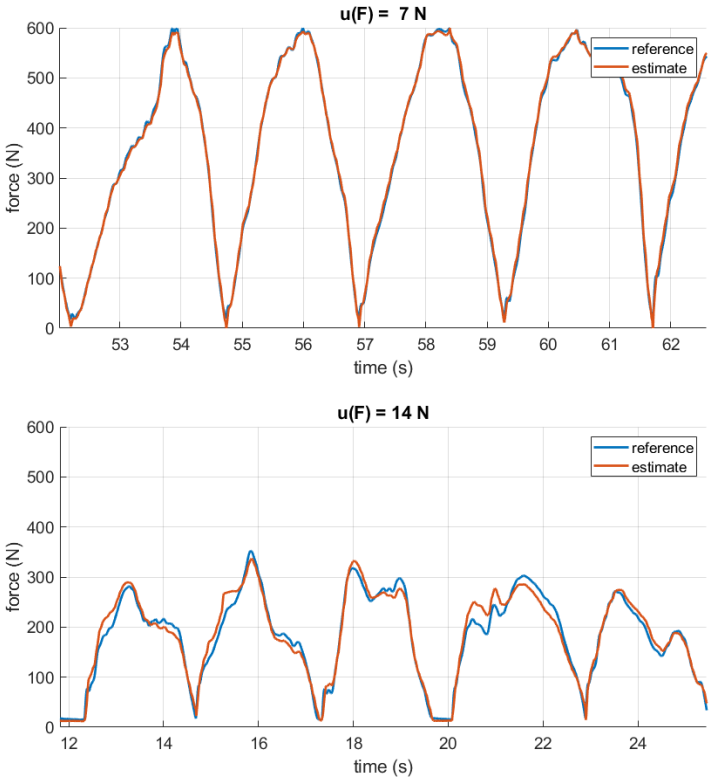

a)

b)

Figure 8: Comparison between the reference force and the estimated value. a) Load applied along the crutch's axis in the vertical position; b) Load applied on the crutch while walking.

The new version of instrumented crutches, unlike the previous one, measures the axial forces only, since the load is mainly applied on the principal axis as demonstrated in [28], [29], [57], in which the peak values of the shear forces are about 3-5% of the axial load. The current configuration in Figure 9 is composed of 6 biaxial (90°) strain gauge rosettes positioned at 60°, forming a Wheatstone full-bridge with 3 strain gauges for each branch.

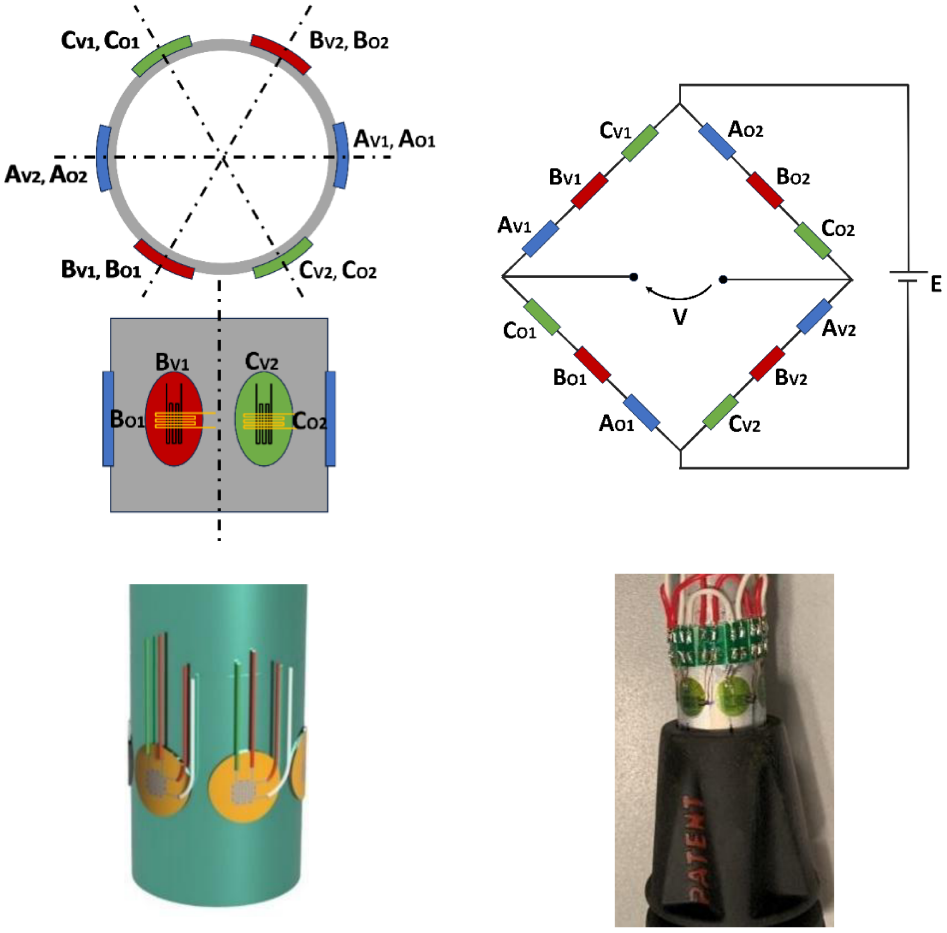

Figure 9: Full-bridge configuration of the instrumented crutches.

From the full-bridge configuration, where R is the strain gauge's nominal resistance, the voltage V is:

$$V = \frac{E}{4} * \frac{1}{3} * \left(\frac{\Delta R_{v1}}{R} - \frac{\Delta R_{o1}}{R} + \frac{\Delta R_{v2}}{R} - \frac{\Delta R_{o2}}{R}\right) \quad \textbf{Eq. 1}$$

Since:

$$\frac{\Delta R}{R} = K_G \varepsilon \qquad \textbf{Eq. 2}$$

and:

$$\begin{aligned}
\frac{\Delta R_{v1}}{R} &= \frac{\Delta R_{Av1}}{R} + \frac{\Delta R_{Bv1}}{R} + \frac{\Delta R_{Cv1}}{R} \\
\frac{\Delta R_{o1}}{R} &= \frac{\Delta R_{Ao1}}{R} + \frac{\Delta R_{Bo1}}{R} + \frac{\Delta R_{Co1}}{R} \\
\frac{\Delta R_{v2}}{R} &= \frac{\Delta R_{Av2}}{R} + \frac{\Delta R_{Bv2}}{R} + \frac{\Delta R_{Cv2}}{R} \\
\frac{\Delta R_{o2}}{R} &= \frac{\Delta R_{Ao2}}{R} + \frac{\Delta R_{Bo2}}{R} + \frac{\Delta R_{Co2}}{R}
\end{aligned} \qquad \textbf{Eq. 3}$$

the previous equation can be written as:

$$\begin{aligned}
\frac{V}{E} = \frac{K_G}{4} * \frac{1}{3} * (&\varepsilon_{Av1} + \varepsilon_{Bv1} + \varepsilon_{Cv1} - \varepsilon_{Ao1} - \varepsilon_{Bo1} - \varepsilon_{Co1} + \varepsilon_{Av2} \\
&+ \varepsilon_{Bv2} + \varepsilon_{Cv2} - \varepsilon_{Ao2} - \varepsilon_{Bo2} - \varepsilon_{Co2})
\end{aligned} \qquad \textbf{Eq. 4}$$

The axial load component affects all the strain gauges with ε_N deformation if they are vertically aligned and $-\nu\varepsilon_N$ when horizontally aligned. Assuming then that a bending moment M_f is applied on the rod (also including the shear forces), it causes a deformation $+\varepsilon_{Mf}$ on one face and -ε_{Mf} on the opposite side. The temperature variation causes an apparent deformation ε_t on all strain gauges.

$$\begin{aligned}
\varepsilon_{Av1} &= \varepsilon_{N_{A1}} + \varepsilon_{Mf_A} + \varepsilon_t & \varepsilon_{Av2} &= \varepsilon_{N_{A2}} - \varepsilon_{Mf_A} + \varepsilon_t \\
\varepsilon_{Bv1} &= \varepsilon_{N_{B1}} + \varepsilon_{Mf_B} + \varepsilon_t & \varepsilon_{Bv2} &= \varepsilon_{N_{B2}} - \varepsilon_{Mf_B} + \varepsilon_t \\
\varepsilon_{Cv1} &= \varepsilon_{N_{C1}} + \varepsilon_{Mf_C} + \varepsilon_t & \varepsilon_{Cv2} &= \varepsilon_{N_{C2}} - \varepsilon_{Mf_C} + \varepsilon_t \\
\varepsilon_{Ao1} &= -\nu\left(\varepsilon_{N_{A1}} + \varepsilon_{Mf_A}\right) + \varepsilon_t & \varepsilon_{Ao2} &= -\nu(\varepsilon_{N_{A2}} - \varepsilon_{Mf_A}) + \varepsilon_t \\
\varepsilon_{Bo1} &= -\nu\left(\varepsilon_{N_{B1}} + \varepsilon_{Mf_B}\right) + \varepsilon_t & \varepsilon_{Bo2} &= -\nu(\varepsilon_{N_{B2}} - \varepsilon_{Mf_B}) + \varepsilon_t \\
\varepsilon_{Co1} &= -\nu(\varepsilon_{N_{C1}} + \varepsilon_{Mf_C}) + \varepsilon_t & \varepsilon_{Co2} &= -\nu(\varepsilon_{N_{C2}} - \varepsilon_{Mf_C}) + \varepsilon_t
\end{aligned} \qquad \textbf{Eq. 5}$$

Substituting Eq. 5 into Eq. 4 we obtain:

$$\frac{V}{E} = \frac{K_G}{4} * \frac{(1+\nu)}{3} * \left(\varepsilon_{N_{A1}} + \varepsilon_{N_{B1}} + \varepsilon_{N_{C1}} + \varepsilon_{N_{A2}} + \varepsilon_{N_{B2}} + \varepsilon_{N_{C2}}\right) \quad \textbf{Eq. 6}$$

Since the strain gauges are manually placed, the deformation ε_N will change according to the angular displacement [58], and the ε_{Mf} difference between the opposite faces will depend on the alignment matching. Placing the 6 biaxial strain gauge rosettes at 60° allows to mitigate the misalignment effects. Moreover, the previous analysis assumes that all gages in a bridge are perfectly matched and have the same gage factor. All the strain gauges are from the same lot as recommended by manufacturers, but gauge factor variability is still expected. Repeating the tests with the described full-bridge configuration in both the Perpendicular Calibration and Walking Test, the obtained errors are respectively 3 and 7 N, as shown in Figure 10. From Figure 11b it can be observed that the overestimates in the first half of the stance phase and the underestimates in the second half are still present, but with lower magnitude with respect to the previous approach in Figure 8b.

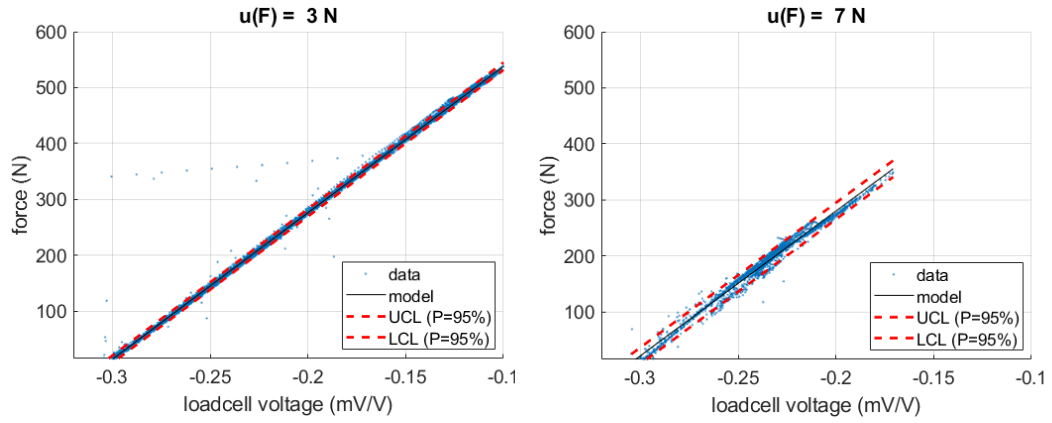

Figure 10: Comparison between linear regressions of the last version of instrumented crutches. a) Load applied along the crutch's axis in the vertical position; b) Load applied on the crutch while walking.

a)

b)

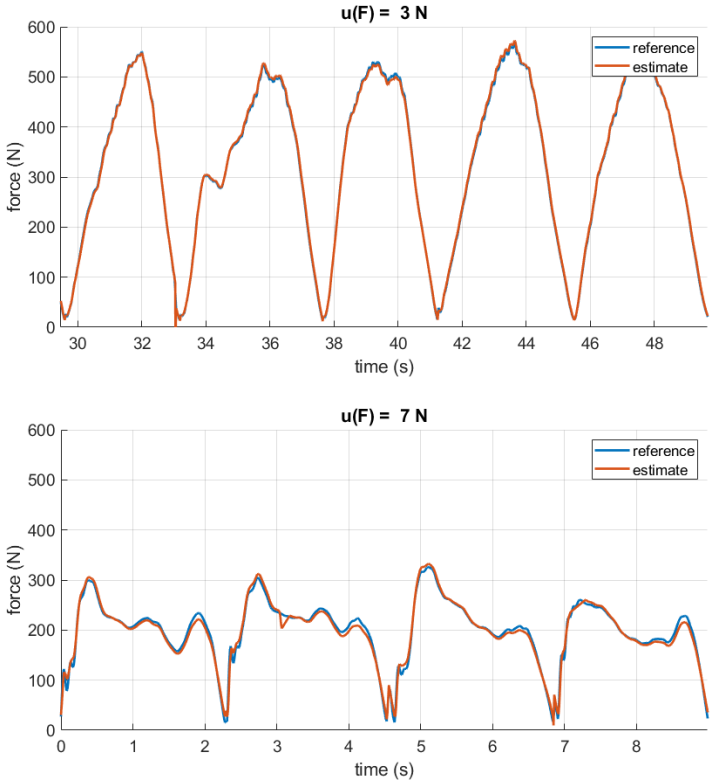

Figure 11: Comparison between the reference force and the estimated value acquired by the last version of instrumented crutches. a) Load applied along the crutch's axis in the vertical position; b) Load applied on the crutch while walking.

5.2.3 Step phases detection

In gait analysis, measuring and analysing data related to these specific phases of the stride can provide detailed information about the biomechanics of walking. Displaying data relative to the phase of the stride rather than in time allows for consideration of the cyclic and rhythmic nature of human walking. This can help identify and analyse any anomalies or irregularities in the stride phase [59], and it can enable better comparability across different subjects normalizing individual differences. Finally, it can be useful for evaluating and monitoring specific pathologies or conditions related to walking [59].

Most of the prototypes of instrumented crutches available in the literature [13], [28], [29], require external motion capture devices to perform a gait analysis and to report the load applied on the crutches with respect to the gait cycle. Motion capture systems that utilize markers necessitate a controlled laboratory setting with

cameras, whereas IMU-based systems are more portable, although requiring the user to be instrumented [13]. The authors in [60] have developed a version of instrumented crutches that allows measuring the axial forces and detecting the gait phases during a two-point assisted walking thanks to the cameras mounted on the lower part of the crutches. The system requires nothing but crutches and a PC, avoiding any user instrumentation aiming to bring gait rehabilitation out of laboratory conditions. The instrumented crutches, schematized in Figure 3, allow the axial forces measurement with 14 N (P=95%) of uncertainty and capture the depth images from a D435I Intel Realsense camera. The camera is placed on the lower part of the crutch looking at the contralateral foot and it acquires at 15 fps.

In [60] the algorithm takes the depth image acquired and applies depth filtering with a pre-selected threshold to isolate the foot's point cloud from the background, as in Figure 12. Then the floor plane is extracted using a RANSAC algorithm and its points are excluded from the point cloud. For all the remaining points, that should belong to the foot, the point-floor distance is calculated. Five percentiles of the foot-floor distance distribution are then used as features to train and test a Modified Random-Forest model. In [60] the model was created from images acquired during a 2-point contralateral walking pattern and the foot phase reference was obtained by manually labelling each frame.

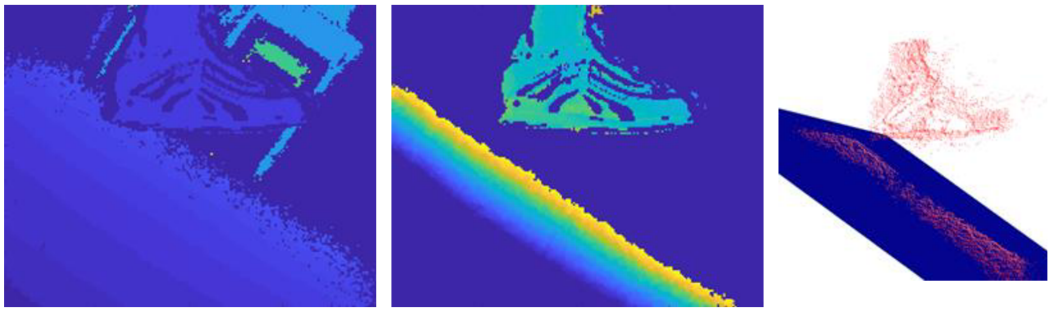

a) b) c)

Figure 12: a) Depth image acquired by the camera mounted on the lower part of the crutch; b) Floor and contralateral foot point cloud after depth filtering; c) Floor plane recognition.

However, the described approach has robustness issues due to the foot's point cloud isolation mainly for the occlusion of the contralateral foot by the ipsilateral foot and the inclusion of undesired objects in the point cloud. The contralateral foot occlusions can't be avoided since the camera is mounted on the opposite crutch and

the ipsilateral foot must pass in the field of view. Moreover, since the depth filtering thresholds are pre-selected, if the crutch is placed at an unusual distance the contralateral foot may be excluded and the ipsilateral foot included in the final point cloud.

Aiming to improve gait detection and its robustness, a new algorithm has been developed following a similar approach to [60]. As shown in Figure 13, due to the camera orientation and the walking pattern, more objects are usually included in the point cloud: the floor, the ipsilateral foot, the contralateral foot, the contralateral crutch, and background objects. Each depth frame is filtered in distance with a depth threshold of 1 meter just to exclude undesired distant objects.

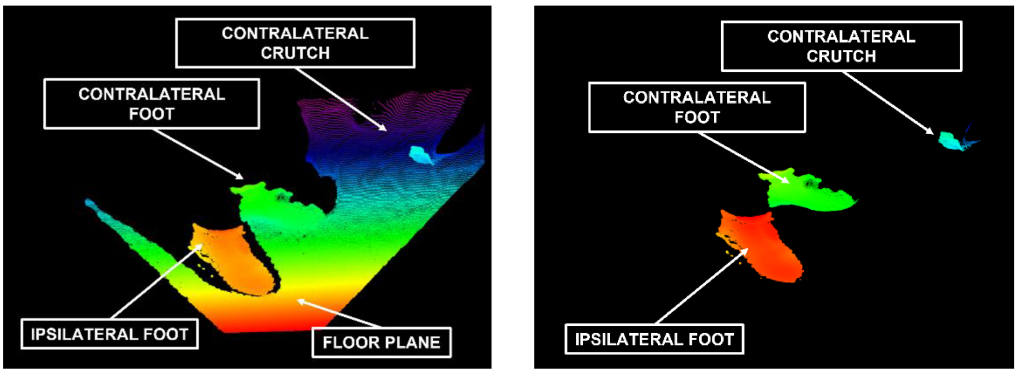

a) b)

Figure 13: a) Point cloud acquired by the depth camera mounted on the lower part of the crutch; b) Point cloud after the floor plane removal.

The floor surface is extracted again using a RANSAC algorithm and the point cloud without the floor is then passed to a recursive k-means clustering to separate each element, as schematized in Figure 14. For each iteration, the R parameter is calculated as the root mean square value of the distances from the point cloud's centroid. If R is greater than a pre-selected threshold, the point cloud is divided into two with a traditional k-means method and the new point clouds undergo another iteration. The iterations end when all the point clouds have R lower than the threshold. Since the contralateral crutch's point cloud, if it is present, is the farthest element from the camera as in Figure 15, it should be composed of a few points. An empirical threshold of 1% of the resolution points number is chosen to remove all the clusters under this value. The remaining clusters should belong to the ipsilateral and contralateral feet. The cluster with the maximum distance of the centroid from the camera is then selected as the contralateral foot's point cloud.

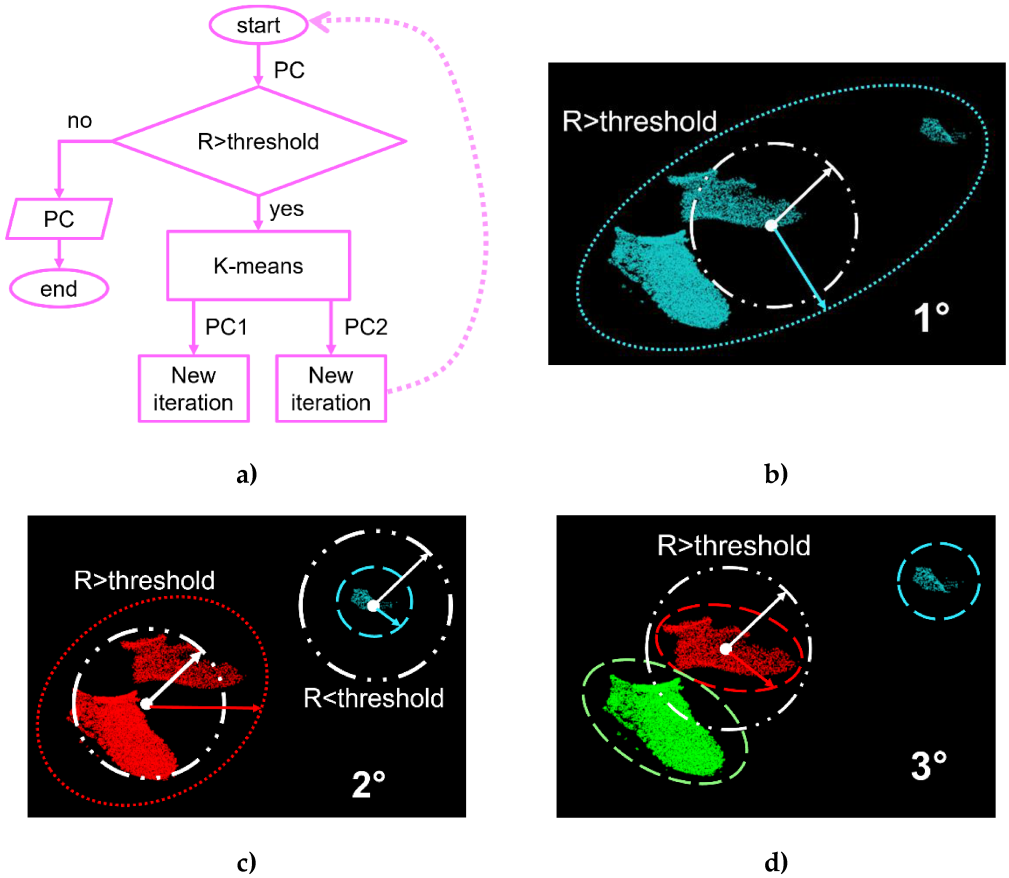

Figure 14: Recursive k-means method to separate objects in a point cloud. a) Algorithm scheme; b) First iteration; c) Second iteration; d) third iteration.

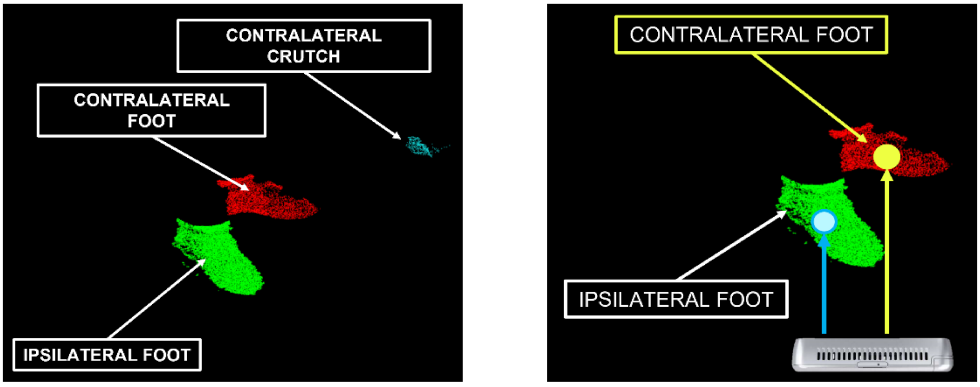

Figure 15: On the left, the point clouds of the remaining objects after the recursive k-means clustering; On the right, the contralateral foot's point cloud identification after the contralateral crutch exclusion.

For each point, the point-plane distance is computed, and five percentiles are extracted from the distribution. Since during the two-point walking pattern, a swing phase of the contralateral foot imposes a stance phase in the ipsilateral foot, the percentiles extracted by both crutches are useful to predict the step phases. To take advantage of the chronological sequence of the recorded frames a Neural Network with three fully connected layers is trained passing the percentiles from the i-9 frame to the i+9 frame from both the crutches (PCA enabled with 95% of explained variance).

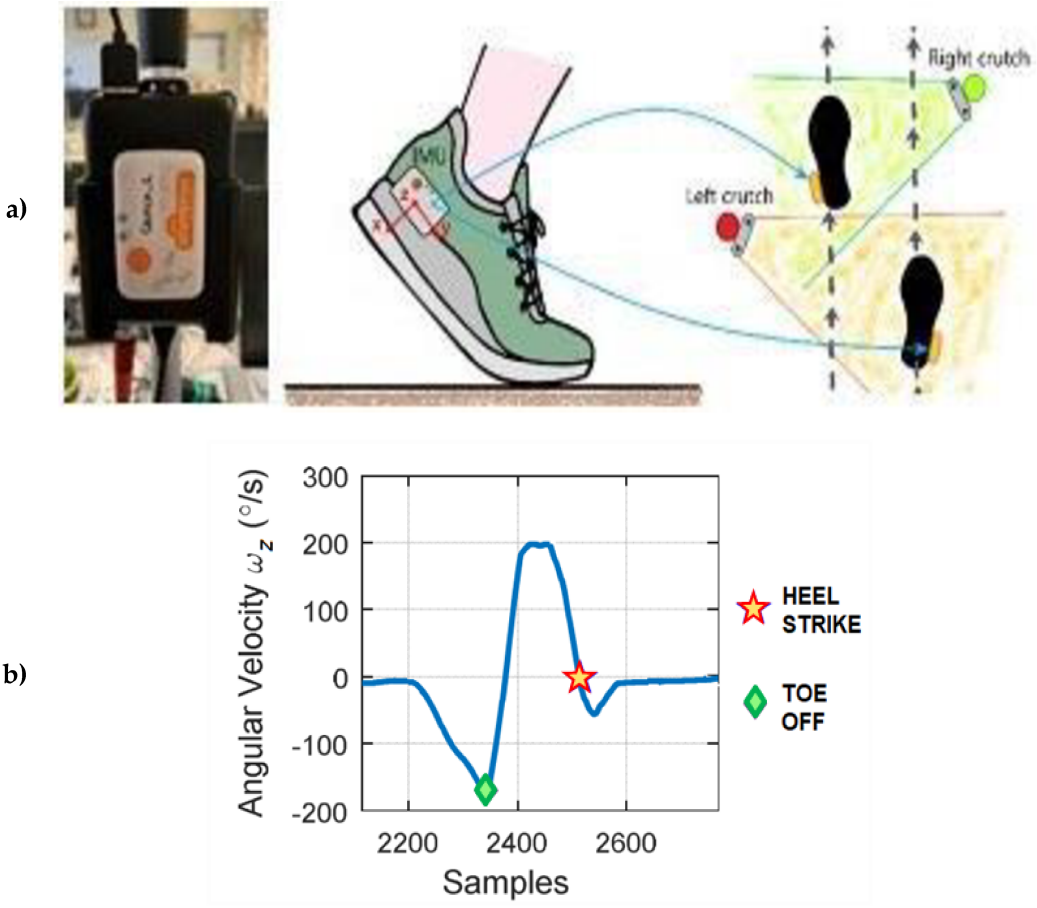

Figure 16: a) IMUs placement on the feet and the crutch; b) Heel strike and toe-off event detection from the angular velocity.

The test campaign involves 13 young healthy subjects (gender: 10 male and 3 female; age: 29.3 ± 5.1 years; height: 1.76 ± 0.05 m; weight: 74.6 ± 12.5 kg). The participants are asked to perform a two-point contralateral assisted walking [13] on a flat indoor surface of 25 meters with self-selected speed. The walk is repeated at

least three times, and the subjects must load a partial of their body weight on the crutches. To get the step phase references a set of four external IMUs are used during the tests. Two IMUs are placed on the shoes and another two are fixed on the crutches as shown in Figure 16. With an approach like the one used in [61], the gait events are identified from the angular velocity ω_z along the z-axis in Figure 16. Another two IMUs are fixed on the crutches to allow data synchronization comparing the accelerations with the signals recorded by the instrumented crutches' IMUs.

The k-fold cross-validation is used for training and validation of the algorithm [62]. The dataset is divided in 5 folds and each fold is composed of different subjects' data. The results reported as accuracy, F1-score, True Positive Ratio (TPR) and True Negative Ratio (TNR) are shown in Table 1. The global confusion matrix is shown in Figure 17.

Table 1: Statistical results of the trained classification model.

	ACCURACY	F1-SCORE	TPR	TNR
FOLD 1	93%	95%	96%	89%
FOLD 2	86%	89%	87%	83%
FOLD 3	90%	93%	91%	88%
FOLD 4	87%	91%	91%	79%
FOLD 5	85%	90%	89%	78%
GLOBAL	**88%**	**92%**	**91%**	**83%**

Considering the overall performance of the model, it achieved an accuracy of 88%, indicating a reasonable level of overall correctness in classification. The accuracy is comparable to the previous method [60] in which was 87% with 14% of unclassifiable samples. The F1-score was 92%, indicating a good balance between precision and recall. The TPR was 91%, indicating a good ability to identify the stance phase, while the TNR was 83%, indicating a moderate ability to identify swing phase. Performances drop for the swing phase prediction, but it is expected because both the crutch (and camera) and foot are moving during the swing phase worsening the camera framing and the quality of images captured.

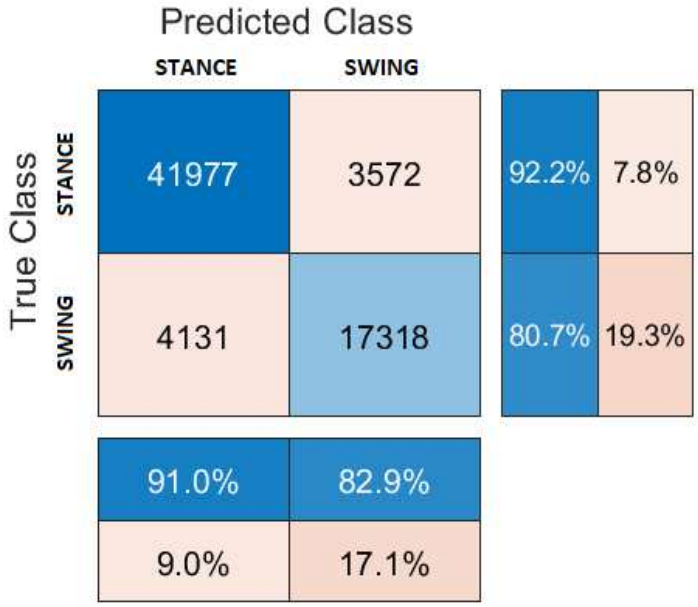

Figure 17: Test confusion matrix of the gait phase predictions.

The robustness has been improved reaching a measurement independent from the foot distance, but the database should be expanded, also including subjects with walking disorders and different gait patterns to cover more rehabilitation approaches. The instrumented crutches with gait detection can also be used for outdoor environments without requiring extra instrumentation. Table 2 reports an intra-subject comparison among the predictions and the reference results computing the root mean squared error (RMSE). The load applied on the crutches of the same subset can be shown with respect to the gait cycle, as in Figure 18. For example, since the 2-point walking pattern, it is expected that the load on the right crutch will be increased during stance on the left side.

Table 2: Intra-subject comparison of gait parameters.

Foot side	*Stance time (ms)*		*Swing time (ms)*	
	mean	*RMSE*	*mean*	*RMSE*
left	1164	87	544	61
right	1167	78	541	44

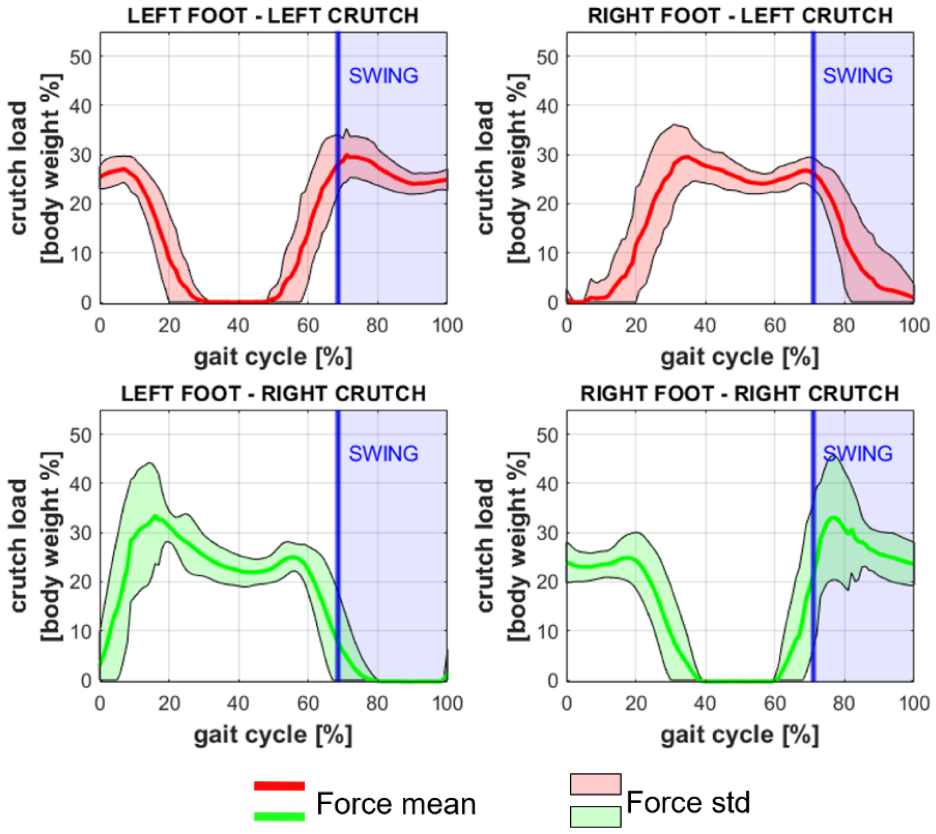

Figure 18: Outcomes visualization example: load applied on the crutches with respect to the gait cycle of the foot.

5.3 Synchronizer

In biomechanics, several kinematic and kinetic devices can be needed for human motion evaluation in different conditions. Gait analysis laboratories are equipped with sensors like motion capture systems (inertial measurement units (IMUs), vision systems), electromyography (EMGs), force platforms, or pressure/force sensors. Most of these sensors are either commercial or closed solutions, often hardly embeddable in a distributed network typical of industrial environments. Biomechanics experiments usually rely on simpler synchronization protocols, that mostly depend on the sensor availability and the experiment about

to be conducted. The practical requirements of the synchronization concern the correlation in the time domain of the operations and involve (i) the detection of the time delay among independent signals, (ii) the compensation for the delay, and (iii) the implementation of a protocol to guarantee the accurate synchronized operations [63].

Time delay evaluation can be realized by clock timestamps or by common input/output triggering signals at the synchronized elements. Classic protocols and synchronization solutions generally require specific hardware and communication modules for their implementation [64], [65], [66], [67]. These requirements and implementation are often not justified or affordable in a typical research measurement setup. A common way to synchronize the acquisition of different systems is through a common signal path or triggers [68]. In biomechanics, a predefined human motion can be recognized by more systems, defining a clear moment in the timeline of the different devices. However, this technique requires more post-processing efforts and more data to be acquired [69]. Trigger signals can synchronize the start/stop of the acquisition of different systems [68], but still, some systems might not be equipped to support the handling of trigger signals. The adoption of a synchronized timestamp from the different devices represents one of the preferred solutions to synchronize different signals that can be acquired at a different sampling rate, reducing the efforts needed in the post-processing synchronization of the data recorded. One of the most used technologies is the GPS (Global Positioning System) [70]. Although GPS was developed as a navigation solution, several applications can rely on its technology for clock synchronization. However, GPS remains an expensive solution outside of its main application fields. Other more accessible technologies for machine synchronization are the Network Time Protocol (NTP) [71] and the Precision Time Protocol (PTP) [72]. While PTP (defined in IEEE 1588 [71]), can provide higher accuracy synchronization (in order of μs) [72], NTP results in a less expensive implementation and is now the established Internet standard protocol used to organize and maintain the clock synchronization of a PC to a reference time. The sensor's software might not often include the possibility to add an absolute time reference in the data sent, rather they can provide timing information relative to the data that start the acquisition. From this point of view, NTP can represent a suitable tool for the synchronization of different PCs and acquisition units but a shared time reference in all the sensing units can still be missing.

A strong tool for developing early-stage robot applications is the ROS [55]. A ROS application is composed of several independent programs called nodes, each of which communicates with other nodes using a topic-based Publish/Subscribe design pattern [73]. An already developed acquisition software can be adapted to support ROS communication and publish the received data that will be shared with all the systems under the network. Each message published is completed with the related machine timestamp in EPOCH format, allowing an easy synchronization of all the messages published in the network. However, this ROS integration can be problematic with some specific instrumentation. Commercial systems often don't allow the user to access their online data, hampering their inclusion in a ROS-based network. Systems that still rely on external trigger signals for their data acquisition shall be somehow able to synchronize their records with those compatible with ROS.

The work published in [74], and further detailed, proposes a simple and low-cost solution for the synchronization of data in a ROS network and from analogic trigger-based systems. This solution wants to overcome and simplify the synchronization protocols that are normally employed in biomechanics laboratories offering a bridge to and from devices that fall outside a ROS network.

5.3.1 Materials and Methods

A Raspberry Pi 3 B+ mounting Raspbian GNU/Linux 9 with ROS kinetic distro is used as a trigger box (TB). A ROS node in the Raspberry handles the synchronization as follows:

- A PC or any other device in the ROS network can publish a ROS standard message of type Int8MultiArray (std_msgs/Int8MultiArray) in a ROS topic (*/enable).*
- The first element of the message array represents the ROS trigger, which is set to "1" when enabled, while the following values are the addresses (IDs) of the ROS devices intended to be triggered by the message.

The TB has a unique ID set in the ROS node and subscribes to the topic */enable*. When the TB reads an active ROS trigger value in the first array location and finds its unique ID included in one of the following array locations, a trigger is declared, and a digital output (GPIO) is set to HIGH (3.3V) for a predefined amount of time.

As soon as the GPIO is set to HIGH, a ROS standard message of type Header (std_msgs/Header) is published by the TB in a ROS topic /*enable_ack*. This Header message includes a timestamp in EPOCH format and an additional field where the ID of the publisher is declared.

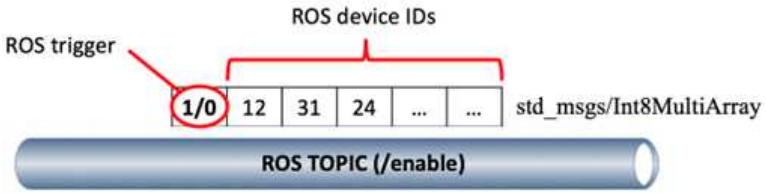

Figure 19: The ROS topic /enable with the relative ROS message. The first element can be 0 or 1 depending on the ROS trigger activation status. The IDs of the device intended to be triggered are added in the following locations.

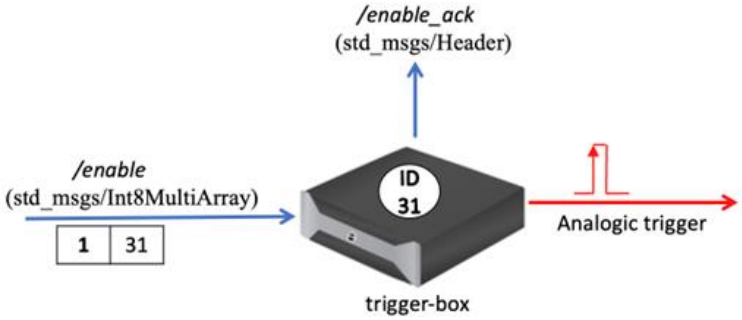

Figure 20: trigger-box functioning principle. The trigger-box reads the topic /enable and if a trigger is declared including the trigger-box ID, an analogic trigger is sent through a digital output while a timestamp is published in the topic /enable_ack. In this example, the TB has ID 31.

The published timestamp can be saved from any device subscribing to the topic /*enable_ack*, collecting a time reference in which the analogic trigger signal has been sent from the TB. To make the collected timestamps consistent among all the devices and the data shared in the ROS network, the TB and the devices in the network are synchronized through NTP to the same source.

For the validation test of the proposed solution, the following components are used:

- Raspberry Pi 3 B+ used as TB and connected as in Figure 21.
- 1 NI CompactRIO (cRIO) 9022

- 1 NI Analog Input module 9215
- 1 Modem/Router NETGEAR N750
- 1.5m ethernet cable Cat.5
- 1 Computer mounting Ubuntu 18.04

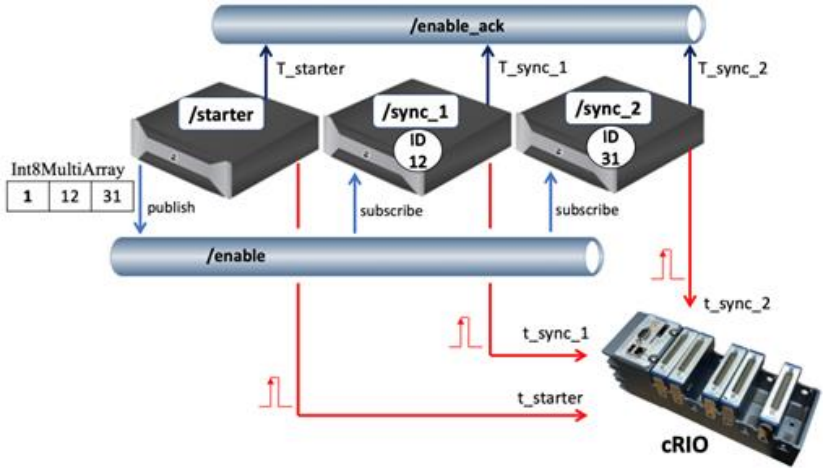

Figure 21: Connection and interaction of the components. Blue arrows represent the ROS-world communications while red arrows represent the analogic trigger transmissions.

Each TB is represented as a ROS node:

- Node /*starter*: Executed in the first TB, publishes the start message on the topic /*enable* composed by a "1" to start the ROS trigger followed by the device IDs of the other TBs. When the message is published, a physical trigger is sent to the cRIO, and a timestamp is published on the topic /*enable_ack*.
- Node /*sync_1*: Executed in the second TB, subscribes the topic /*enable* and when a "1" together with its unique ID is found, a physical trigger is sent to the cRIO, and a timestamp is published on the topic /*enable_ack*.
- Node /*sync_2*: Same as /sync_1 executed in the third TB.

The ROS master runs on a PC that saves all the timestamps published on the topic /*enable_ack* while the cRIO saves the timestamps in which the physical triggers are acquired.

All the devices, including the 3 TBs, the cRIO, and the master PC are synchronized through NTP to the same server (server 1.it.pool.ntp.org). All the

systems are connected through ethernet to the network. The network ping packet request-response rate was 2 ms. Download and Upload velocities were 900.20 Mbps and 420.74 Mbps respectively performed with a speed test. With the setup proposed in Figure 19, the test is conducted as follows:

- The TB /starter publishes a ROS trigger at 2Hz while the cRIO acquires any trigger signal in input at 50kHz. The TBs update their clock through NTP every 3 minutes while the cRIO performs an update every 30 seconds.

- All the system runs for 39 hours while all the timestamps in the topic /enable_ack are saved in the master PC and the cRIO saves the timestamps for any physical trigger acquired. Globally, 70000 samples are recorded.

The time values considered in the protocol are:

Table 3: Time values considered in the protocol.

$t_{starter}$	time in which the cRIO has received the physical trigger from the TB /starter.
t_{sync_1}	time in which the cRIO has received the physical trigger from the TB /sync_1.
t_{sync_2}	time in which the cRIO has received the physical trigger from the TB /sync_2.
$T_{starter}$	timestamp published from the TB /starter on the topic /enable_ack.
T_{sync_1}	timestamp published from the TB /sync_1 on the topic /enable_ack
T_{sync_2}	timestamp published from the TB /sync_2 on the topic /enable_ack.

We hypothesize that the time elapsed between the publication of the ROS trigger from the TB /starter on the /enable topic and the GPIO rising from the same device is negligible. Under this assumption, the metrics in Table 4 are considered for the system evaluation.

Table 4: Metrics to evaluate the synchronization performance.

$cRIO_{recorded\ delay} = (t_{sync_2} - t_{sync_1})$	The delay recorded between the two analogic signals sent from /sync_1 and /sync_2 to the cRIO.
$TB_{published\ delay} = (T_{sync_2} - T_{sync_1})$	The delay recorded between the two timestamps published by /sync_1 and /sync_2 on the topic /enable_ack.
$published\ error = TB_{published\ delay} - cRIO_{recorded\ delay}$	The difference between the timestamps published by the 2 /sync and the difference between the 2 trigger signals sent to the cRIO.

5.3.2 Results

Figure 22 collects the distribution of the metrics $cRIO_{recorded\ delay}$ and $TB_{published\ delay}$. The mean $cRIO_{recorded\ delay}$ is 0.07 ms with a standard deviation of 0.30 ms. Similarly, mean $TB_{published\ delay}$ is 0.1 ms but its standard deviation differs in order of magnitude measuring 3.5 ms. The $cRIO_{recorded\ delay}$ is used as a true reference for scaling the $TB_{published\ delay}$ and informing the real error introduced by the system. By removing the cRIO delay from the TB delay we can obtain the real delay introduced by the system. Figure 23 shows the $published\ error$ distribution with an RMS of 3.5 ms.

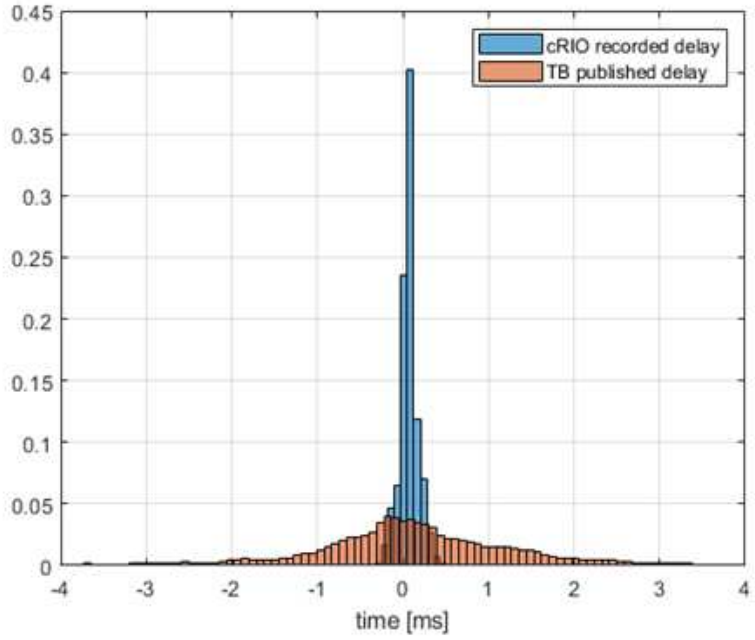

Figure 22: cRIO (blue) and TB (orange) recorded delay. The vertical axis is the relative frequency on 70000 recorded samples.

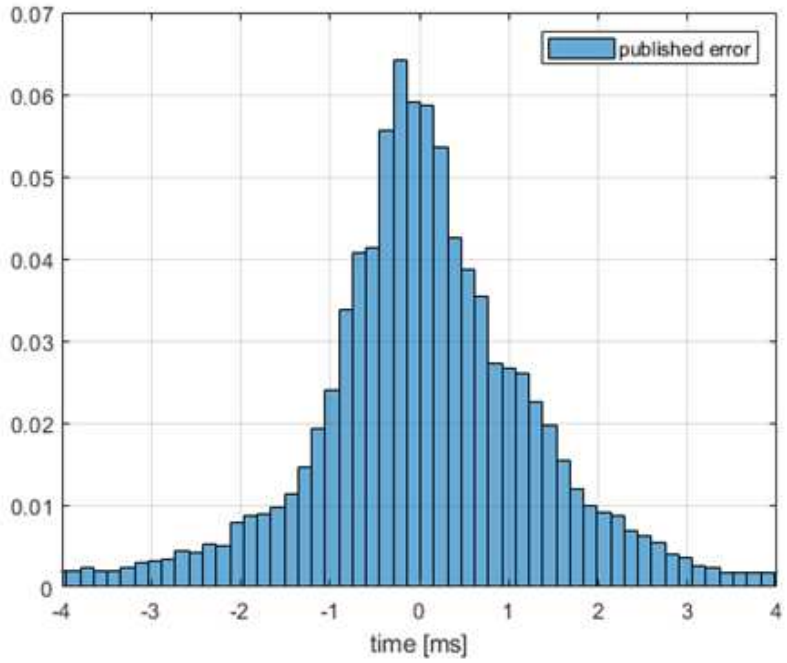

Figure 23: System delay of published times. The vertical axis is the relative frequency on 70000 recorded samples.

5.3.3 Discussion

We proposed a simple and cheap solution for synchronization between ROS and analogic trigger-based devices. The solution can be implemented with a Raspberry, is easy to program, and adapts to the application. We think that flexibility represents one of the main advantages of the proposed solution.

The ROS node in the Raspberry can be easily modified to work with both triggers input and output. Furthermore, timing can be managed in the script by controlling the duration and delay of the signals. From this point of view, this solution can match the simplicity, limited cost, and flexibility required in biomechanical tests, where different devices might require customized input/output signals. The proposed solution supports multi-publishers and subscribers to the same topic by addressing each device with a unique ID. One device can indeed trigger a portion of the devices subscribing to the ROS topic and record the same relative portion of the published timestamp by triggering and looking at the desired device IDs.

The analogic trigger signals from the TBs (sync_1 and sync_2) were recorded at the same instant by the cRIO system. The two signals acquired by the cRIO came from two identical devices and the time dispersion depends on the cRIO time resolution. The cRIO delay can be considered as the real delay between the considered signals. This is important for considering the cRIO recording as our true value in this validation. Both mean values from the data in Figure 22 are negligible with respect to their standard deviation. The standard deviation was a fraction of ms in the case of the recorded analogic trigger, while between the ROS timestamps, it was 10 times bigger. Nevertheless, as for the published error, 3.5 ms is a promising result considering the application this solution was meant for. Biomechanics scenarios involve human motions with frequencies in the order of a few Hertz while data are typically recorded at a sample rate from 50 to 200Hz. For these reasons, we can consider the recorded delays widely suitable for a biomechanics test.

The presented system allows easy synchronization from the ROS world with devices that are suited to be synchronized through analogical triggers. However, no solutions are presented for devices that cannot handle any input/output trigger. This solution relies on a ROS network together with its limitations in matter reliability

and data safety. The performance of the network influences the overall performance of the system.

The presented results widely achieve the needed requirements. However, this validation is performed with a specific test for several hours, under controlled and predefined conditions. A reliable network and proper NTP synchronization are key factors for the achievement of the desired performance. All the presented results are considered the best outcome for the system proposed. Still, our results have a wide tolerance considering the proposed application, entrusting the system validity even in view of performance degradations.

5.4 Partial weight-bearing and shoulder loads estimator

Gait laboratories are not always available and accessible because of their cost, required space and personnel competence. Estimators for the Partial Weight-Bearing (PWB) and the shoulder loads are then validated in [75] minimizing the required instrumentation and increasing ease of use and accessibility.

Incremental weight-bearing is common during post-surgery gait rehabilitation to minimize implant failures and enhance the healing of the soft tissue. The PWB method involves gradually increasing the weight load on the limb over time, a process that is tailored to each patient based on the severity of their injury and the clinician's discretion [76], [77]. Walking aids, such as crutches, can help reduce instability and they are typically prescribed to support weight-bearing on the affected weak lower extremity [78]. During rehabilitation, physiotherapists typically offer prompt feedback to patients on their posture, load, and step sequence, based on their perception and experience. Consequently, the outcome is contingent on the therapist's proficiency, and the patient's progress is assessed subjectively by the therapist [34]. Multiple studies have indicated that patients generally fail to comply adequately with lower extremity PWB protocols [79], [80], [81]. In [81], none of the patients were able to follow the prescribed reduction of 30% of their body weight (BW), and one-third of them were not aware of their inability to follow the instructions. Another study highlighted that none of the participants managed the prescribed load on the operated limb, especially patients who were 60 years old or older [82].

It is necessary to monitor not only consequences on the affected limb but also secondary symptoms involving the upper extremities, which can be stressed during daily activities if crutches are involved [83], [84], [85]. In [86], shoulder force magnitudes up to 170 %BW were measured during crutch-assisted walking with partial or complete unloading of the lower limb. Moreover, the number of repetitions during long-lasting crutch use could lead to shoulder problems as a long-term consequence.

To verify compliance with the rehabilitation goals, force platforms and motion capture systems are commonly used to extract kinematics and kinetics information of the gait also when performed with walking aids. Even if gait laboratories could perform highly accurate measurements [87], some limitations must be considered in clinical applications: they are expensive to set up and operate [88]; patients may need to travel to a specialized gait laboratory, and this can be challenging for individuals who have limited mobility; the controlled environment of the laboratory may be a rough simulation of a patient's real-life walking patterns; and the test takes place over a relatively short period of time [89]. Moreover, information related to the reaction forces of the shoulders is not usually available in real-time since it requires post-process analysis of the acquired data.

Recently, numerous wearable technologies have emerged with the objective of facilitating gait analysis in non-laboratory settings. Several instrumented insoles are employed to gather data during daily activities, and while many of these devices allow for real-time data acquisition, they generally require preliminary calibration to ensure accurate measurement of forces [24], [26], [88], [90], [91]. Several research groups have created instrumented crutches because they allow the estimation of the patient's performance during walking and provide feedback to improve rehabilitation [24], [26], [28], [29], [30], [31], [92]. In [26], [28] vibratory and audio feedback was added to inform the user of overloading or underloading, and in [93], patients showed higher compliance to the rehabilitation goals when audio feedback was provided.

In [75], it provides a preliminary methodological validation of an estimator of the PWB of the lower limbs and the shoulder joint's reaction forces during a walk with instrumented crutches. The estimate is provided by a pair of instrumented crutches to measure the ground reaction forces along their principal axis, and the forces are acquired and processed in real-time, which is suitable for collecting data or providing feedback. The system is validated on six healthy subjects, and since

the estimation of the load on the lower limbs during PWB is affected by dynamics factors ignored by the model, the tests were performed varying the walking cadence and the load on the crutches. Two force platforms by BTS were used to collect the reference values of the legs' load. The models to estimate the shoulder reactions were identified and tested using the reference values obtained by inverse kinematics using the biomechanical model described in [85] and an optoelectronic motion capture system by VICON. The estimator could produce accurate estimates of shoulder forces, although its torque estimates were less accurate. However, as schematized in Figure 24, it does not require motion capture devices to extract the subject's kinematics, and the system can also be used outdoors, bringing the analysis to environments outside the laboratory's conditions. Since neurological conditions, orthopaedic problems, and medical conditions could lead to alterations in gait behaviour [94], this preliminary validation aimed to promote future investigations to confirm and reinforce the method by expanding the sample size and including impairments.

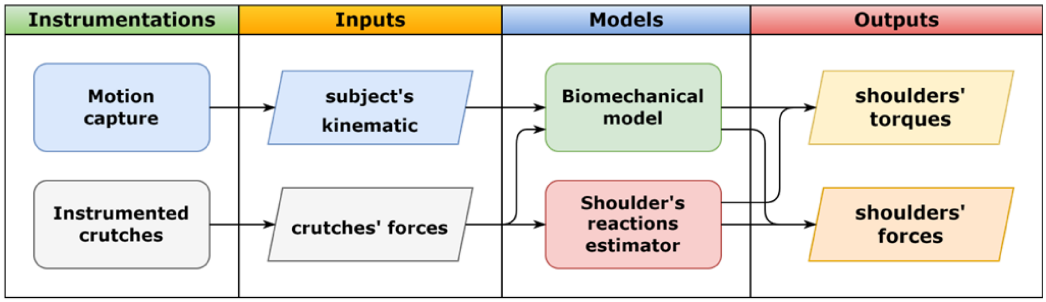

Figure 24: Comparison between the flowcharts of the biomechanical model approach and the shoulder reactions estimator.

5.4.1 Protocol

The instrumentation used and described in the following chapter is summarized in Table 5, and the main details are listed.

The instrumented crutches, shown in Figure 25, measure the force exerted along their principal axis and the crutch's orientation during assisted walking. Data are shared wirelessly in a ROS network [55], and a PC under the same network collects them. The force is measured at 60 Hz in a range from 0 to 600 N with 7 N of measurement uncertainty. The total mass of a single crutch, including the acquisition board and the power unit attached close to the handle, is about 1 kg.

In addition to the instrumented crutches, the experimental configuration comprised two force plates from BTS Bioengineering, which were utilized to gauge the ground reaction force of each foot. Furthermore, a marker-based motion capture system from Vicon Motion Systems, comprising eight cameras, was deployed to capture the subject's kinematics. The sampling frequencies were different for the three systems: the force plates acquired data at 1 kHz, the motion-capture system acquired data at 100 Hz, and the crutches acquired data at 60 Hz, so a resampling procedure was required before starting data processing. The Vicon Full Body Plug-In Gait model was used, as shown in Figure 23, for the placement of the markers on the subject's body [95].

Table 5: Summary of instrumentations and methods in the experimental setup.

Instrumentation	Details
Instrumented crutches	● Range: 0–600 N ● Uncertainty: 6 N (P = 95%) ● Crutch mass: 1 kg ● Sampling frequency: 60 Hz ● Data sharing protocol: ROS ● Time synchronization: NTP server
Optoelectronic motion capture system (Vicon Motion Systems Ltd, UK)	● Cameras: 8 ● Volume: 6 × 3 × 3 m ● Marker protocol: full body VICON plug-in gait (39 markers) ● Markers on each foot ● Markers on each crutch ● Sampling frequency: 100 Hz
LockLab Control Box (Vicon Motion Systems Ltd, UK)	● Time synchronization: generates trigger output
BTS force platforms (BTS S.p.A., Garbagnate Milanese, Italy)	● Dimensions: 0.8 × 0.6m ● Range: 2 kN ● Sampling frequency: 1 kHz ● Time synchronization: receives start/stop trigger from LockLab
Crutches Trigger box	● Available I/O channels: 3 ● Data sharing protocol: ROS ● Crutch time synchronization: NTP server ● System time synchronization receives a start/stop trigger from LockLab

The trigger box previously detailed in the section "5.3 Synchronizer" was used for data synchronization between the motion capture system, the force platforms,

and the instrumented crutches [74]. The internal clock of the trigger box was synchronized with the same NTP server as that used for the instrumented crutches, and when it received a starting trigger from the mocap system, it published its timestamp through the ROS network. The published timestamp was then associated with the first sample of the motion capture system and the force plates. The crutches were already synchronized with the NTP server, and they saved their timestamp labels. Please note that this configuration was required for validation only; when the instrumented crutches are not used simultaneously with other devices, they can be controlled independently using the user interface of Figure 4.

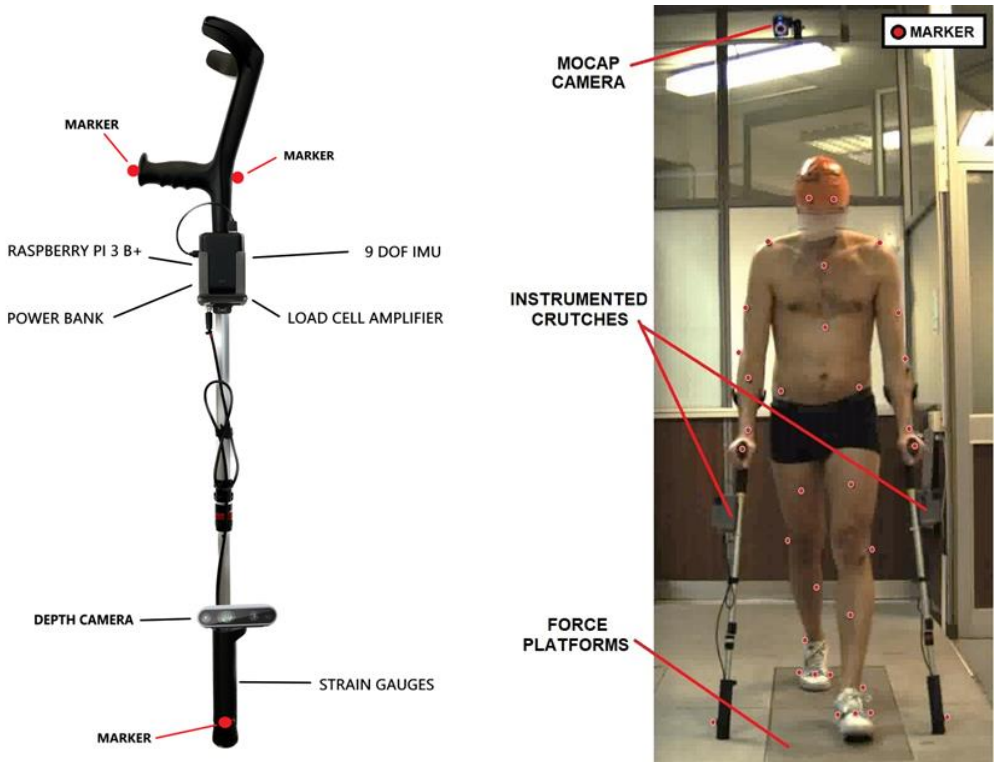

a) b)

Figure 25: a) Instrumented crutches and marker placement; b) subject walking with instrumented crutches during validation. Red dots highlight the visible markers from the frontal point of view.

The experimental protocol aimed to acquire data useful for validating the proposed PWB and shoulder reaction estimators. Since the effect of the gait dynamics was somehow neglected in the model that determined the PWB from crutches' forces, the protocol included three different pacing conditions during

walking: normal or the subject's preferred rhythm and slow and fast cadence rhythms. These different conditions enabled the verification of the dynamic effects of the proposed approach. A metronome helped the subjects follow a cadence of 50 or 90 steps/min, with the goal of covering reasonable boundaries of a walking cadence with crutches [15], [96]. Subjects were asked to walk using the 2-point contralateral pattern and then the tests were repeated with the 3-point partial weight-bearing (3-point PWB) walking pattern [13]. Walking patterns are shown in Figure 26.

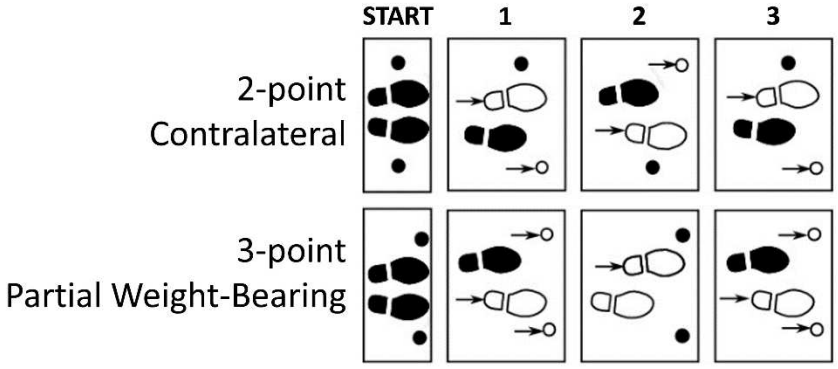

Figure 26: Walking patterns with crutches [13]**.**

Finally, in order to achieve weight-bearing values on the lower limbs that are consistent with those typically prescribed by clinicians, the subjects were required to load 20% or 40% of their BW onto the crutch. In this way, during the 2-point contralateral pattern, the PWB should range between 60–80 %BW, and during the 3-point PWB pattern, it should range between 20–60 %BW. In order to verify subject repeatability, at least three trials were conducted for every condition. Prior to the tests, the subjects underwent a training session lasting approximately 10 minutes to familiarize themselves with walking patterns, cadences, and crutch loads.

The experimental protocol was applied to 6 subjects, 5 male and 1 female with a weight of 78 ± 12 kg, a height of 1.77 ± 0.03 m, and an age of 38 ± 12 years old (mean ± STD). Since at this stage, we were interested in the validation of the proposed approach and not in clinical validation, we performed the tests on healthy subjects only. The study was conducted in accordance with the Declaration of Helsinki, and informed consent was obtained from all subjects involved.

5.4.2 The partial weight bearing estimator

Since during assisted walking, the external forces applied to the subject are the ground reaction forces on the feet and the crutches, the authors believed that the load supported by the user's lower limbs could be estimated by subtracting the left crutch force (LCF) and the right crutch force (RCF) from the total subject body's weight (BW), which is the sum of the instrumented crutches' weight and the user's weight. The load is then normalized and expressed as a percentage of the total subject's weight:

$$PWB = \frac{TW - LCF - RCF}{BW} \quad \textbf{Eq. 7}$$

The Guide to the Expression of Uncertainty in Measurement is applied to the PWB estimate with all the parameters used in the analytical formula of the measurand, along with their associated uncertainties. The following parameters' uncertainties are used:

- The subject's body mass: since the crutches could be used in clinics or domestic environments where body mass is measured with domestic scales, the associated uncertainty is obtained from [94] that analysed the mean and standard deviation of domestic scales. The standard uncertainty is equal to 1.1 kg.
- The crutch load: the crutches are calibrated using force plates and the standard uncertainty obtained is 7 N.
- The crutch mass: each instrumented crutch weighs 0.95 kg. A standard uncertainty of 0.05 kg is considered due to manufacturing differences.

The standard uncertainty is calculated by combining all the individual sources of uncertainty using the law of propagation of uncertainty once all the parameters and their associated uncertainties are identified. The uncertainty propagation is then repeated for some of the possible combinations of the subject's body mass (40, 80, and 120 kg) and the crutches' loads (2.5, 12.5, 20.0, 37.5, and 47.5 %BW). As shown in Figure 27 lower values of PWB have higher standard uncertainty and it also depends on the subject's body mass. When the load on the crutches is lower, which means higher PWB values, the contribution of the crutch load uncertainty increases up to 50% for both crutches measurements.

Of course, the inertia contribution in dynamic conditions could worsen the results since is neglected in the PWB estimator, so a specific testing protocol was proposed to verify this point, varying the user's walking pace and the crutch loads.

a)

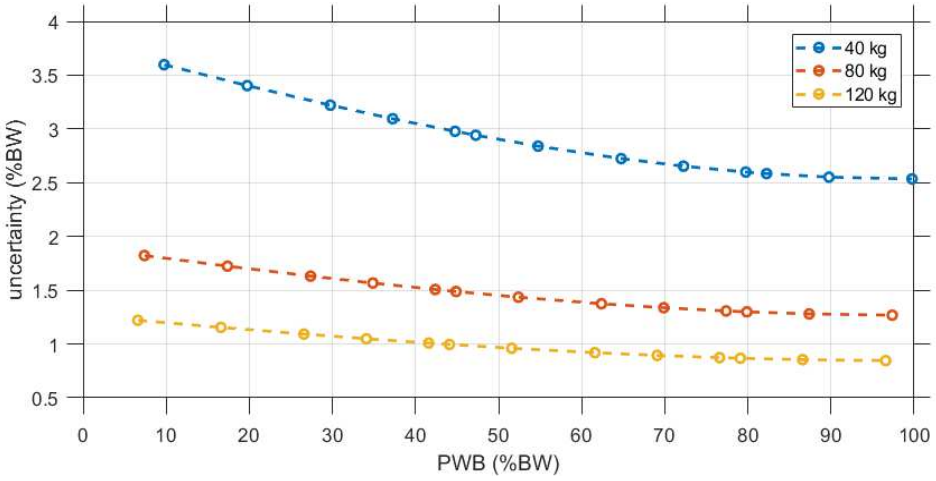

b)

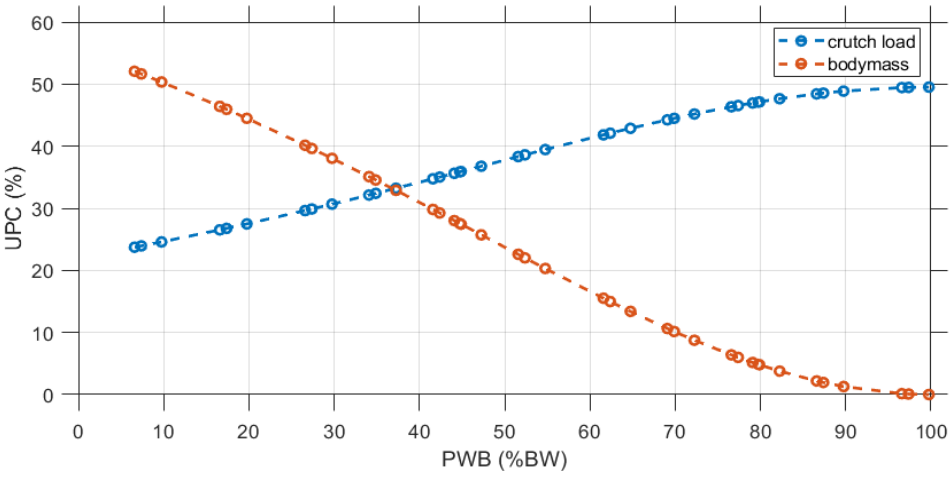

Figure 27: a) Uncertainty of the PWB estimate with respect to the PWB value. b) Uncertainty Percentage Contribution of the subject's body mass and the crutch force measurement.

The reference values are obtained from the sum of the left platform force (LPF) and the right platform force (RPF), normalized by the total subject's weight:

$$\widehat{PWB} = \frac{LPF + RPF}{BW} \qquad \textbf{Eq. 8}$$

The difference between the two values is considered the error:

$$ERROR = PWB - \widehat{PWB} \qquad \textbf{Eq. 9}$$

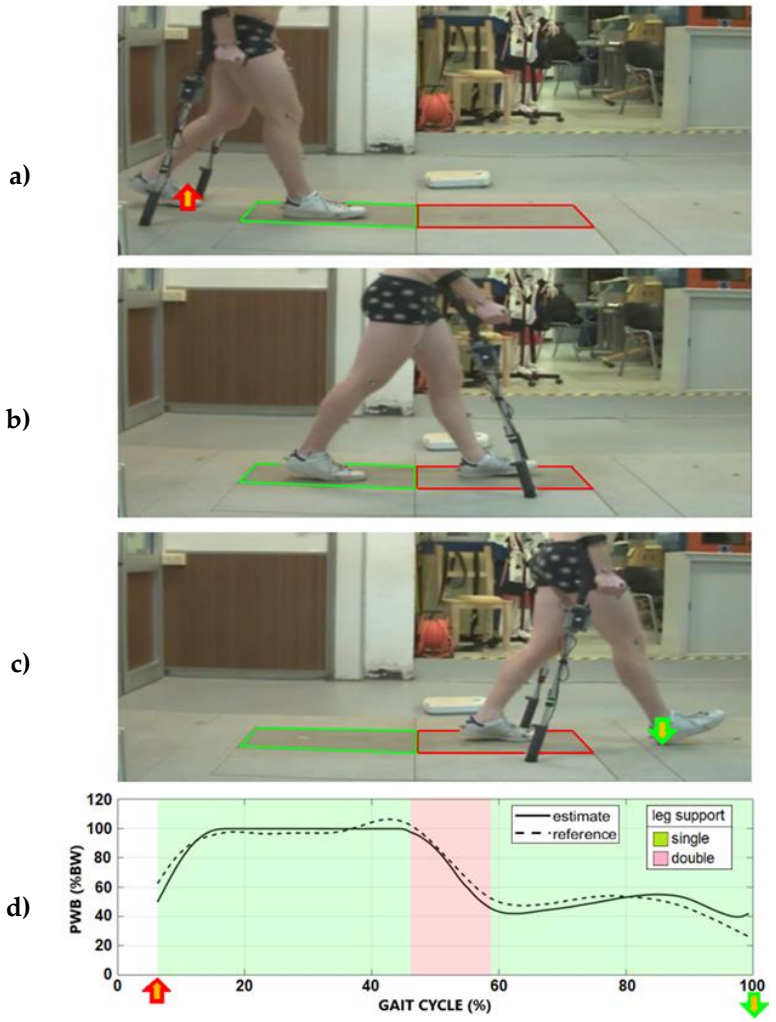

Figure 28: a) The gait event at the start of the interval for the validation of the PWB. The single support phase of the right leg started from this event until the next left foot's heel contact. b) The double leg support phase with all external forces measured by instrumented crutches and force plates. c) The gait event at the end of the interval for the validation of the PWB. The left leg's single support phase was between the last toe-off and the next heel contact of the right foot. d) Comparison between the PWB estimated by the instrumented crutches and the reference value from the force plates, shown in the right leg's gait cycle. The blank background is due to the interval with unknown external forces applied to the foot still resting on the floor.

Table 6 reports the analysis of variance (ANOVA) results of the PWB error. The walking pattern was not statistically significant while all the other parameters (cadence, crutch load, subject, and support status) were statistically significant. The support status of the legs has the highest F value, followed by the cadence. Figure 29 shows the boxplots of the PWB error for all the parameters divided by the gait support since it had the highest F-value.

The PWB's reference, estimate, and error are shown with respect to the time in Figure 30 and with respect to the gait cycle in Figure 31. The data are compared between the gait pattern and the cadence in Figure 30 and the crutch load in Figure 31; moreover, the double-leg support is shown in the background.

Table 6: The ANOVA of the PWB's error.

Parameter	Sum of Squares	Degrees of Freedom	Mean Squares	F	*p*-Value
Cadence	1346	1	1346	46	<0.05
Crutch load	361	1	361	12	<0.05
Pattern	37	1	37	1	0.26
Subject	1336	5	267	9	<0.05
Support	10,177	1	10,177	348	<0.05
Error	7471	256	29		
Total	20,961	265			

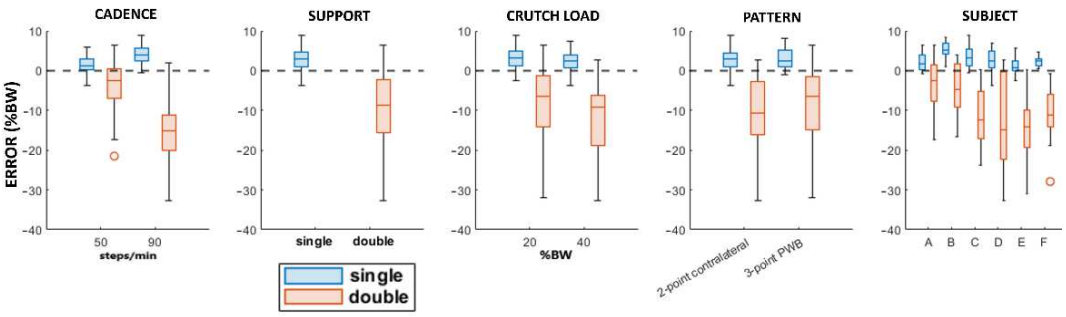

Figure 29: Boxplots of the PWB's error.

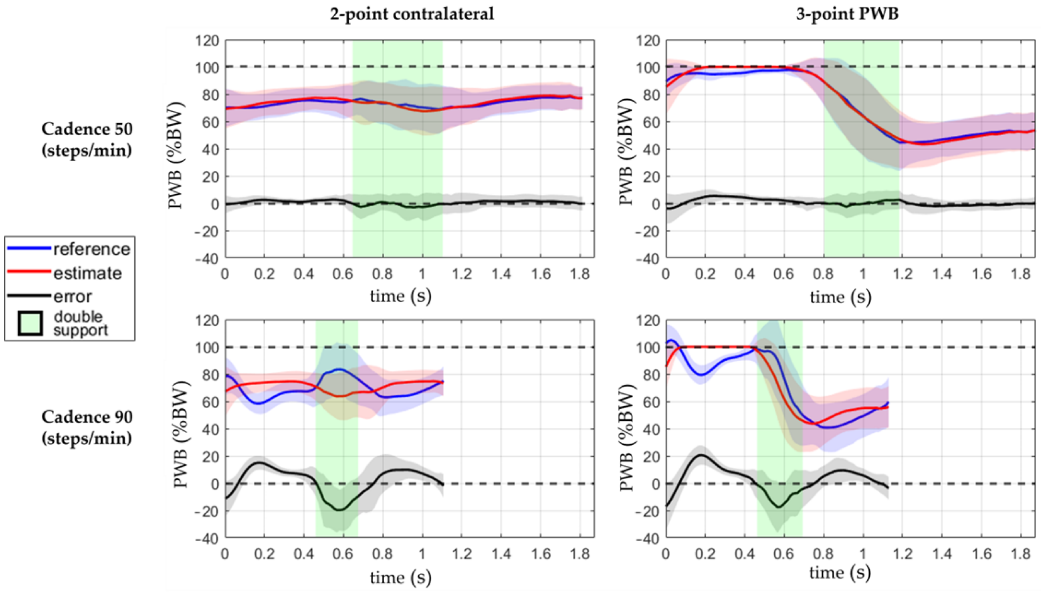

Figure 30: Comparison between the estimated PWB and the reference against the time. The line represents the mean value, and the standard deviation is shown with the coloured band around the mean. The green background indicates the double-leg support interval.

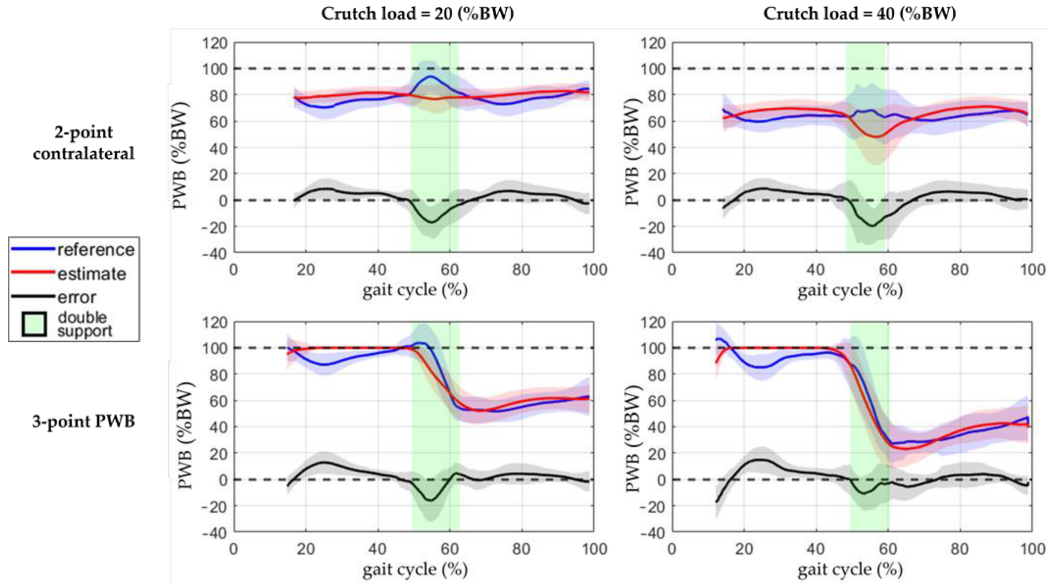

Figure 31: Comparison between the estimated PWB and the reference against the gait cycle. The line represents the mean value, and the standard deviation is shown with the coloured band around the mean. The green and red backgrounds indicate the gait cycle interval with double-leg support. The missing data between 0–15% of the gait cycle are due to the interval with unknown external forces applied to the foot still resting on the floor.

The presented approach estimated the PWB from the measurement of a pair of instrumented crutches. The ANOVA results of Table 6 show that the error was strongly influenced by the cadence and the legs' support. A higher walking pace produced a higher inertia contribution, and the double-leg support also included the toe-off and heel contact events, which generated higher accelerations than the midstance phases. This confirmed that higher dynamic conditions worsen the PWB estimation. The highest error is observed during double-support walking at a speed of 90 steps/min. When the cadence was about 90 steps/min the error reached 11 %BW, which is more than twice the 5 %BW of error reached walking at 50 steps/min. This means that real-time values are more reliable with lower cadence and speed, as could happen during the first rehabilitation days. Typical values of cadence for assisted walking with crutches are 73.2 ± 8.5 steps/min [15], [96]. If the relation between cadence and the PWB error is determined and the gait phases are detected (so cadence and legs support status), the PWB estimation can be corrected by removing the known trend, but it requires a deeper investigation not achievable with the cadences analysed in this work. However, several devices can be used to assess gait phases, but they may have limitations. IMUs or instrumented insoles require the patient to wear the device and sometimes require calibration. Fixed RGB or infrared cameras must be installed in some motion capture systems, which limits their use to specific locations. These devices also require a post-processing stage sometimes and cannot provide real-time feedback. While our instrumented crutches may provide gait phase detection, as previously detailed in section "5.2.3 Step phases detection", the process still needs to improve the reliability and elaborate data in real-time [60], [92].

5.4.3 The shoulder loads estimator

Shoulder reaction reference values were obtained by the biomechanical model outcomes described in detail in [85]. The model is based on an inverse kinetics analysis of the upper limbs. It was originally created to analyse torques in the sagittal plane, and then it was extended to the other planes, including coupled three-dimensional effects. The inputs required are the subject's anthropometry, the kinematics of the crutches and the subject's upper limbs, and the force measured on the crutches. The model considers the hand rigidly connected to the crutch, so the upper limb is described by three rigid segments: the crutch plus the hand, forearm, and arm. The torque and the internal forces are computed at the proximal end of the shoulder or arm. The biomechanical model's main goal was to obtain an online

estimation of the overall shoulder torque; for this reason, a purely mechanical model was considered; this model considers the overall torque required in the articulation to realize the measured movement, and it does not include the forces produced by active muscles on the articulation.

As previously described in the introduction, the purpose of the shoulder loads and torque regression model is to obtain their estimates without measuring upper limb kinematics. In such a way, the biomechanical model is not required, and an online, rough indication of shoulder loads and torque can be directly given to the patient and to the physician. Since the biomechanical model does not need the ground reaction forces on the feet, any gait cycle is valid to create the regression dataset to compute the shoulder values.

The wide dataset was then divided into identification and validation datasets. For this separation, we considered that, in accordance with the test protocol, each condition was repeated at least three times, so one trial was randomly assigned to the validation dataset, while the remaining trials were assigned to the identification dataset. With this procedure, we maintain a balanced representation of the population and conditions between the datasets with good numerosity: 2/3 for the identification and 1/3 for the validation. The model estimated the peaks and the root mean square (RMS) of the shoulder torques and forces, calculated by the biomechanical model in every stance phase of the crutches. Each subject performed at least two stance phases of the crutch on both sides in every trial.

Since the purpose is to give an online indication to the therapist or the patient, the time histories of the loads at the shoulders are not required, while peak and root mean square values are certainly more informative. The corresponding values were computed for each crutch cycle and the force is normalized by the subject's weight while the torque is normalized by the subject's weight times the subject's height.

In the first regression attempt, we considered forces in the sagittal plane (anterior-posterior and vertical directions) and the torque exerted along an axis perpendicular to this plane (mediolateral). These directions were the most significant in a previous study [85], as they include the force in the vertical direction and the torque needed to manoeuvre the crutches during the gait cycle. To simplify the model and focus only on relevant predictors, we investigated the correlation between possible influencing factors and shoulders' forces and torques before proceeding with the regression. We considered the overall set of available

parameters, including the most evident crutch force, anthropometric parameters, kinematic parameters, stance time, and walking pattern. Then, we included all possible couple interactions. For both shoulder forces and torques, we classified possible predictors in decreasing order of correlation with a clear discrimination at a certain correlation level, enabling a clear selection of the most significative parameters for our purposes.

According to the procedure described, we ordered the possible predictors, including their interaction, according to their Pearson correlation coefficient with shoulder forces and torque, and we obtained a clear separation for parameters above 0.65 for the torque and 0.90 for the force. We considered a regression model including such parameters and their interactions with the possibility of considering a second-order model. The parameters above the Pearson correlation index thresholds (0.65 for torques and 0.90 for forces) are shown in Table 7.

Table 7: Pearson correlation coefficients between the shoulder load and torque and some of the parameters investigated. The * (multiplication) operator yields the product of its operands.

Parameters	Correlation with Shoulder Vertical Force		Correlation with Shoulder Mediolateral Torque	
	RMS	**Peaks**	**RMS**	**Peaks**
Crutch force RMS	1.00	0.96	0.74	0.74
Crutch force RMS * height	1.00	0.96	0.73	0.73
Crutch force RMS * height^2	0.99	0.95	0.71	0.71
Crutch force peak	0.93	0.98	0.68	0.74
Crutch force peak * height	0.93	0.98	0.67	0.73
Crutch force peak * height^2	0.93	0.98	0.66	0.71
Crutch force RMS * BMI	0.86	0.86	0.54	0.56
Crutch force RMS * body mass	0.86	0.86	0.52	0.54
Crutch force peak * BMI	0.80	0.87	0.49	0.56
…	…	…	…	…

Moreover, in order to maintain a clear physical correspondence of the model, we considered the same predictors set for both force and torque, so we assume that this parameter set is significant for the general shoulder load.

Figure 32 and Figure 33 show the regressions of the shoulder joint force and torque. Table 8 and Table 9 display the RMSE values for the shoulder joint force and torque.

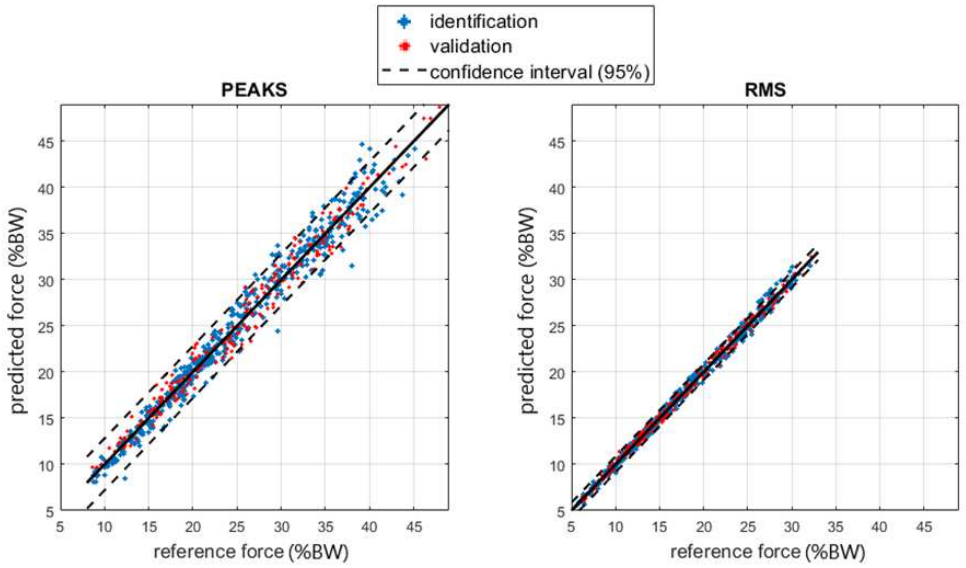

Figure 32: Regression of the shoulder joint force RMS and peaks. The force is shown as a percentage of the subject's BW.

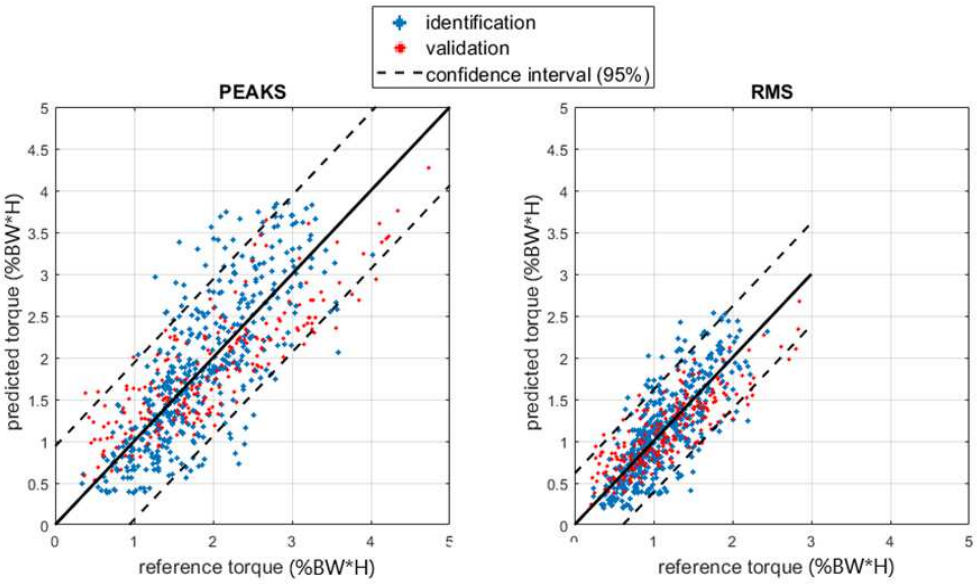

Figure 33: Regression of the shoulder joint torque. The torque is shown as a percentage of the BW times the height (H) of the subject.

Table 8: RMSE and R2 values of the shoulder joint force.

Shoulder Joint Force	RMSE (%BW)	R^2	Dataset
RMS	0.45	1.00	Identification
	0.42	1.00	Validation
Peak	1.5	0.97	Identification
	1.4	0.98	Validation

Table 9: RMSE and R2 values of the shoulder joint torque.

Shoulder Joint Torque	RMSE (%BW*H)	R^2	Dataset
RMS	0.34	0.61	Identification
	0.32	0.68	Validation
Peak	0.55	0.61	Identification
	0.52	0.69	Validation

The shoulder regression model involved the RMS and the peak values for crutch force and their interaction with the subject's height and squared height, as reported in Table 7. The regression was good regarding shoulder force (R2 about 1), while it was more critical for torques (R2 about 0.6). The residuals for the RMS and peak force regression models followed a normal distribution, as shown in the normal probability plots in Figure 34, so the random behaviour of the residuals was confirmed.

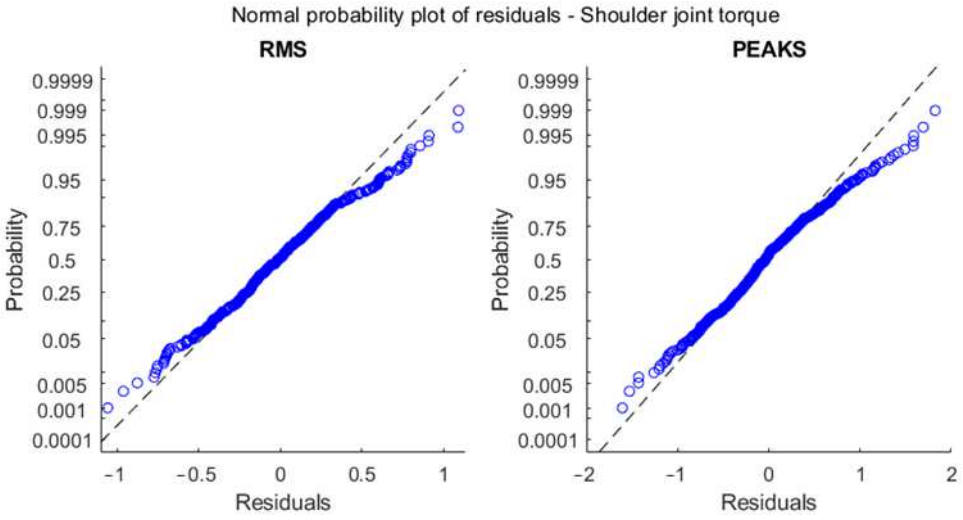

Figure 34: Normal probability plots of regression residuals of the identification subset for RMS and peak shoulder force.

Regarding torque, the R^2 was lower, and residuals were less normal. A possible justification relies on the equations describing the inverse dynamics: they are based on some anthropometric parameters determined with the help of statistical tables based on specific population samples. Precise evaluation of the effect of anthropometric parameters uncertainties on the inverse dynamics results uncertainty is complex due to non-linearities in the model equations, a large number of possible influence factors, and the recursive relation that moves the results from a distal to a proximal element. A previous investigation [97] applying the simplification principles described in [98] evidenced that anthropometric parameters may heavily affect the inverse kinetics analysis and, in our case, the reference shoulder torque and force. In the force case, equations included only segment masses and their centre of mass acceleration. Torque computation also requires the segment's inertial properties, which generally suffer from a larger uncertainty. Moreover, the correlation analysis excluded anthropometric parameters such as mass and height from the regression due to their poor correlation. The prediction error for torque as a function of the BMI anthropometric parameter can be checked with the box plots in Figure 35, in which no explicit dependency is shown, so the model validity was confirmed, and the reason for the lower torque prediction performance is not clear yet. Of course, a more complex regression model including a larger set of factors improves the correlation at the expense of introducing a large set of quantities in the description. Since our intention here was to give a rough but immediate and easily obtainable estimation to the patient and the clinician to improve gait management, we prioritized model simplicity. To this end, the regression proposed seems to be sufficiently accurate. Shoulder forces were estimated with an RMS error of about 1.5 %BW, while for torques, the RMS error was about 0.5% of the product BW times height on a scale ranging up to 4.0 %BW*H, i.e., about 12% of the full scale of the values recorded. Such values are sufficient for a rough indication to the end user and the therapist.

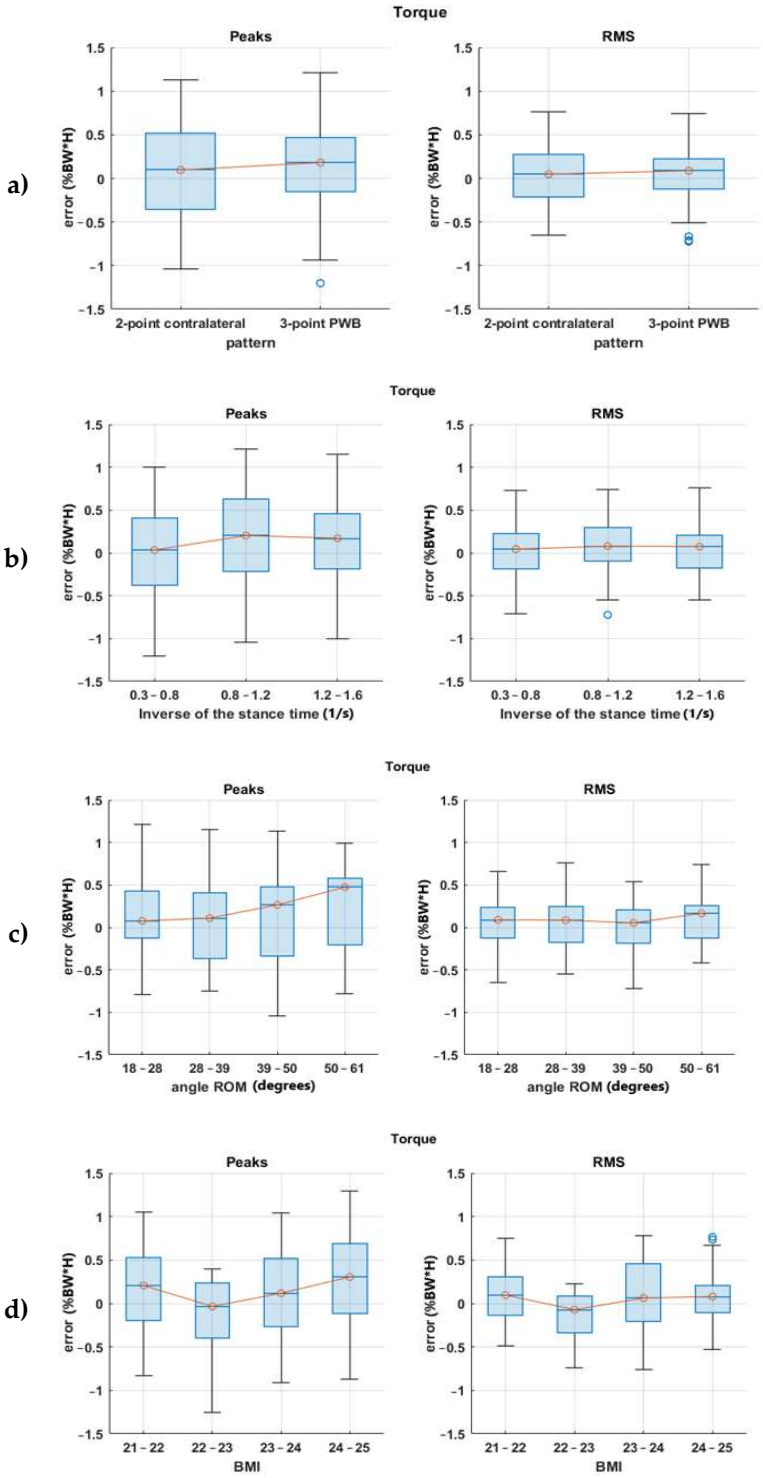

Figure 35: Shoulder torque RMSE boxplots for (a) walking pattern; (b) the inverse of stance time; (c) crutch angle range of motion; (d) BMI.

5.4.4 Conclusions

The presented approach estimated the PWB using instrumented crutches, and the results showed that the error was strongly influenced by walking cadence and leg support. Higher walking speeds and double-leg support result in higher errors in the PWB estimation. The real-time PWB values were more reliable with lower cadence and speed, which were typical values for assisted walking with crutches, and the RMSE was not influenced by crutch load. In the three-point PWB gait pattern, PWB estimation during the unaffected limb's single support was saturated at 100 %BW, but this is not useful for rehabilitation purposes. The study also developed a regression model for estimating shoulder force and torque during crutch-assisted gait. The model is based on RMS and peak values of crutch force and considers the subject's height and squared height. The regression model provided good estimates for shoulder force (R^2 about 1) but was less accurate for torque (R^2 about 0.6). The less normal distribution of the torque residuals was possibly due to uncertainties in the anthropometric parameters used in the inverse dynamic equations, and a more complex regression model would improve the correlation.

The inclusion of a larger sample size and a more balanced gender distribution could have provided more generalizable results. Nevertheless, this preliminary study provided promising results that demonstrate the validity and effectiveness of the load estimator system. Additionally, future studies should consider testing the system under different walking conditions, such as different ranges of speeds, inclines, and terrain types to further validate its accuracy and effectiveness. Furthermore, the estimator should also be checked with different impairments since the deviations in the gait could alter the predictions.

5.5 Tests on field

In collaboration with the Domus Hospital (Brescia, Italy) and ExoAtlet (Luxemburg) the walking loads applied on the crutches have been analysed in tests involving two exoskeletons.

5.5.1 ReWalk

In a case study, a woman suffering from an incomplete spinal cord injury (SCI), was monitored during 13 rehabilitation sessions (2 or 3 times per week) using the instrumented crutches. The patient walked assisted by the Rewalk powered exoskeleton (Argo Medical Technologies Ltd., Yokneam Ilit, 20692, Israel) shown in Figure 36. The robot step movement is initiated by an inclination of the subject torso in the sagittal plane, without any input from the therapist. The 2-point contralateral walking pattern [13] shown in Figure 37 was self-selected by the patient. Each rehabilitation session lasts about 1 hour.

Figure 36: The ReWalk exoskeleton.

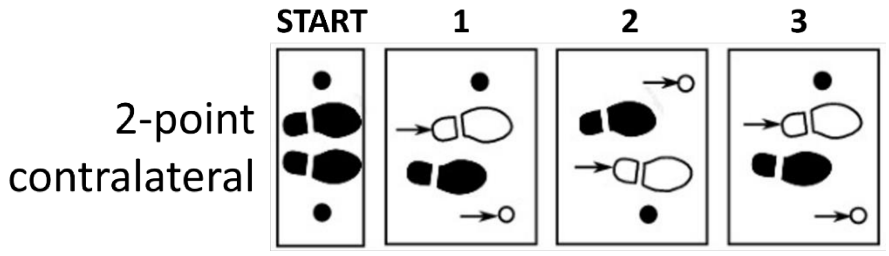

Figure 37. Thee 2-point walking pattern with crutches [13]**.**

The therapist is not aware of the forces applied either real-time or after the session but provides indications to the patient as in a common rehabilitation approach. The aim is to explore if during the rehabilitation the pilot changes the load on the crutches.

As shown in the example of Figure 38, the left and right peak forces and the peaks of the sum of both sides are identified. Forces are then normalized and reported as %BW. Figure 39 and Figure 40 show the boxplots and the standard deviations (respectively) of the crutch's forces peaks against the session number.

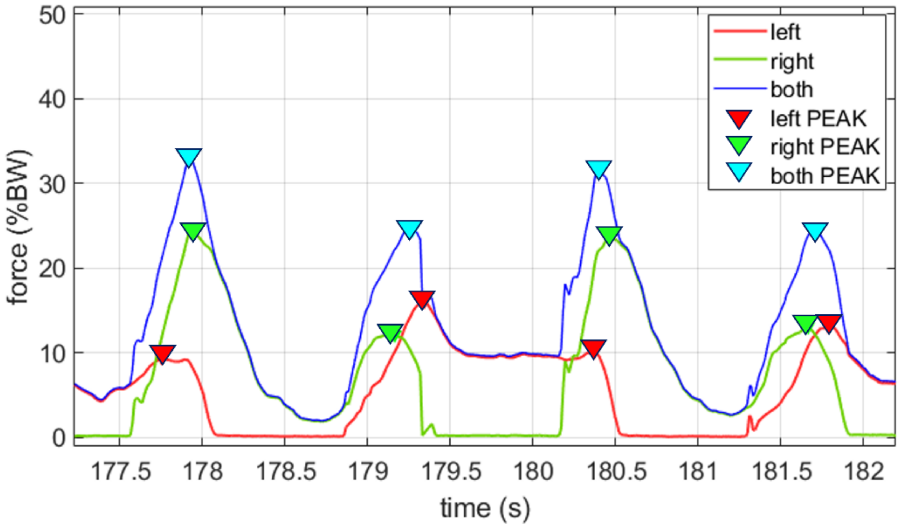

Figure 38: Example of a force peak identification during a 2-point contralateral walking. The blue line is the sum of the left and right forces (red and green lines respectively).

The peak forces exerted by the right crutch are significantly higher than those of the left side, and this tendency does not decrease during the sessions. Additionally, the standard deviation of the peak forces exerted by the left crutch is consistently lower than that of the right crutch. As demonstrated in the literature [84], [99], load asymmetries can be observed in conditions such as incomplete spinal injuries, where one side of the body may be weaker than the other. This asymmetry was not corrected during the sessions, possibly because the therapist failed to notice it or did not identify a suitable method to minimize the difference.

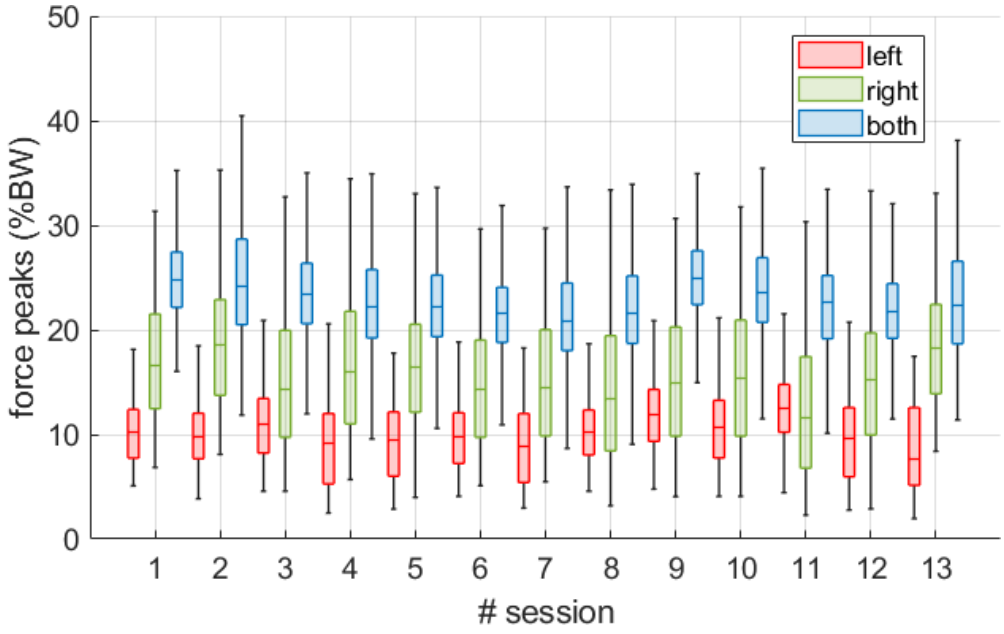

Figure 39: Boxplots of the crutch force peaks of the tests with the ReWalk.

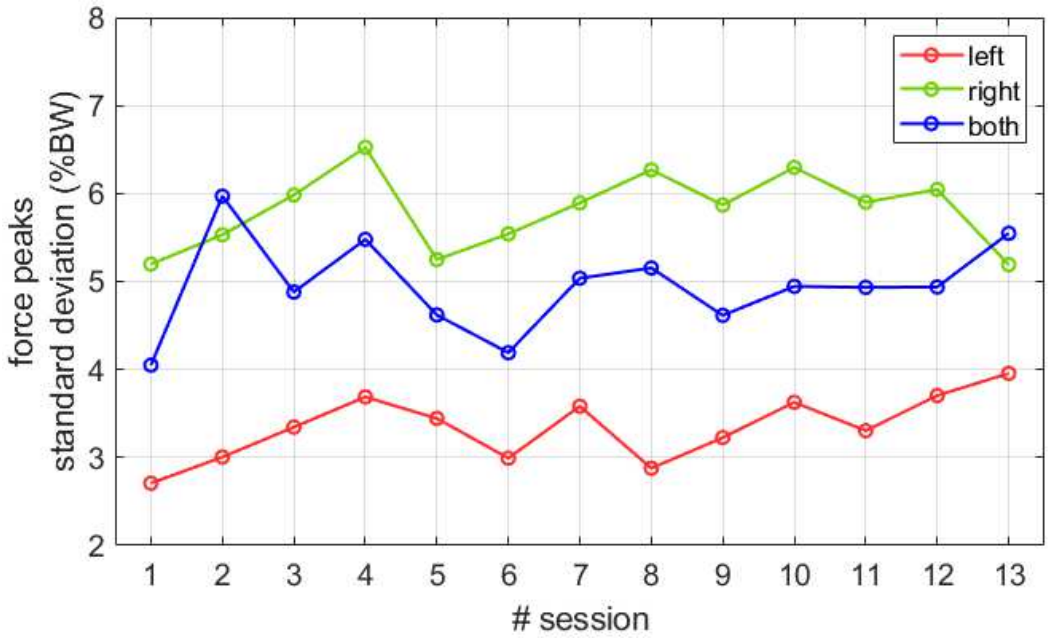

Figure 40: Standard deviation of the crutch force peaks of the tests with the ReWalk.

5.5.2 ExoAtlet

The ExoAtlet I, in Figure 41, is a powered exoskeleton for robotic-assisted walking rehabilitation in patients with locomotor disorders [100]. Since 2017, ExoAtlet has supported clinical research projects with pathologies such as spinal cord injury, cerebral palsy, stroke, multiple sclerosis, traumatic brain injury and arthropathy. As detailed for the Eurobench projects in [101], comparing exoskeletons for rehabilitation is a key stage to identify the best solution in specific situations. A preliminary study on 7 healthy subjects (height: 1.77 ± 0.04 m, body mass: 71 ± 6 kg, age: 28 ± 8 years old) has been conducted with ExoAtlet I exoskeleton aiming to compare the loads applied on crutches walking with different patterns. Since walking with exoskeletons often requires not only the use of crutches but also the support of the therapists who follow and guide the patient during the walk, the ExoAtlet has been tested with and without the therapist's help. The test conditions are then the parallel, ipsilateral, and contralateral walking patterns supported by the therapist, and the contralateral walking pattern without the therapist's support. The walking patterns are shown in Figure 42 and each pattern has been repeated at least 3 times in a 10-meters walking test.

a) **b)**

Figure 41: a) The ExoAtlet I exoskeleton; b) Test walking with ExoAtlet and instrumented crutches.

A pair of instrumented crutches introduced in the section “5.2 Instrumented Crutches – A New Version” has been used to acquire the forces applied to them. As shown in the example of Figure 43, the peaks of the left and right forces and the peaks of the sum of both sides have been identified on each crutch stance phase. Forces are normalized and reported as %BW.

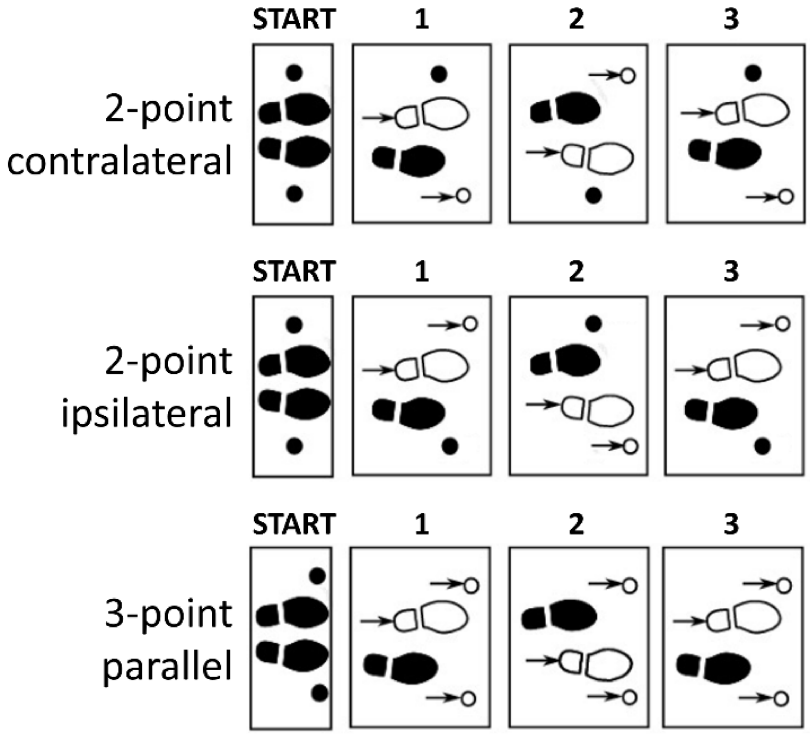

Figure 42: Walking patterns used to test the ExoAtlet exoskeleton [13]**.**

Figure 44 shows the boxplots of the crutch’s forces peaks against the walking pattern. The paired t-test (P value < 0.05) for the condition without the therapist’s support is only performed by comparing it with the tests with the therapist’s help during the contralateral pattern. The inter-pattern t-tests are only conducted between the same crutch side. The intra-pattern t-tests are only conducted between the left and right sides. The force exerted on the crutches without the therapist's support is significantly higher than in the case with their support, demonstrating that the therapist's contribution alleviates the loads applied to the upper joints [31]. Of course, the therapist’s presence limits the exoskeleton pilot's autonomy. When the therapist is present, the pattern that induces higher loads on the crutches is the parallel gait, as opposed to the ipsilateral and contralateral gait.

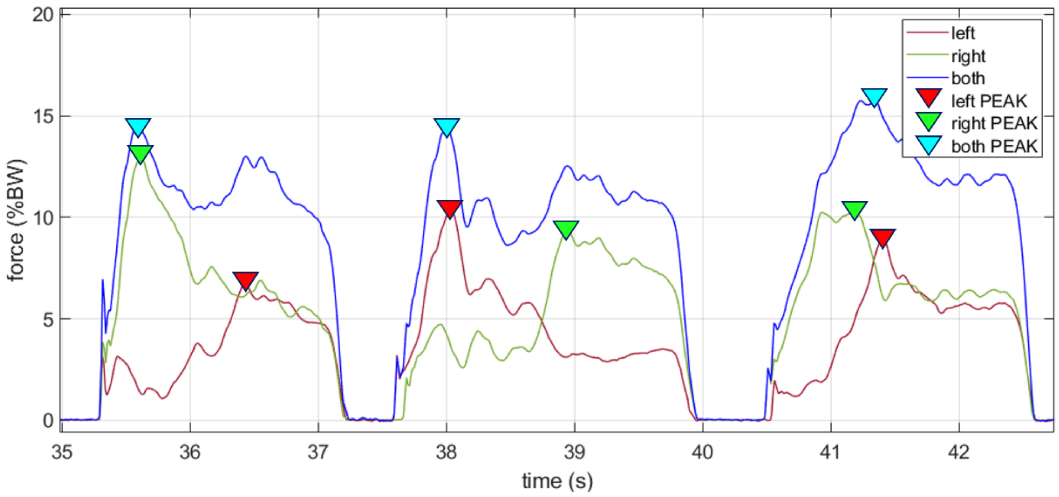

Figure 43: Example of a force peak identification during a 3-point parallel walking. The blue line is the sum of the left and right forces (red and green lines respectively).

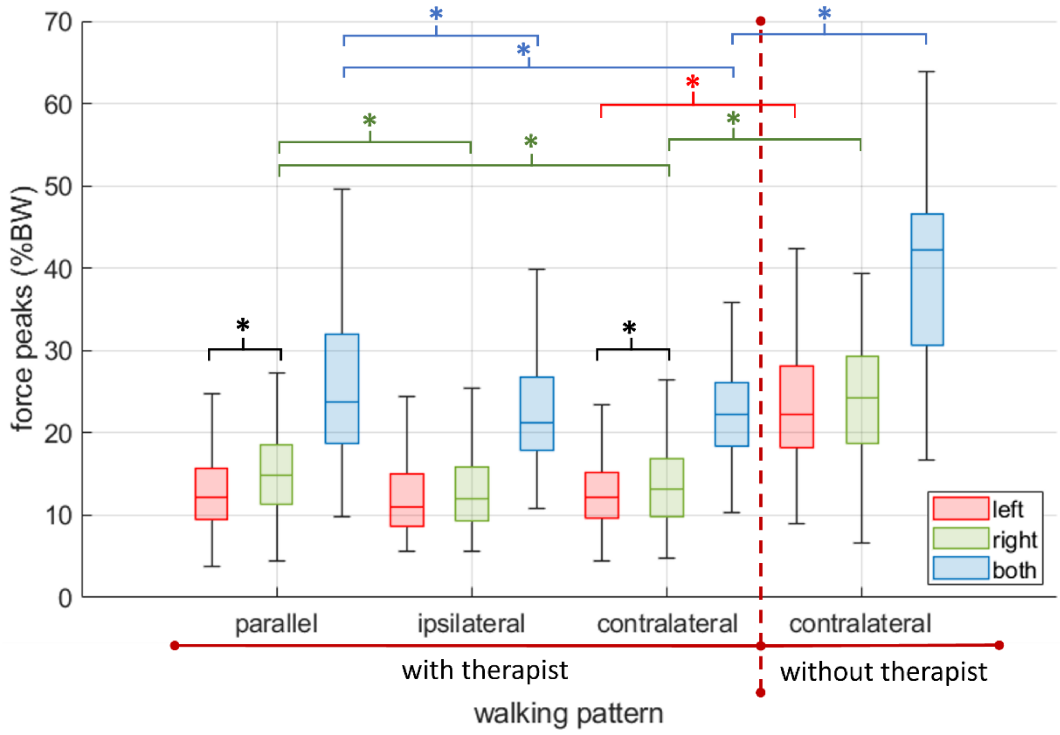

Figure 44: The crutches force peaks walking with the ExoAtlet exoskeleton. *two-sided p-value < 0.05 with the unequal variances t-test.

5.6 Instrumented Walker

In collaboration with the exoskeleton manufacturer MEBSTER (https://mebster.com/en/), an instrumented walker has been developed to measure load and torques applied during assisted walking.

Figure 45: Unilexa passive exoskeleton and the walker.

The enterprise aims to monitor and evaluate the support given by the walker during the walk with the Unilexa exoskeleton, shown in Figure 45. Unilexa is a passive exoskeleton, and it can require higher support from the upper arms if compared to powered exoskeletons.

2.6.1 Force measurement

The vertical load and the torques are measured using four Wheatstone bridges in full-bridge configuration for bending, displaced as in Figure 46. The acquisition board of the instrumented crutch, as described in section “5.2 Instrumented Crutches – A New Version”, is used to acquire the voltage from the full-bridge. Two boards equipped with two loadcell amplifiers (HX711) collect voltages and send them to a PC through a ROS network. Acquired voltages are then combined

to estimate the force applied on the y-axis, according to the reference system of Figure 46, and the torques along the x and z axes.

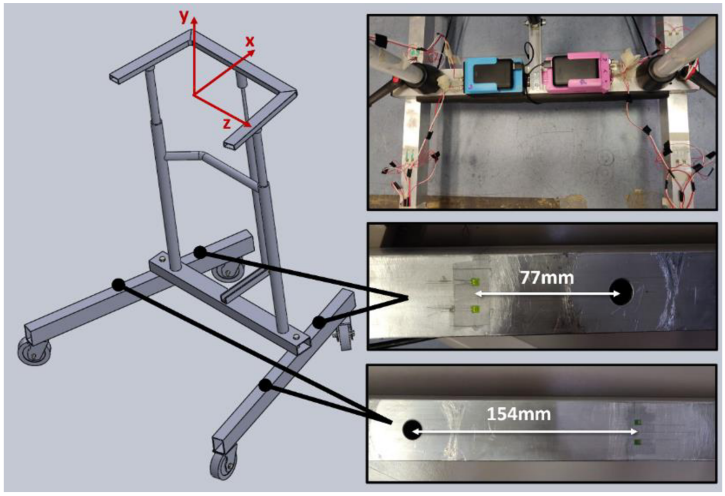

Figure 46: Strain gauges displacement on the walker.

The loads measurements are calibrated using known masses fixed on the walker at different positions. With the aid of four bars fixed on the walker's top frame, the masses are applied on the walker as in Figure 47, and they range from 0.75 kg to 30.00 kg.

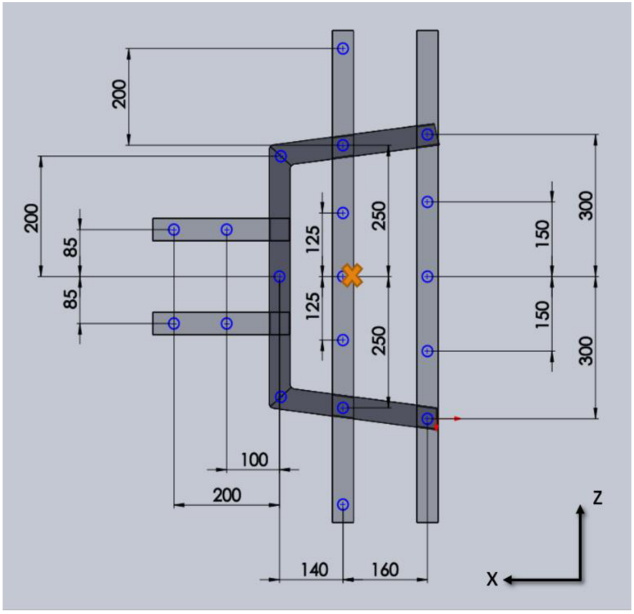

Figure 47: Top view of the known masses' displacement for the calibration.

The walker height is kept at 1 meter from the floor, and 25 masses are used to sweep across the range on each of the 19 positions of Figure 47. A total of 475 combinations are collected in random order. A multivariate multiple linear regression is applied, and the results are summarized in Table 10. Figure 48 shows the linear regressions and the residuals with respect to the reference.

Table 10: Multivariate multiple linear regression results.

	F_y	T_x	T_z
Range	0:300 N	-50:100 Nm	-150:150 Nm
R^2	0.99	0.99	0.99
RMSE	8.2 N	3.0 Nm	3.3 Nm

The coefficient of determination (R^2) for all three output parameters is 0.99, indicating a strong correlation between the input strains and the output forces and torques. The root mean square error (RMSE) for F_y is 8.2 N, indicating the average deviation between the predicted and actual values of F_y is approximately 8.2 N. Similarly, RMSE values show an average deviation between the predicted and actual values of 3.0 Nm for T_x and 3.3 Nm for T_z. These results demonstrate a high level of accuracy in the regression model, as evidenced by the high R^2 values and relatively low RMSE values for all three output parameters.

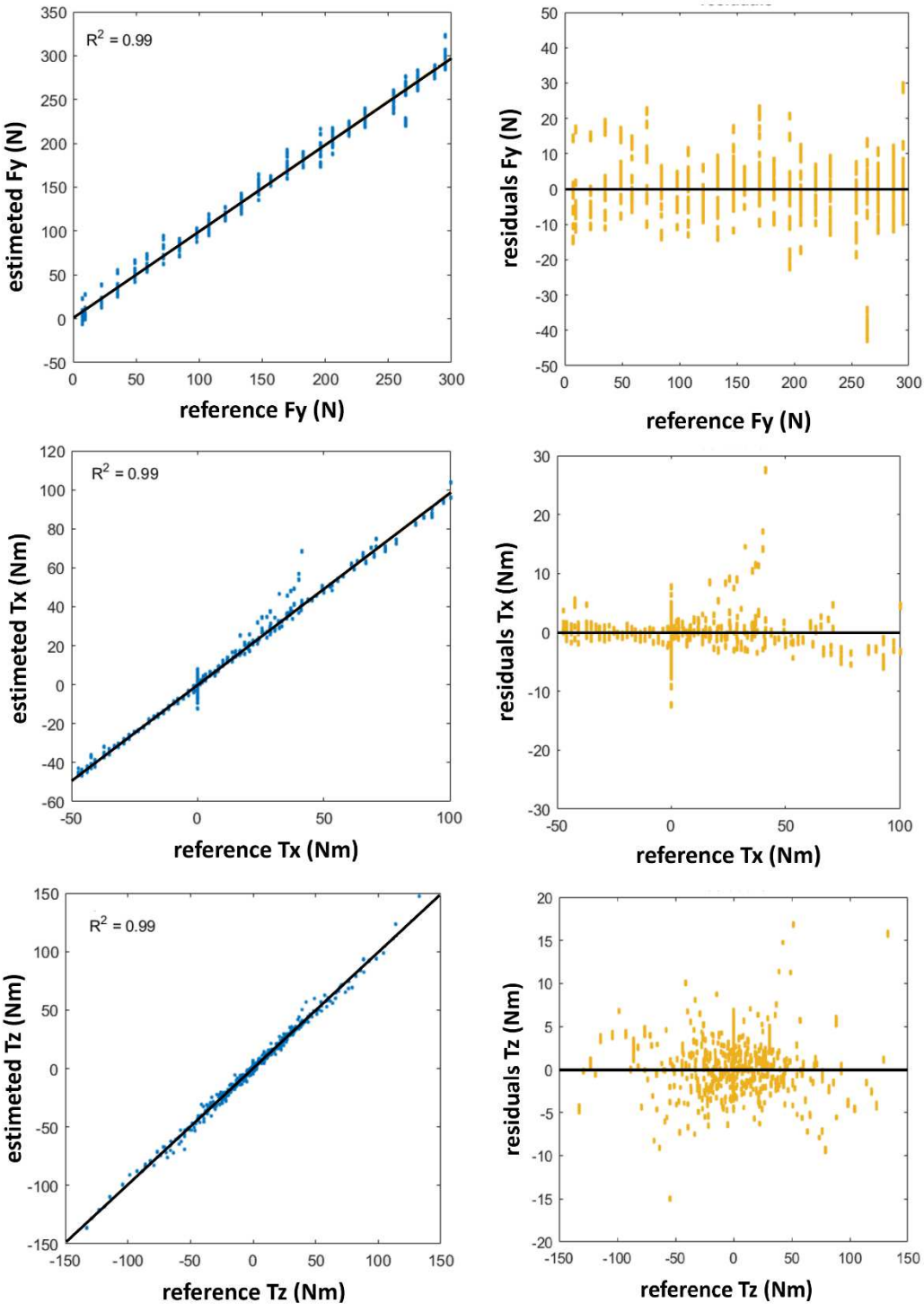

Figure 48: Multivariate multiple linear regression.

Augmented Reality Feedback

Therapists play a vital role in guiding and monitoring the rehabilitation process, ensuring optimal outcomes for patients. In recent years, the emergence of AR technologies has opened up new possibilities for enhancing the effectiveness and engagement of rehabilitation interventions. This chapter presents the development and evaluation of an AR interface designed to support therapists in monitoring walking rehabilitation using instrumented crutches. By overlaying digital information in the real world, AR can provide therapists with real-time feedback, visualizations, and guidance during rehabilitation sessions. Instrumented crutches offer a valuable tool for objective assessment and monitoring of gait performance. However, the effective integration of force measurement data with an AR interface tailored to the needs of therapists and patients remains an open challenge. The design process employed a participatory design approach, ensuring that the development of the AR interface incorporates the perspectives and insights of the end-users – therapists and patients. Through collaborative design sessions and iterative feedback loops, the interface design was shaped to align with their requirements and preferences. This involved interviews, observations, discussions, and prototyping to identify the specific requirements for an AR interface. This approach aimed to enhance usability, user acceptance, and overall effectiveness of the AR system in supporting the rehabilitation process. A comprehensive test campaign was conducted involving both therapists and patients aimed to gauge the interface's impact on therapists' ability to monitor and guide rehabilitation sessions effectively. Objective measures, such as usability, workload, and attention metrics,

were collected along with interviews. The results provide valuable insights for future development and implementation in clinical settings.

6.1 Participatory codesign

Participatory co-design is an approach that involves end-users, stakeholders, and experts in the design and development process of a product or application [102] which fosters collaboration, empathy, and shared decision-making. It ensures that the final application reflects the collective expertise and insights. By involving therapists in the design process, the application is more likely to meet the specific needs of therapy sessions, enhance the therapeutic experience, and ultimately improve patient outcomes. The participatory co-design process starts with an initial exploration phase, where therapists and designers collaborate to understand the requirements, objectives, and challenges of using AR in crutch-assisted gait therapy. During this phase, therapists provide insights into the specific needs of their patients, the therapeutic techniques they usually employ, and the potential benefits and limitations of incorporating AR technology.

The first meeting was held online with a total of 12 experts, including some representatives of the Department of Rehabilitation of the Rīga Stradiņš University and the Latvian National Rehabilitation Centre “Vaivari” (NRC Vaivari). Firstly, the therapists explained the conventional method to a patient who needs to learn the correct technique for walking with crutches. During this process, therapists closely observe and assess several key parameters to guide and correct the patient's walking technique [103]. These parameters include:

1. Crutch positioning and support: Therapists pay close attention to how the patient holds and positions the crutches. They check the height of the crutches, the handgrip placement, and the patient's arm and hand positioning. Adjustments are made to ensure proper support and stability during walking.

2. Weight-bearing: Therapists assess how much weight the patient is placing on their affected or injured limb while using crutches. They provide guidance to ensure proper weight distribution, which helps prevent further injury and promotes stability.

3. Posture and alignment: Therapists observe the patient's overall posture and alignment while using crutches. They check if the patient's body is properly aligned, with the head, shoulders, hips, and feet in a straight line. Corrections are made to maintain a balanced posture, reducing strain on the body.

4. Step length and rhythm: Therapists monitor the patient's step length and rhythm to ensure a smooth and coordinated walking pattern. They guide the patient to take steps of appropriate length, promoting a natural gait.

Secondly, we explained the principles of the instrumented crutches previously described in the section “5.2 Instrumented Crutches – A New Version” with their advantages and limitations. We also showed the available AR glasses, the Microsoft HoloLens 2 in Figure 49, with their main characteristics and technological advantages that could be useful for the design.

Figure 49: The Microsoft HoloLens 2 glasses for AR.

The HoloLens 2 provides a wide field of view allowing users to see and interact with holographic contents; an accurate tracking technology enabling the glasses to maintain stable holographic overlays aligned with the real-world environment; hand and gesture tracking capabilities enabling intuitive interaction with holographic elements, such as grabbing and manipulating virtual objects. Everything with a lightweight design with a balanced centre of gravity, adjustable headband, and flip-up visor, making it more comfortable for extended use and easy transition between augmented and real-world views. Moreover, data can be shared in real-time between the AR glasses and the instrumented crutches.

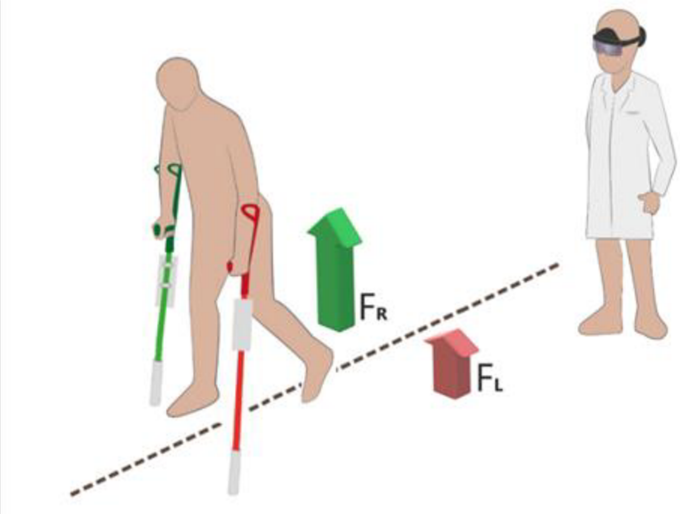

Figure 50: A draft of the AR interface. The forces are represented as arrows with a label of the measured value.

The last part of the meeting focused on a brainstorming session to explore all the ideas from both sides. The main request from the therapists was to not only consider the crutches' forces but also the load applied on the legs. The holographic representation identified was the three-dimensional arrows with a label of the measured value, as sketchy in Figure 50. The arrow increases its vertical size according to the force magnitude. Moreover, some of them asked if the holographic projections could follow the patient's movements during the walk. Since the gait phase detection is still not provided in real-time but it requires minutes to obtain predictions, it has been decided to exclude this parameter at this stage of development and keep it in consideration in future developments.

The next step is the prototyping phase, where therapists' and designers' ideas for the application become low-fidelity demos. Prototyping is a crucial stage in participatory co-design, and it involves creating early versions of the application to gather feedback from users.

To satisfy the therapist's request to receive feedback about the legs' load (PWB) some solutions have been evaluated and explored. Devices like force platforms are the most accurate technology to measure ground reaction forces, but they require space, and specialized personnel and their cost is often not negligible. Instrumented insoles have a more affordable cost, but they usually require calibration and time to correctly adjust them in shoes. The solution identified was

the PWB estimator [75] detailed in the section “5.4 Partial weight-bearing and shoulder loads estimator”, which only requires the already necessary instrumented crutches, and a domestic scale to measure the patient’s body mass. The PWB measurements are less accurate than the outcomes from force plates or instrumented insoles, but the simplicity of use and the reduced assessment time it was prioritized.

Placing the holograms near the patient can potentially reduce the mental workload required by the therapist. This is particularly relevant when considering the existence of multitasking overload, as suggested in existing literature [104]. While there is currently no research specifically investigating the therapist's workload during observational gait assessment, it can be argued that such assessments involve the utilization of multiple cognitive resources, including visual, auditory, cognitive, and responsive processes. The visual process comprises both searching for and observing the patient. When the AR feedback holograms are located far from the patient, the therapist needs to consistently engage in the searching task to locate the patient's position. By placing the holograms close to the patient, the need for frequent searching is reduced, while still maintaining the essential observation phase. This adjustment has the potential to alleviate cognitive demands.

a) **b)**

Figure 51: a) Human body tracking; b) QR code to track.

In trying to place the holograms close to the patient, several approaches were examined to track the patient’s pose. Accessing the frontal webcam of the HoloLens 2 it is possible to run a human body skeletonization on the RGB images [105], as

in Figure 51a, but it lags and requires a lot of processing power critically limiting the battery life. Another approach is to track a QR code marker placed on the back of the patient as in Figure 51b, but the tracking performance gets worse if the patient-therapist distance increases (>3 m).

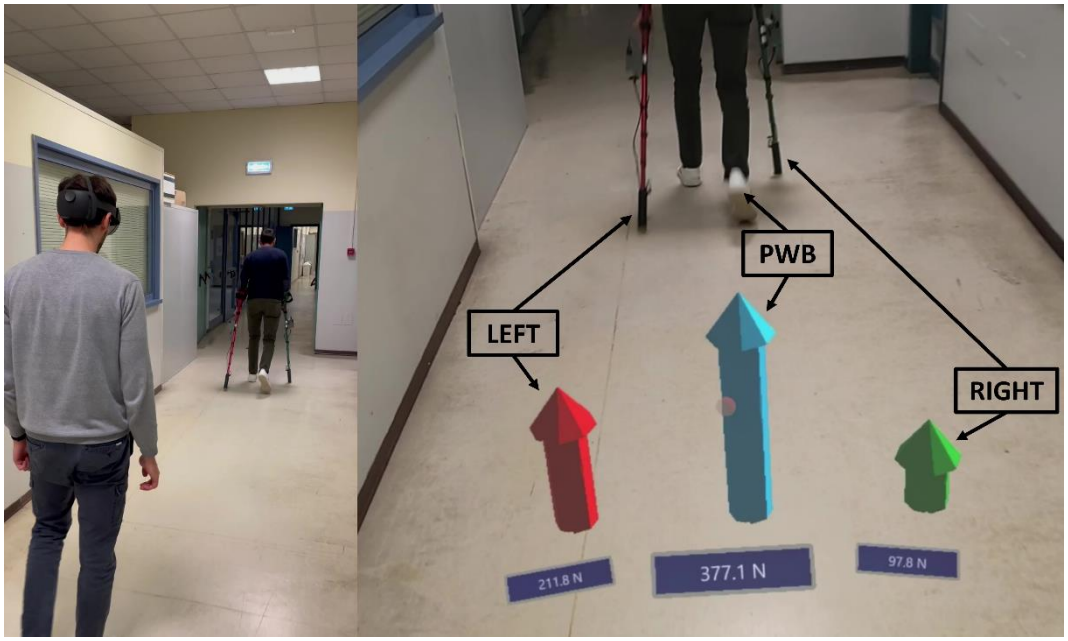

Figure 52: User interface demo with loads represented as arrows.

The first demo developed is shown in Figure 52 and it includes the arrow representation of the load associated with its value in Newton in the lower label. The arrows are placed on the floor surface, and they only follow the therapist's position since a reliable solution for patient tracking has not been found yet. Another meeting was held in person at the NRC Vaivari (Riga) since it was critically important that therapists familiarize themselves with the AR glasses and try the demo. Twelve therapists, specialized in gait rehabilitation, were involved and everyone tested the application and provided their opinion. Comments are summarized in Table 11 divided into topics.

Table 11: Comments of the therapists after the first demonstration.

	(Topic 1) Quantity to be displayed
1.	Unit of measure of the loads as "%BW" and not "N".
2.	Unit of measure of the loads as "kg" and not "N".
3.	PWB estimation for each foot separately.
4.	Show the last maximum of the load.
	(Topic 2) Labels aspect
1.	Too many digits.
2.	The font size should be bigger.
	(Topic 3) Placement of holograms in the space
1.	Holograms should move with the therapist's head.
2.	Holograms should follow the patient and be aligned with the crutches.
3.	Holograms along the crutches.
4.	Holograms are placed according to the patient's side.
	(Topic 4) Others
1.	Difficult to directly compare left and right crutch loads based on their arrow height.
2.	The patient should use the application to understand how much "%BW" is applied.
3.	Not only with crutches but also quadripodes and walkers.
4.	Sounds to improve gait rhythm.

For therapists, it's hard to figure out the forces if expressed in N while they are more used to working with the %BW or the kilograms. To make the comparison between loads easier, the arrows are substituted with the graphical representation in Figure 53. The load bar scale is normalized on the patient BW. The current load is displayed by the bar high and the lower label in kilograms, while the last peak reached is displayed by the upper label in %BW and the associated notch. The current load labels have a resolution limit of 5 kg to improve readability during quick fluctuations, and the most recent peak label is restricted to the unit place. The bars on the side show the load applied on the crutches (red for the left crutch and green for the right crutch). The middle bar in blue is the estimated load applied on the legs.

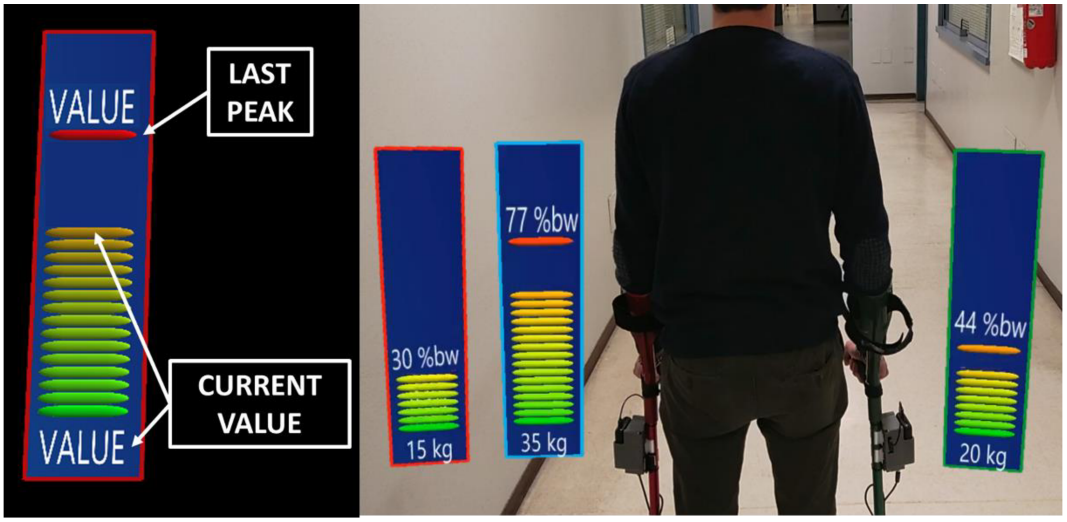

Figure 53: Final interface with bar representation of the load.

Based on the previous consideration, two working modalities were developed:

- **In-place mode**: Feedback holograms are placed on the patient's side, and they are about 30-40 cm over the floor as in Figure 54a.
- **Display mode:** holograms are projected in a virtual monitor which follows the therapist's head movements. The data are displayed on the side in the virtual display to keep the central view free from any holograms.

a)

b)

Figure 54: a) In-place mode; b) Display mode.

To solve the patient tracking, another HoloLens 2 is worn by the patient and used as a tracking device to get his/her pose in real-time. The absolute position of the patient in the therapist's reference is assessed by sharing the patient pose with respect to a QR code, tracked as in Figure 54. The patient pose is then used to place the holograms in the in-place modality, but it is also used in both modalities to

visualize the crutches' load bars according to the patient side with respect to the therapist's view, as in Figure 55.

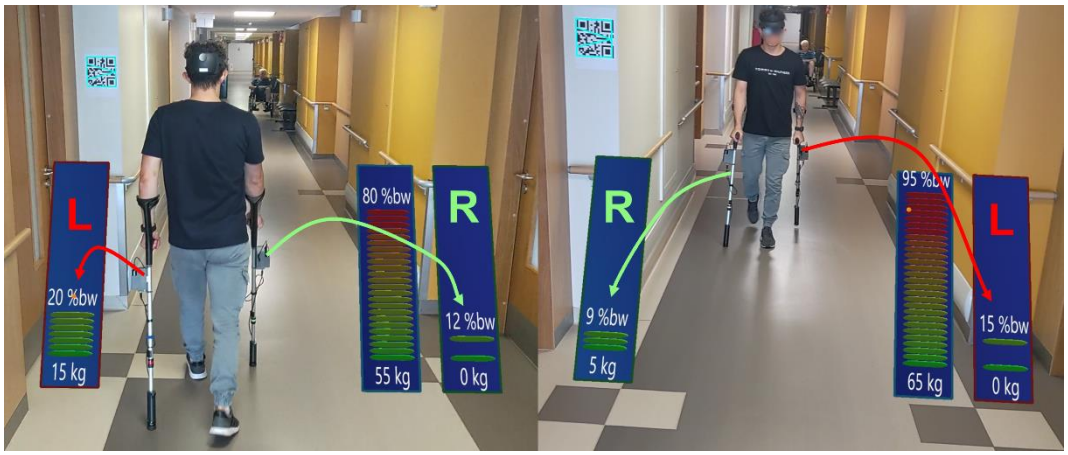

Figure 55: Loads' bars position according to the patient's orientation from the therapist's point of view.

A selection menu appears if the user looks at his/her left-hand palm as in Figure 56. The user can choose the working modality between the display mode or the in-place mode.

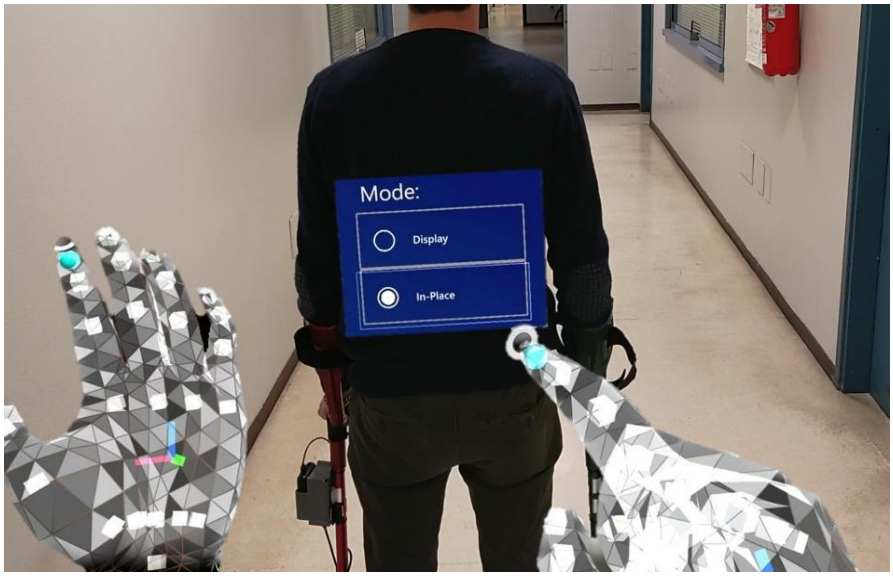

Figure 56: Working mode selection menu.

6.2 Application framework

The AR application has been developed with Unity (editor version 2020.3.28f1) and OpenXR, an API that aims to solve development fragmentation between platforms, as schematized in Figure 57. The Microsoft HoloLens 2 are integrated into the same ROS network of the instrumented crutches implementing a ROS-TCP-Connector [106]. Through ROS is possible to access the loads measured by the instrumented crutches and the patient's weight, which is necessary to properly scale the load bars. A second HoloLens 2 is worn by the patient to track his/her pose. Both the therapist and patient's glasses track a common QR code and the relative position of the patient with respect to the therapist can be computed. The accuracy of the HoloLens 2 self-tracking is about 2 cm [107] and it is considered acceptable for this application. The Mixed Reality Toolkit 2 is used for the user interface's components (backgrounds, fonts, radio buttons, etc.) and the gaze tracking. The gaze tracking uncertainty is about 9 cm (P=99%) in walking conditions with the target at a 4 m distance [108]. Holograms are placed at a larger distance from each other to ensure correct identification of the observed target.

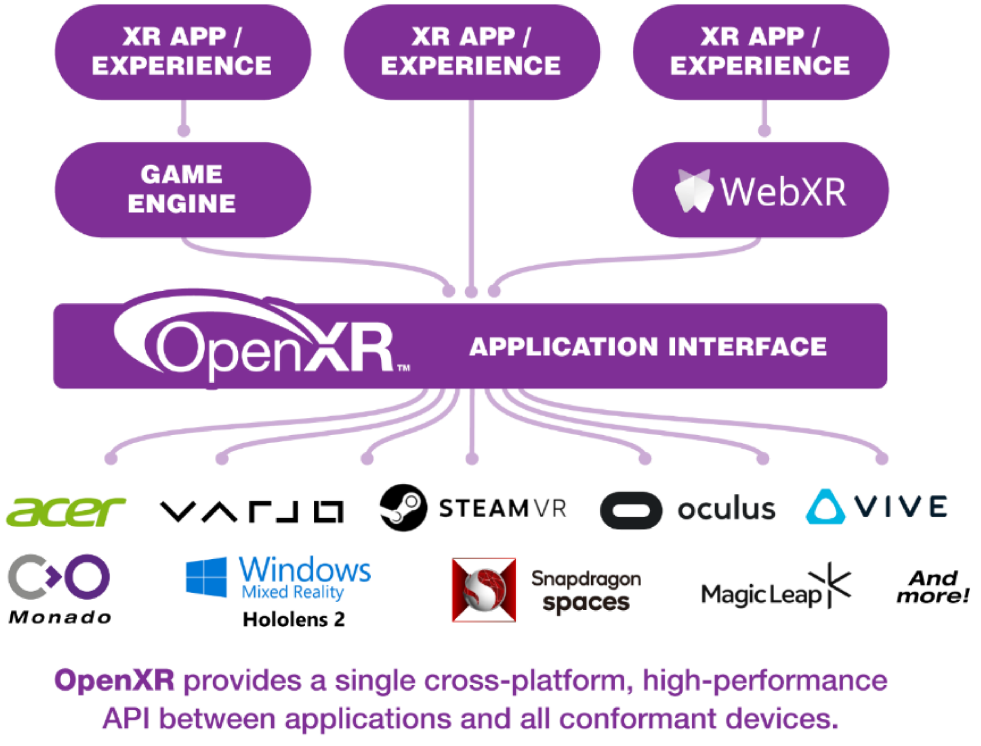

Figure 57: The OpenXR API.

6.3 Usability and attention tests

The preliminary results obtained using AR in rehabilitation show improvements in many parameters even better than the results with traditional therapies [41], [53], [109], [110], [111]. AR has important relevance in promoting interactions between patients and therapies, and bringing benefits to the effect of rehabilitation, but should be verified the engagement of the users to avoid cognitive overloads or distractions from the main task. Even the usability of the AR solutions should be investigated to continuously improve the technologies and simplify their use, leading to a wider spread of innovative rehabilitation techniques. Another key evaluation when AR or VR are involved is on symptoms of visually induced motion sickness (VIMS) [112]. Although VIMS symptoms are less inclined to compare with AR glasses, it should be investigated during development to reduce the influence of sickness on the usability results [113], [114].

To face all the previous arguments a specific test protocol has been defined for their assessment in the AR application developed during the co-design phase.

6.3.1 Test protocol

To ensure the reliability and generalizability of the evaluation results, the attention testing and usability assessments are conducted in real-life conditions. Therapists and patients perform the tasks and exercises of actual rehabilitation scenarios, closely resembling the challenges faced during routine therapy sessions. This realistic setup allows for a comprehensive understanding of the application's performance and suitability for clinical use. Table 12 lists the inclusion and exclusion criteria for both therapists and patients participating in the study.

Table 12: Therapists and patients' inclusion and exclusion criteria.

Subject	Inclusion criteria	Exclusion criteria
• Both	• Age: between 18-85 years old. • Gender: any. • Must be able to follow instructions and demonstrate learning skills.	• Skin problems (for example, sores) that prevent the use of tools. • Cognitive or behavioural impairment affecting understanding or execution of the experiment. • Severe disorders of the visionary system. • Severe disorders of the auditory system. • Non-willingness to provide informed consent.
• Therapist		• Suffering from pre-existing medical conditions that may be exacerbated using the AR headset.
• Patient	• Height: 1.40-2.00 m	• Any medical problem that prevents the full load or intolerance to exercise with the forearm crutches (e.g., orthopaedic disorders, pain, spasticity...). • Ability to walk correctly and independently without external support. • Persistent orthostatic hypotension.

Based on the test condition, the HoloLens 2 glasses perform the following tasks:

1. **Holograms projection**: virtual objects are displayed through the glasses lens to be visible to the user. Holograms representing bars are used to visualize the load information to the user as in Figure 53. A selection menu, as in Figure 56, appears if the user looks at his/her left-hand palm and the therapist can choose the working modality between the display mode or the in-place mode.
2. **QR-tracking**: the webcam is enabled and QR markers are tracked. Only the marker with a specific code is processed and shared in a ROS topic.
3. **Pose-tracking**: the glasses share their pose through a ROS topic.
4. **Eye-tracking**: the user gaze is recorded, and the objects hit by the gaze are saved in log files.
5. **Audio recording:** the audio is recorded by the device's microphone.
6. **Video recording**: the webcam stream is saved, and holograms are displayed in the record if visible and stay in the user's field of view.

During the test, the AR glasses mix the tasks described previously. QR-tracking, audio, and video recording are always enabled in every condition. The patient's glasses do not display anything, but only the pose-tracking is enabled. The gaze tracking is always enabled for the therapist's glasses and an orange dot is captured in the video recording to know how the therapist distributes his/her attention. The instrumented crutches are always enabled and share forces through the ROS network. The coordinator's computer records the force data during the test.

The working modalities available for the therapist are:

- **transparent mode:** nothing is displayed to the user.
- **in-place mode:** feedback holograms are placed on the patient's side, as in Figure 54a.
- **display mode:** holograms are projected in a virtual monitor which follows the therapist's head movements, as in Figure 54b.

The following questionnaires are included in the test protocol, along with their respective meanings:

- **The Visual Activities Questionnaire (VAQ):** for assessing visual characteristics in colour discrimination, glare disability, light/dark adaption, acuity/spatial vision, depth perception, peripherical vision, visual search, and visual processing speed [115]. Visual skills can be strongly related to the experience with AR glasses.

- **Simulator Sickness Questionnaire (SSQ):** for checking if motion sickness is present and influences results. Recent findings suggest that the symptoms of cybersickness and motion sickness are not different [116], [117]. In the therapist's demographic questionnaire, we collect information regarding previous AR experience since previous exposure to provocative environments influences susceptibility to motion sickness. Over repeated, intermittent, short exposures to such environments, habituation may occur in which symptomatology decreases. Individuals who repeatedly experience these environments may build a tolerance to sickness-inducing stimuli and thus learn adaptive behaviours that minimize adverse effects [118].

- **NASA Task Load Index (NASA-TLX):** for assessing the workload required while receiving feedback with AR during gait rehabilitation [119]. If high-demanding tasks are present, they should be better managed to reduce the stress and fatigue of the operator [120].

- **Post-Study System Usability Questionnaire (PSSUQ):** it consists of 16 items that measure the user's satisfaction, ease of use, and perceived usefulness of the system. The PSSUQ provides valuable insights into the overall user experience and helps identify areas for improvement in the system's usability [117].

The test is conducted for each patient-therapist pair according to the following schedule:

1. Participants sign the informed consent.
2. The therapist compiles a demographic questionnaire.
3. The therapist compiles the VAQ.
4. The therapist compiles the SSQ.
5. Training session with AR glasses. The HoloLens 2 are calibrated on the therapist. The therapist learns how to manage the HoloLens 2 and the feedback received by the instrumented crutches in both display modalities.
6. The patient compiles a demographic questionnaire.
7. Both therapist and patient wear the HoloLens 2. The therapist uses the transparent mode, instead, the patient uses the pose-sharing mode. Subjects

do not receive any feedback and perform a traditional rehabilitation session with normal interaction strategies.

8. Both therapist and patient wear the HoloLens 2. The patient uses the pose-sharing mode. The therapist must use the first AR feedback modality.
9. Both subjects rest.
10. Both therapist and patient wear the HoloLens 2. The patient uses the pose-sharing mode. The therapist must use the second AR feedback modality.
11. The therapist compiles the SSQ.
12. The therapist compiles the NASA-TLX questionnaire.
13. The therapist compiles the PSSUQ questionnaire.
14. The therapist and patient provide feedback (if any) on what they liked or disliked. They can suggest what and how the AR feedback can be improved.

During the rehabilitation session, with or without AR feedback, the patient walks back and forth along a straight corridor for a minimum distance of 10 meters, and it is repeated at least 4 times. The order of the feedback modality is randomized (first display then in-place mode, or vice versa), otherwise learning effects from the first session with AR could influence the therapist's behaviour in the second session.

A total of 12 therapist-patient couples were tested according to the protocol, and their demographic information was recorded and presented in Table 13.

Table 13: Demographics of the subjects (MEAN ± SD).

24 subjects	**Gender**	**Age**	**Height**	**Body mass**	**Pathology**
Patients	2 females 10 males	52 ± 18 years old	1.71 ± 0.06 m	85 ± 13 kg	5 amputees 7 orthopaedics
Therapists	3 females 9 males	27 ± 3 years old	1.78 ± 0.07 m		

6.3.2 Results

Figure 58 shows the VAQ scores collected from the therapist during the initial assessment. Every visual function has a low score indicating generally good vision skills.

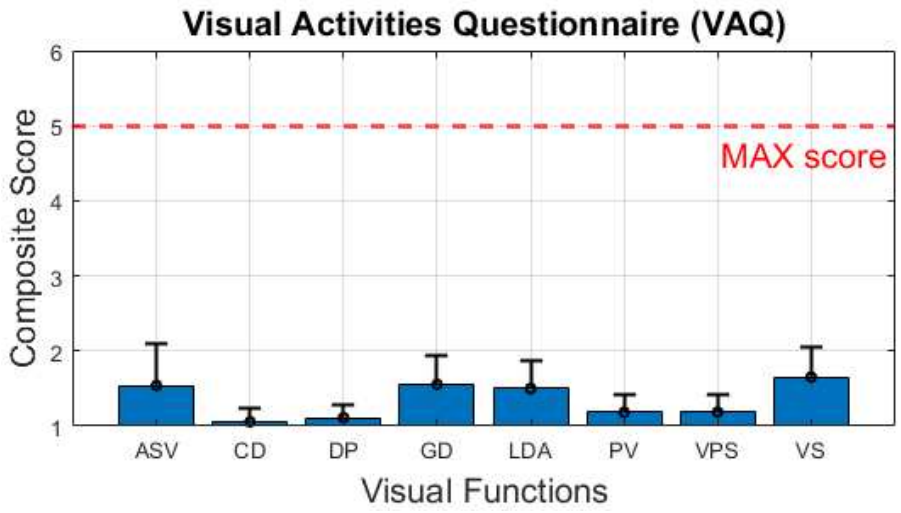

Figure 58: VAQ scores. Visual functions: Acuity/Spatial Vision (ASV); Color Discrimination (CD); Depth Perception (DP); Glare Disability (GD); Light/Dark Adaptation (LDA); Peripheral Vision (PV); Visual Processing Speed (VPS); Visual Search (VS).

Figure 59 shows the scores of the SSQ collected before and after the test. Results of non-parametric Wilcoxon tests with Bonferroni correction revealed no significant differences for all the scales. The post-SSQ's median value for the nausea was $M = 5$ ($SD = 10$), for the oculomotor disturbance $M = 8$ ($SD = 16$), for the disorientation $M = 0$ ($SD = 21$), and for the total score $M = 6$ ($SD = 16$). All the symptoms can be classified as minor according to Stanney et al.'s [121] classification. In general, the VIMS symptoms are negligible, but just one therapist has reported medium-severe oculomotor disturbance (score from 0 to 53) and disorientation (score from 0 to 69) while nausea slightly increases (score from 0 to 19). As in [114] and shown in Figure 60, a detailed look at the differences regarding individual symptoms shows the greatest pre- and post-exposure differences for eyestrain, fullness of head, and blurred vision.

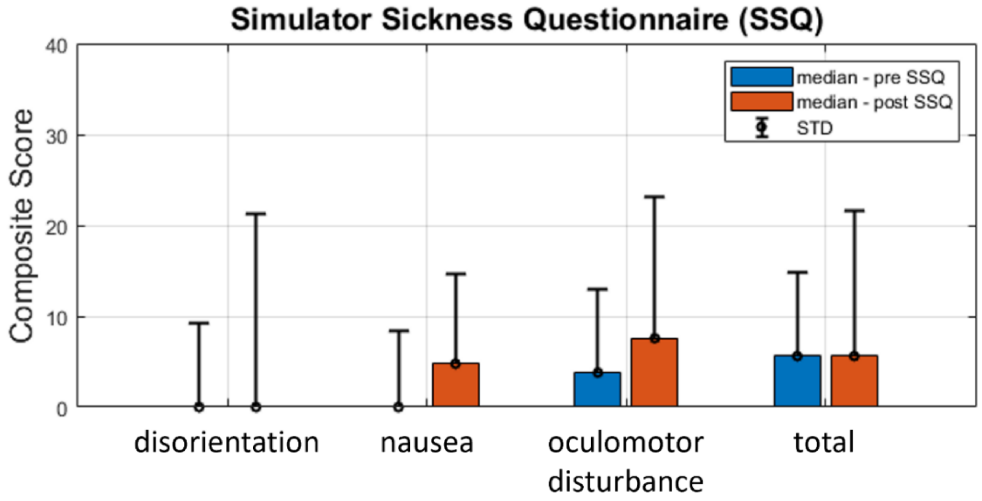

Figure 59: Pre-SSQ (orange) and post-SSQ (blue) scores comparison.

All therapists reported having minimal experience with AR, as they do not regularly use AR and have only briefly used it for a few minutes. Due to the therapists' limited AR experience, the relationship between the attenuation of VIMS symptoms and AR experience level will not be examined in this study.

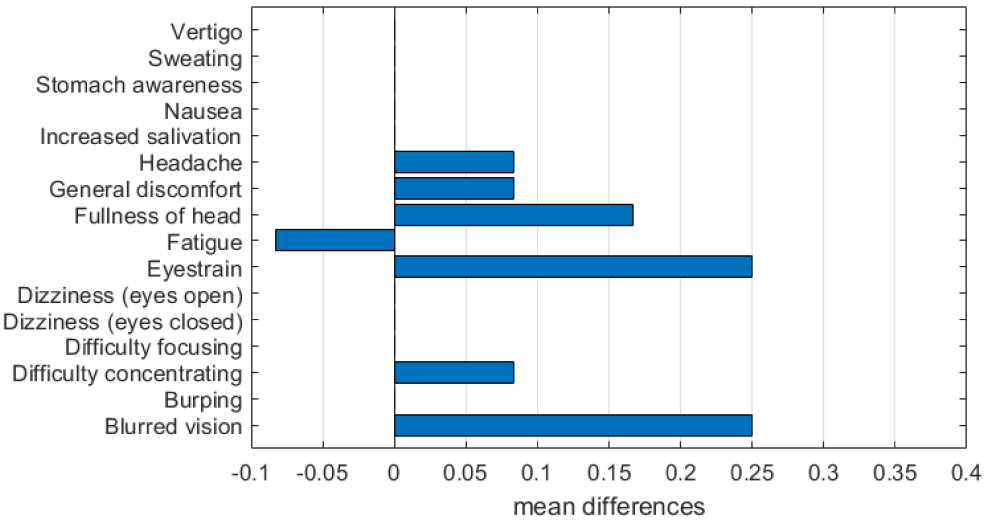

Figure 60: Mean pre- and post-exposure differences for all items of the SSQ.

Figure 61 shows the NASA-TLX scores. Referring to the interpretation scores of the NASA-TLX [119], the physical demand is low (<10) while all the other items are in the medium range (10-29).

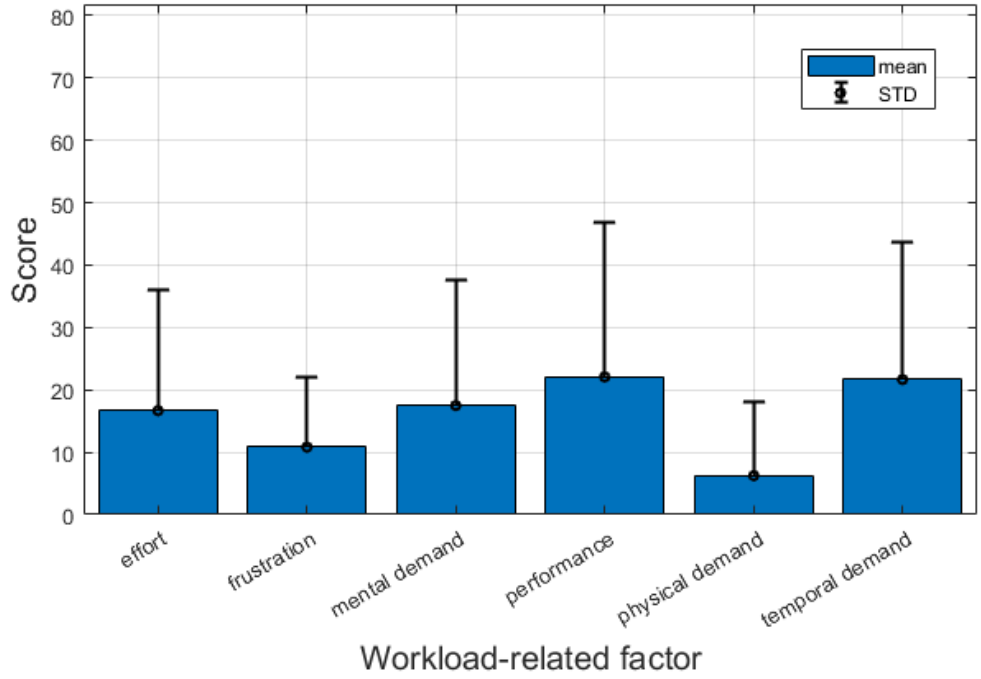

Figure 61: NASA-TLX scores.

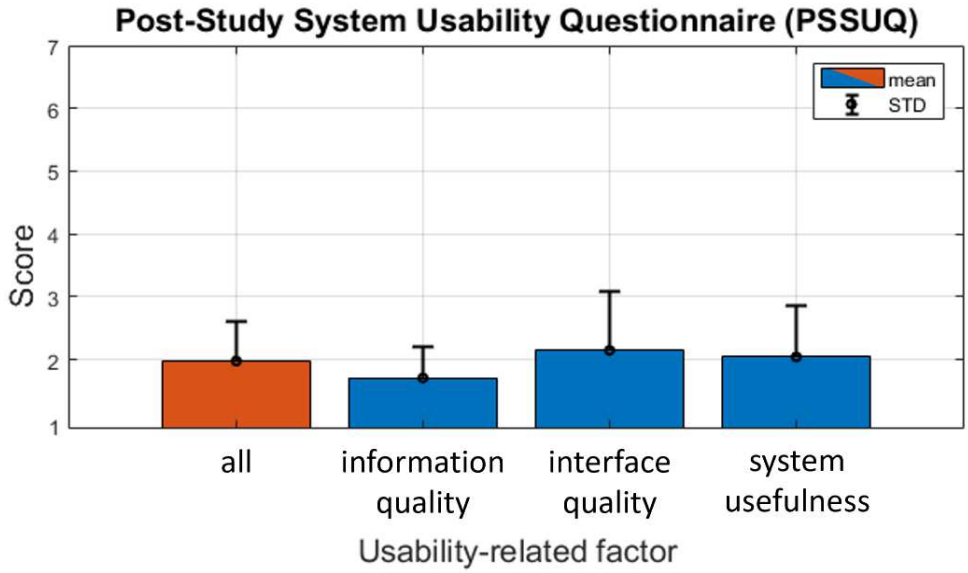

Figure 62: PSSUQ scores.

The PSSUQ scores are shown in Figure 62. PSSUQ score starts with 1 (strongly agree) and ends with 7 (strongly disagree). The lower the score, the better the performance and satisfaction. However, 4 is neutral but may not be the average and

a score below 4 does not indicate that your application has performed above average. Interpretation scores are referred to [122] (system usefulness: 2.80, information quality: 3.02, interface quality: 2.49, overall: 2.82). All the mean scores are lower than the interpretation scores indicating a level of good acceptance of the proposed solution.

The therapist's attention and behaviour are analysed with gaze and movement tracking. Samples of the therapist's movement and gaze are kept only if the patient has started walking and is not turning back to repeat the 10 meters path in the opposite versus, as schematized in Figure 63.

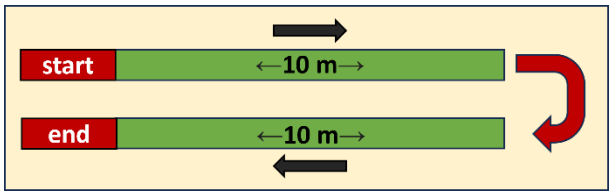

Figure 63: Patient walking path and valid intervals.

The walking velocity of the therapist has been calculated to investigate if the visualization modality causes different behaviours. The velocity is derived by the AR glasses recorded position. As shown in Figure 64, a low significance of the therapist velocity against visualization modality and a high significance against the subject are present. Since therapists have self-selected their positions, the movements are not influenced by the working modality but depend on the therapist's decision.

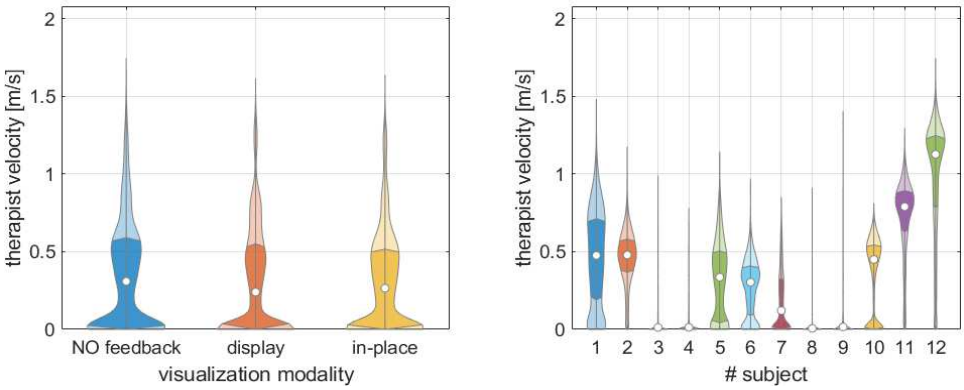

Figure 64: The therapist's walking velocity. The white dot represents the median and the shaded area represents the interquartile range (25-75%).

The heatmaps of Figure 65 show the relative position of the therapist with respect to the position and orientation of the patient's head. The spread points mean that the therapist doesn't keep a constant distance from the patient. As for the walking velocity, the relative position is not influenced by the visualization modality and in every condition the therapist decides to follow the patient or watch him/her in a static position. In the in-place modality, the median of the relative distance slightly increases with respect to the other conditions (without feedback: 1.5 m, display mode: 1.6 m, in-place mode: 2.1 m).

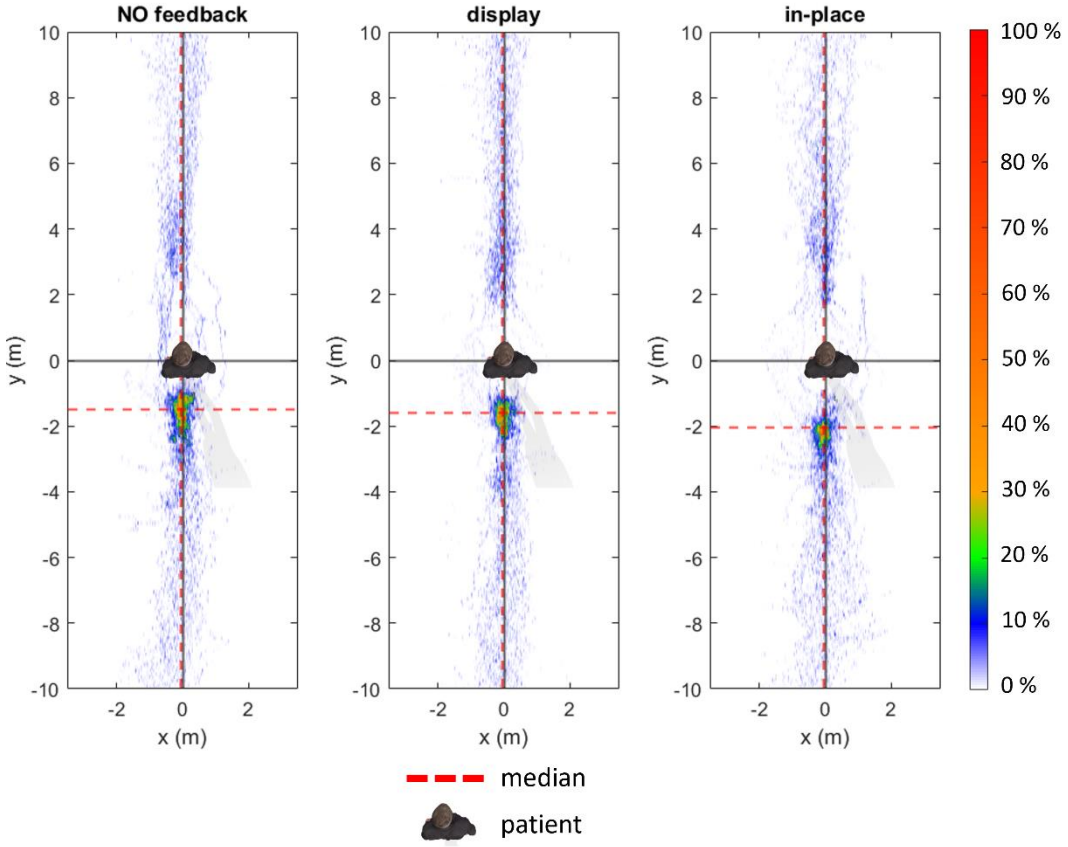

Figure 65: The therapist's position with respect to the position and orientation of the patient's head. The red line represents the median.

The gaze of the therapist is analysed to investigate preferences, strategies and patterns followed during the gait rehabilitation with or without AR feedback. Fixations are extracted from the gaze using the I-VT algorithm based on velocity threshold [108], [123]. Then each fixation is manually assigned to an area of interest (AOI) reproducing the video capture during the fixation interval and visualizing an

orange dot in correspondence with the gaze position, as in the example of Figure 66. The operator can choose between five AOIs: left crutch's load bar (AOI Bar Left), right crutch's load bar (AOI Bar Right), PWB's load bar (AOI Bar PWB), patient (AOI Patient), and not applicable (NA) if none of the previous AOIs.

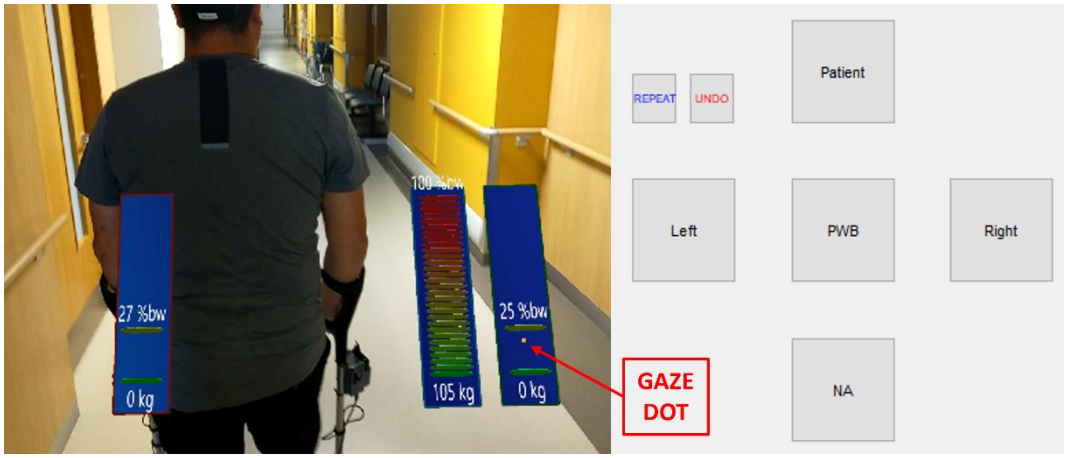

Figure 66: Manual labelling interface. On the left side, the video capture is reproduced in the fixation interval showing an orange dot to represent the gaze position. On the right side, the user can select the last reproduced fixation AOI.

Figure 67 and Figure 68 show the fixation ratio of the AOIs as a percentage of the total time. The fixation duration for each AOI is shown in Figure 69 divided by the working modality.

In Figure 67 the holograms' AOIs are merged into a unique category AOI Feedback. The therapist's average time spent on the patient is 83% (SD=8%) without AR feedback, 34% (SD=15%) in display mode, and 22% (SD=13%) in in-place mode. The therapist's average time spent on the AR feedback is 50% (SD=16%) in display mode and 64% (SD=13%) in in-place mode. The time dedicated to the patient decreases when AR feedback is present, and the lowest value is reached in the in-place modality. All the differences are statistically significant. The time dedicated to AR feedback is statistically significantly higher in the in-place mode compared to the display mode. The remaining time in every condition is dedicated to saccades or other objects.

Figure 68 shows that the attention time difference between the three sources of information (left and right crutch loads, and the PWB estimate) is not statistically significant in intra-condition tests. The time dedicated to the PWB estimate is

statistically significantly higher in the in-place mode compared to the display mode. Unlike the display mode, the time dedicated to the patient is not statistically significantly different from the time spent on a single information source.

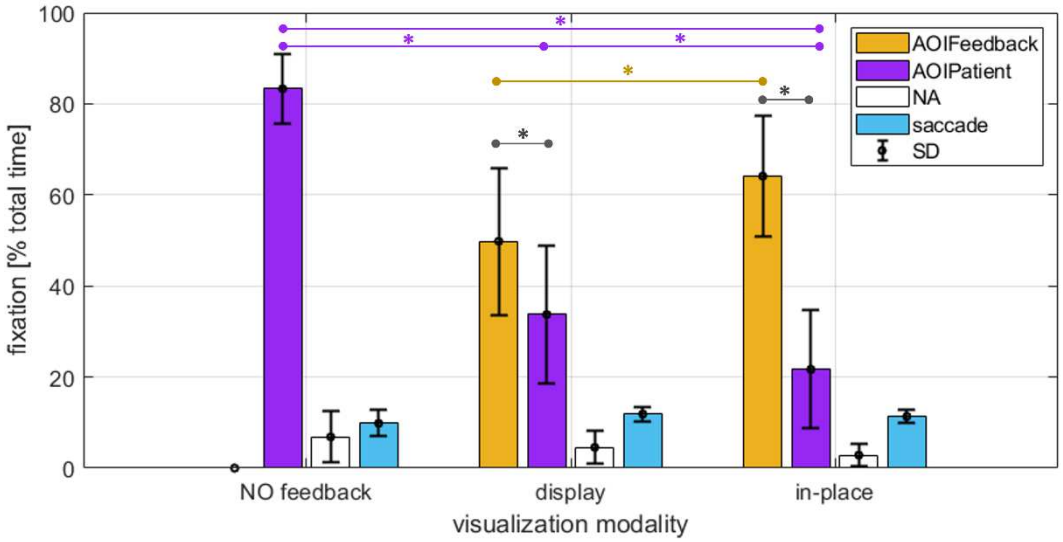

Figure 67: AOI's fixation ratio. Holograms' AOIs are merged into a unique category (AOI Feedback). *two-sided p-value < 0.05 with the unequal variances t-test.

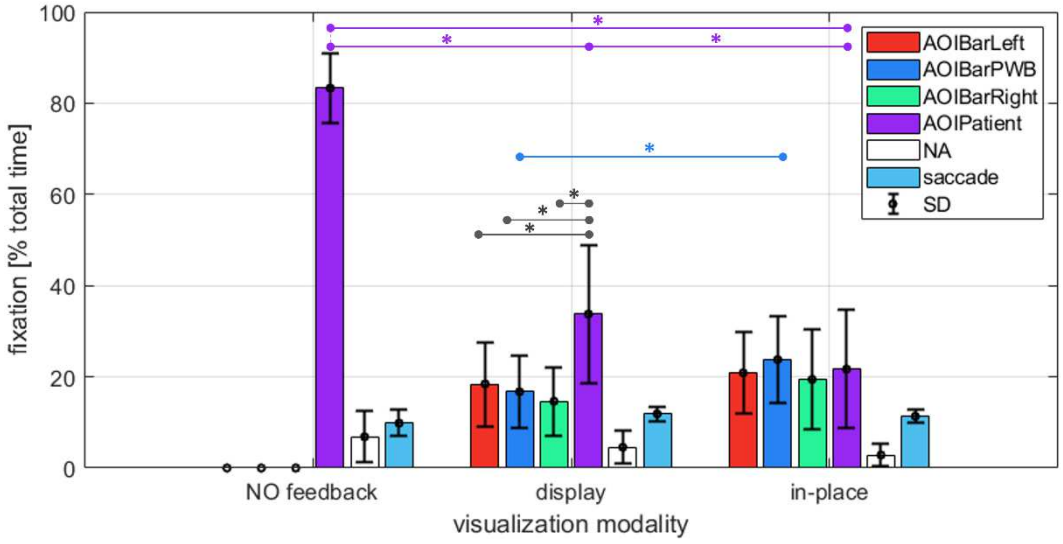

Figure 68: AOI's fixation ratio. *two-sided p-value < 0.05 with the unequal variances t-test.

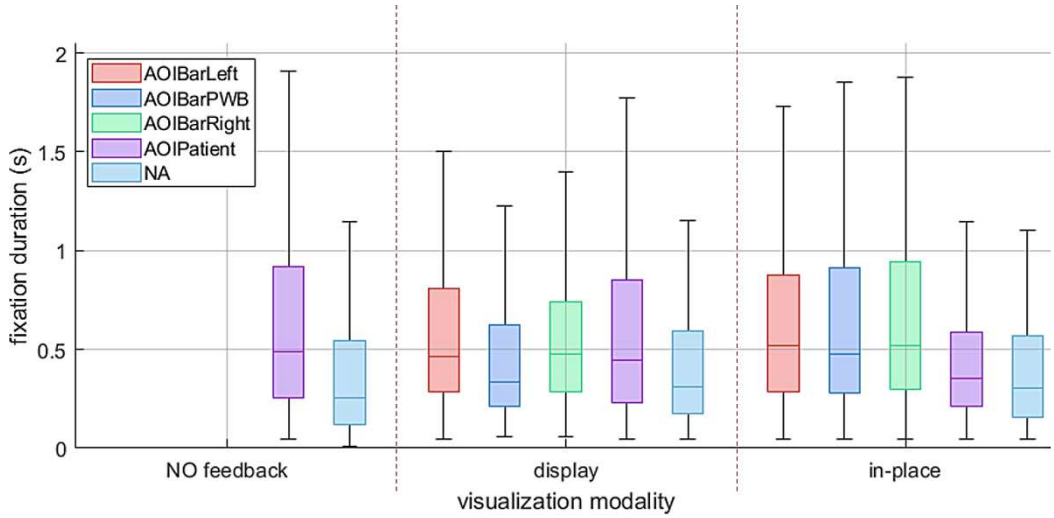

Figure 69: The fixation duration against the visualization modality and divided by the AOI.

The following tables, Table 14 and Table 15, present the eye transitions for the two different feedback modes, expressed as percentages of the total number of transitions starting from an AOI. These tables provide insights into the eye movement patterns during different working modes, shedding light on the visual attention allocation. Eye transitions are also represented in the Sankey diagrams of Figure 70.

Table 14: Eye transitions for the in-place mode. Eye transitions are expressed as percentages of the total number of transitions that start from an AOI.

		TO				
		Bar Left	**Bar PWB**	**Bar Right**	**Patient**	**NA**
FROM	**Bar Left**	-	23%	47%	27%	2%
	Bar PWB	29%	-	29%	38%	4%
	Bar Right	48%	26%	-	23%	4%
	Patient	28%	40%	21%	-	11%
	NA	14%	23%	9%	54%	-

Table 15: Eye transitions for the display mode. Eye transitions are expressed as percentages of the total number of transitions that start from an AOI.

		TO				
		Bar Left	**Bar PWB**	**Bar Right**	**Patient**	**NA**
FROM	**Bar Left**	-	22%	49%	27%	2%
	Bar PWB	29%	-	22%	40%	9%
	Bar Right	55%	16%	-	25%	3%
	Patient	28%	39%	19%	-	14%
	NA	20%	23%	6%	52%	-

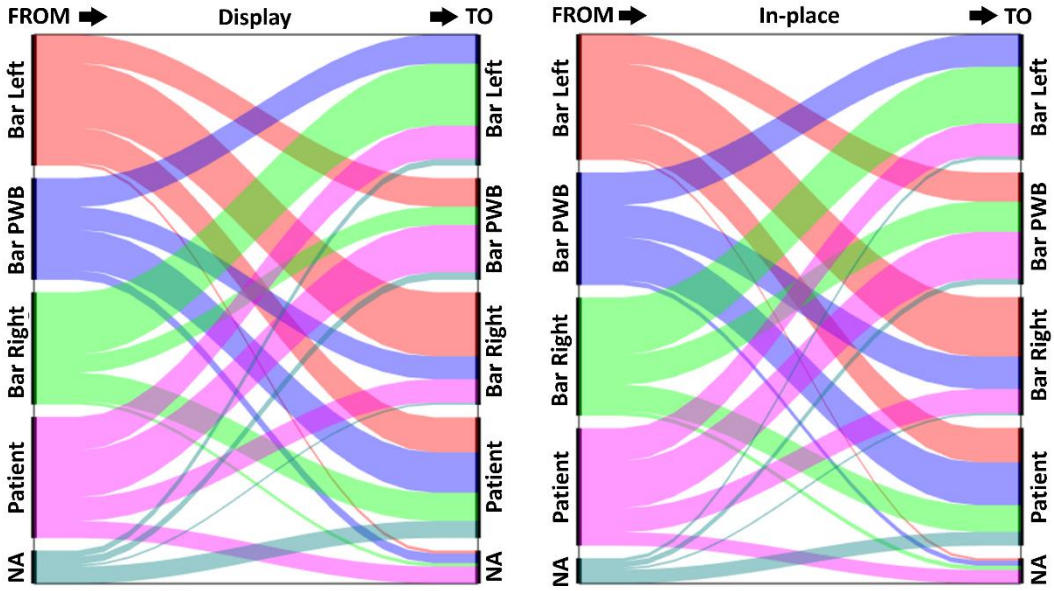

Figure 70: The eye transition between fixations of the display mode test on the left and the in-place mode test on the right. The thick black bar represents the frequency of transition from or to the corresponding AOI. The width of the branch represents the flow amount of eye transitions.

Finally, the feedback collected after every test is listed in Table 16.

Table 16: Therapists' comments during the post-test interviews.

Comment 1	"I believe it's very useful to perform a check now and then."
Comment 2	"High setup time."
Comment 3	"In in-place modality, I can see the subject's legs while looking at the information in place with peripheral vision, while in display mode, I can focus on either the patient or the information."
Comment 4	"I prefer the display mode because the quality of the holograms doesn't deteriorate when the patient moves away."
Comment 5	"I was confused at first, but then I got used to it."
Comment 6	"I prefer the in-place mode, but only if the holograms are not blurry."
Comment 7	"I was interested in the pelvic movement, and the in-place mode information was too low."
Comment 8	"A tutorial to explain how to use it would be helpful."
Comment 9	"I prefer the display mode because I can see the information even when closely following the patient."

3.3.3 Discussion

The AR interface developed has reached a general good acceptance from the end-users. The scores of the PSSUQ in Figure 62 show that the quality of the information and the interface is adequate for the task. Users also believe that the application can be useful for assisting their work. A therapist said that could be a useful technology to assess the patient's condition when needed or to verify if there are improvements in gait after a rehabilitation session. Moreover, looking at this comment "I was interested in the pelvic movement, and the in-place mode information was too low", the position of the holograms should also consider the target of the patient's body that the therapist needs to observe. Another therapist, more interested in the legs' movement, was satisfied with the in-place modality because she was able to check the legs and the information almost contemporarily. Familiarization and setup time appear to pose challenges for some therapists who are concerned about the limited time available for each patient. However, they also

believe that, with tutorials and experience, they can become accustomed to the device, reducing the time needed and enhancing their satisfaction.

The young age of the therapist could be related to their good vision skills influencing positively the AR experience. Nevertheless, in post-test interviews, some therapists expressed concerns about the legibility of the labels, particularly in the in-place modality when the patient is at a distance and the holograms become blurred. The labels' position and the font should be further investigated to provide a higher readability quality according to factors such as ambient illuminance, distance, and background properties [124], [125]. Blurred vision is also observed in the VIMS symptoms (Figure 60), and it remains unclear from the literature whether this is a result of the optical see-through AR technology or its particular application. Yu et al. [126] identified a relationship between the refocusing issue when users shift their attention between the real world and see-through objects, with the primary parameter being the distance from the objects. Nevertheless, it appears that the blurred labels do not cause movements in every therapist, as their velocity and position are not conditioned on the visualization modality, as indicated in Figure 64 and Figure 65.

When analysing the VIMS symptoms, it is important to highlight that there are currently no reliable reference values in the literature for assessing their severity in the context of AR [127], [128], and only a few studies have explored this aspect. Neither the pre-test nor the post-SSQ results (Figure 59) reached a high level of severity when compared to [113], [114]. Prolonged exposure over time can increase the incidence of VIMS symptoms [114], and reduced usage time should be considered for subjects more prone to experiencing VIMS. In our experiments, the average duration of non-continuous usage was approximately 15 to 20 minutes, which also included the training phase. In a real-world scenario, the effective usage time might be further decreased when the solution is operated by pre-trained personnel and only the preferred modality is enabled.

The workload required is investigated through the NASA-TLX questionnaire. Due to the way we designed the protocol, it is not possible to ascertain whether the in-place mode reduces the cognitive load of the therapist by eliminating the visual search component for the target to observe. Moreover, since the workloads induced by the AR interface and the rehabilitation task cannot be isolated, the scores obtained are combinations of both. Nevertheless, the results (Figure 61) show a low/medium level in every factor if compared to the interpretation given by the

questionnaire's creator [119]. Comparing the results to typical outcomes in medical, monitoring, and other scenarios [129], also reported in Table 17, the average global score falls below the 25th percentile, and the impact of the application on the therapist's workload appears to be minimal, even when a searching task is involved.

Table 17: Cumulative frequency distributions of NASA-TLX global workload scores by task type [129]**.**

Task (n)	**Min**	**25%**	**50%**	**75%**	**Max**
Medical (45)	9.00	39.35	50.60	61.45	77.35
Monitoring (174)	20.00	39.97	52.24	62.63	77.00
Video Game (60)	14.08	48.23	56.50	63.72	78.00

The therapist movements reported in Figure 64 and Figure 65 are not influenced by the visualization modality but depend on the therapist's preferences. Observing the therapist's position relative to the patient, it is possible to identify two behaviours. In one case, the therapist maintains a safe distance behind the patient, while in the other, they remain consistently stationary in a frontal or rear position relative to the patient. The patient's impairment severity could be an influencing factor that imposes the therapist-patient distance for safety reasons, but no evidence has been found in the literature to confirm or deny this assumption. However, in this study, the impairment severity was not considered. The option to select an alternative visualization modality could be advantageous. As mentioned by therapists, the display modality may be more suitable when the therapist needs to closely follow the patient, while the in-place modality offers a quicker and more straightforward transition between the information and the patient in safer conditions.

The therapist dedicates less time to watching the patient when the AR feedback is enabled, reaching the lowest value in the in-place modality. In the in-place mode, the time is equally distributed between the patient's AOI and the information sources' AOIs. The same cannot be said for the display modality, in which the patient is observed with a higher ratio. A comment from a therapist suggests that in display mode, shifting focus from the patient to the AR feedback can be challenging. Therapists may prefer to monitor the patient for a longer period before taking a look at the information.

The fixation duration in the in-place mode with respect to the display decreases for the patient's AOI and increases for the PWB's AOI. The variation in fixation duration, along with the differences in time spent on the same AOIs, suggests that in the in-place modality, therapists are more likely to observe the load applied to the legs for a longer time without reducing the time devoted to monitoring the loads on the left and right crutches but reducing the time devoted to the patient. However, it has been demonstrated in the literature that professionals require shorter fixation on the patient than trainees, while describing a higher number of gait abnormalities (the median fixation duration is approximately 400 ms in professionals and 650 ms in trainees) [130], [131]. Therefore, even though the time dedicated to observing the patient is less, it should still be sufficient to accurately assess gait abnormalities, including those not highlighted by AR feedback.

The eye transition and the revisit rate can be useful for understanding the user interest [132] and from Table 14 and Table 15 two gaze patterns can be observed: the therapist's attention usually switches from the left to the right crutch load (and vice-versa) or from the patient to the PWB (and vice-versa). For a particular patient or pathology, a therapist's level of interest in crutch loads or PWB estimates may vary. This distinct preference indicates that in future clinical applications, it might be beneficial to allow the therapist to choose which information to visualize, thereby reducing the unnecessary distractions of holograms that fall outside of their specific AOI.

The reduced sample size, 12 couples of therapist-patient, is mostly related to the difficulties in involving specialized therapists and patients with similar pathologies. Anyway, the sample size is selected to obtain 80% statistical power when performing a paired t-test on the outcomes. A larger sample size could be useful to deeply investigate the relationship between outcomes and deteriorated vision skill. For examples, it is expected to receive more feedback on the aesthetics of the user interface, mostly related to the font size and contrast with the background colour. A larger sample size could also provide insight into the movement strategies of the therapists according to the patient's pathology. It is still not clear whether the therapist decides to strictly follow the patient movements or remains in a static position, and it could be useful to classify the needs of the therapist to provide a more adequate interface. Similarly, since two eye transition patterns were identified, an adaption of the interface based on the therapist interests could improve the visibility, reduce the distraction and enhance the rehabilitation outcomes.

Conclusions

Over the years, several assistive devices have been developed to address the needs of patients, aiming to preserve or restore their functionality and independence. The decline in physical mobility resulting from various medical conditions reduces the motivation to engage in activities and, in severe cases, may even prevent such possibilities. Crutches, walkers, canes, and various other devices can serve as valuable tools to enhance mobility, balance, confidence, and autonomy. Crutches are among the most used devices for assisting walking and, especially if their use is required for long periods, special attention must be applied. Incorrect use leads to falls or injuries, and unbalanced weight-bearing on arms or legs may cause pain in joint articulations or injured limbs. Therapists usually assess their patients' gait searching for abnormalities in posture, rhythm, pattern, and many other factors. Healthcare professionals can employ different strategies aiming to correct the assisted gait: designing exercise programs for strength, balance, and coordination, but also providing encouragement and motivation.

In the field of rehabilitation, researchers have developed various systems to analyse and enhance walking, including instrumented assistive devices, biofeedback, robotics, VR, AR, and games. Instrumented assistive devices are advanced technological tools, such as parallel bars, walkers, crutches, and canes, equipped with sensors to capture parameters like step length, step width, walking speed, ground reaction forces, and orientation. These devices provide quantitative data on a patient's walking patterns and biomechanical characteristics, aiding

healthcare professionals in assessing functional abilities and gait abnormalities. The objective measurements help in evaluating the effectiveness of interventions and personalizing rehabilitation programs for better outcomes and more efficient recovery.

In recent years, there has been a growing interest in using immersive technologies in healthcare and rehabilitation. They have the potential to transform rehabilitation by enhancing patient engagement, improving outcomes, and making the experience more effective and enjoyable. Immersive technologies create interactive virtual environments tailored to rehabilitation goals and allow real-time data tracking. Sensors and tracking devices in these systems can measure parameters like joint movements, range of motion, and force exertion, facilitating progress monitoring and treatment adjustments. Nowadays, only a few works have been conducted on using immersive technologies to support therapists during the observational assessment of patients. The presented work describes an AR solution based on the measurements obtained from instrumented crutches, aimed at providing kinetic information to therapists during rehabilitation or observational gait assessments.

The instrumented crutches have been upgraded to improve the force measurement's reliability adopting a new full-bridge configuration of the strain gauges. The uncertainty was halved reaching 7 N in the walking conditions instead of the previous 14 N. The sensitivity regarding the bending and temperature of the crutches, which is expected due to non-idealities in the strain gauge fixation, still needs to be quantified. The crutches are also equipped with depth cameras to detect the patient's gait phases, and the process has been strengthened to reduce prediction failures by limiting the influence of the subjectivity of crutch usage on the results. Then, as instrumented crutches are frequently used in gait analysis laboratories, a custom data synchronization system has been developed to enhance the integration of the crutches, thereby reducing post-processing time. The described low-cost solution can achieve a time synchronization accuracy of 4 ms and is built upon common approaches like the NTP protocol and analog/digital triggers. Furthermore, it can be connected to a ROS network for real-time information sharing. These instrumented crutches are employed in on-field tests to assess improvements during exoskeleton-assisted walking and compare crutch loads in various walking patterns and therapist assistance levels, allowing for the monitoring of progress and load comparisons under different conditions.

The integration of AR and instrumented crutches into gait assessment during rehabilitation has been addressed through a participatory design approach. Therapists, as the final users, have been engaged in the process through meetings, interviews, brainstorming, and demos to discuss and design the AR user interface. Following this iterative process, a version of the interface has been created based on the therapists' input and the capabilities of the AR technology used. Additionally, to meet the therapists' need for information regarding the load on the legs, a weight-bearing estimator based on measurements from the instrumented crutches has been validated. The weight-bearing estimate is therefore added to the crutches' loads as augmented information of the kinetics involved during the crutch-assisted gait. To assess the usability of the AR interface, a test campaign was conducted in a real-world scenario, comparing two working modalities. In the "display mode," holograms remain on a virtual screen in the therapist's frontal view, while in the "in-place mode", holograms are positioned near the patient. The evaluation included not only usability metrics but also the therapist's attention, behaviour, and workload as well as their well-being to ensure that exposure to AR does not induce severe motion sickness. Results indicate a positive response in terms of information and interface quality, as well as perceived system usefulness among the users. Exposure to AR for this specific application does not induce severe sickness. However, as found in the literature in other cases, eye strain and blurred vision can occur when optical see-through technologies are involved. The required workload remains in the low to medium range and is acceptable when compared to the results of studies that investigate similar tasks. The therapists' behaviour and attention were monitored through their body and eye movements. It cannot be demonstrated that the therapist's position relative to the patient is influenced by the working modality. Instead, it is more likely to be a subjective decision based on the therapist's preferences or the patient's walking independence and safety. The gaze, once the fixations have been extracted and associated with the observed AOI, demonstrates that in the in-place mode, if compared to the display modality, the user spends a shorter period observing the patient and more time on the legs' weight-bearing information. Based on post-test interviews, even though some therapists have expressed a preference for the display mode, it appears that the distance between the holograms and the patient could pose a challenge to the ease of navigating through the AOI. Finally, when analysing the eye transitions between AOIs, two gaze strategies are identified. Depending on the clinical case being assessed, the therapist may be interested in either the left and right crutches' loads or solely in the legs' weight-bearing.

The described results are essential for ensuring a user-oriented system improvement before starting the clinical effectiveness study. The collected information and feedback suggest the following areas for improvement. The setup time should be reduced, and a tutorial implemented. Gait assessments often did not involve the use of both crutches, but instead relied on just one crutch or other support devices like quadripodes or walkers. In light of this, a preliminary study on an instrumented walker has been conducted in collaboration with a passive-exoskeleton manufacturer. Additionally, patients were hesitant to use crutches other than their own, prompting the exploration of alternative solutions for instrumenting assistive devices with fast attachable and detachable force sensors. The AR interface should be made more adaptable to individual user needs, aligning with rehabilitation goals and therapist preferences. Lastly, it is still unclear whether deteriorated vision skills could worsen satisfaction ratings and introduce any side effects. Therefore, future clinical effectiveness studies should continue considering both the VIMS and usability analysis.

Bibliography

[1] J. M. Baker, “Gait Disorders,” *Am J Med*, vol. 131, pp. 602–607, 2018, doi: 10.1016/j.amjmed.2017.11.051.

[2] World Health Organization, “Parkinson disease A public health approach,” Jun. 2022. Accessed: Jan. 12, 2024. [Online]. Available: https://www.who.int/news/item/14-06-2022-launch-of-who-s-parkinson-disease-technical-brief

[3] K. Jahn, A. Zwergal, and R. Schniepp, “Gait Disturbances in Old Age Classification, Diagnosis, and Treatment From a Neurological Perspective”, doi: 10.3238/arztebl.2010.0306.

[4] A. Bronstein and T. Brandt, *Clinical Disorders of Balance, Posture and Gait*, 2Ed ed. CRC Press, 2004.

[5] P. Mahlknecht *et al.*, “Prevalence and Burden of Gait Disorders in Elderly Men and Women Aged 60-97 Years: A Population-Based Study,” *PLoS One*, vol. 8, no. 7, Jul. 2013, doi: 10.1371/journal.pone.0069627.

[6] R. E. Cowan, B. J. Fregly, M. L. Boninger, L. Chan, M. M. Rodgers, and D. J. Reinkensmeyer, “Recent trends in assistive technology for mobility,” 2012. [Online]. Available: http://www.jneuroengrehab.com/content/9/1/20

[7] M. O. A. Aqel *et al.*, “Review of recent research trends in assistive technologies for rehabilitation,” in *Proceedings - 2019 International Conference on Promising Electronic Technologies, ICPET 2019*, Institute of Electrical and Electronics Engineers Inc., Oct. 2019, pp. 16–21. doi: 10.1109/ICPET.2019.00011.

[8] S. M. Bradley and C. R. Hernandez, “Geriatric Assistive Devices,” 2011. [Online]. Available: www.aafp.org/afpAmericanFamilyPhysician405

[9] H. Bateni and B. E. Maki, “Assistive devices for balance and mobility: Benefits, demands, and adverse consequences,” *Arch Phys Med Rehabil*, vol. 86, no. 1, pp. 134–145, 2005, doi: 10.1016/j.apmr.2004.04.023.

[10] R. L. Kirby, H. Y. A. Tsai, and M. M. Graham, “Ambulation Aid Use During the Rehabilitation of People with Lower Limb Amputations,” *Assistive Technology*, vol. 14, no. 2, pp. 112–117, Dec. 2002, doi: 10.1080/10400435.2002.10132060.

[11] G. G. Deaver, “Posture and Its Relation to Mental and Physical Health,” vol. 4, no. 1, pp. 221–228, doi: 10.1080/23267402.1933.10761571.

[12] T. E. Shokp L S Fletcher and B. R. Merrill, “Biomechanics of crutch locomotion.”

[13] F. Rasouli and K. B. Reed, “Walking assistance using crutches: A state of the art review,” *Journal of Biomechanics*, vol. 98. Elsevier Ltd, Jan. 02, 2020. doi: 10.1016/j.jbiomech.2019.109489.

[14] S. Li, C. W. Armstrong, and D. Cipriani, “Three-point gait crutch walking: Variability in ground reaction force during weight bearing,” *Arch Phys Med Rehabil*, vol. 82, no. 1, pp. 86–92, 2001, doi: 10.1053/apmr.2001.16347.

[15] J. W. Youdas, B. J. Kotajarvi, D. J. Padgett, and K. R. Kaufman, “Partial weight-bearing gait using conventional assistive devices,” *Arch Phys Med Rehabil*, vol. 86, no. 3, pp. 394–398, 2005, doi: 10.1016/j.apmr.2004.03.026.

[16] J. C. H. Goh, S. L. Toh’, and K. Bose, “Biomechanical study on axillary crutches during single-leg swing-through gait,” 1986.

[17] R. C. Holliday, C. Ballinger, and E. D. Playford, “Goal setting in neurological rehabilitation: Patients’ perspectives,” vol. 29, no. 5, pp. 389–394, doi: 10.1080/09638280600841117.

[18] World Health Organization, “Assistive technolgy - challenges.” Accessed: Jan. 18, 2024. [Online]. Available: https://www.who.int/health-topics/assistive-technology#tab=tab_2

[19] World Health Organization, “Training in Assistive Products.” Accessed: Jan. 18, 2024. [Online]. Available: https://www.gate-tap.org/

[20] Z. Jin and H. J. Chizeck, “Instrumented parallel bars for three-dimensional force measurement,” *J Rehabil R D*, vol. 29, no. 2, pp. 31–38, 1992, doi: 10.1682/jrrd.1992.04.0031.

[21] A. Fast, F. S. Wang, R. S. Adrezin, M. A. Cordaro, J. Ramis, and J. Sosner, “The Instrumented Walker: Usage Patterns and Forces,” 1995.

[22] A. Sivakumar, K. Bennett, M. Rickman, and D. Thewlis, “An instrumented walker in three-dimensional gait analysis: Improving musculoskeletal estimates in the lower limb mobility impaired,” *Gait Posture*, vol. 93, pp. 142–145, Mar. 2022, doi: 10.1016/j.gaitpost.2022.01.023.

[23] R. A. Bachschmidt, G. F. Harris, and G. G. Simoneau, “Walker-Assisted Gait in Rehabilitation: A Study of Biomechanics and Instrumentation,” 2001.

[24] G. V Merrett, M. A. Ettabib, C. Peters, G. Hallett, and N. M. White, “Augmenting Forearm Crutches with Wireless Sensors for Lower Limb Rehabilitation.”

[25] G. V. Merrett, C. Peters, G. Hallet, and N. M. White, “An instrumented crutch for monitoring patients’ weight distribution during orthopaedic rehabilitation,” in *Procedia Chemistry*, Sep. 2009, pp. 714–717. doi: 10.1016/j.proche.2009.07.178.

[26] G. Chamorro-Moriana, J. L. Sevillano, and C. Ridao-Fernández, “A compact forearm crutch based on force sensors for aided gait: Reliability and validity,” *Sensors (Switzerland)*, vol. 16, no. 6, Jun. 2016, doi: 10.3390/s16060925.

[27] G. Chamorro Moriana, J. R. Roldán, J. J. J. Rejano, R. C. Martínez, and C. S. Serrano, “Design and validation of GCH System 1.0 which measures the weight-bearing exerted on forearm crutches during aided gait,” *Gait Posture*, vol. 37, no. 4, pp. 564–569, Apr. 2013, doi: 10.1016/j.gaitpost.2012.09.018.

[28] Y. Felix Chen, S. Member, D. Napoli, S. K. Agrawal, and D. Zanotto, “Smart Crutches: Towards Instrumented Crutches for Rehabilitation and Exoskeletons-Assisted Walking”.

[29] E. Sardini, M. Serpelloni, and M. Lancini, “Wireless Instrumented Crutches for Force and Movement Measurements for Gait Monitoring,” *IEEE Trans Instrum Meas*, vol. 64, no. 12, pp. 3369–3379, Dec. 2015, doi: 10.1109/TIM.2015.2465751.

[30] M. Lancini, M. Serpelloni, and S. Pasinetti, “Instrumented crutches to measure the internal forces acting on upper limbs in powered exoskeleton users,” in *2015 6th International Workshop on Advances in Sensors and Interfaces (IWASI)*, IEEE, pp. 175–180. doi: 10.1109/IWASI.2015.7184960.

[31] M. Lancini, M. Serpelloni, S. Pasinetti, and E. Guanziroli, “Healthcare Sensor System Exploiting Instrumented Crutches for Force Measurement During Assisted Gait of Exoskeleton Users,” vol. 16, no. 23, pp. 8228–8237, doi: 10.1109/JSEN.2016.2579738.

[32] P. Claire and F. Joyce, “An Instrumented Cane Devised for Gait Rehabilitation and Research,” *Journal of Physical Therapy Education*, vol. 25, pp. 36–41, 2011.

[33] F. Mekki, M. Borghetti, E. Sardini, and M. Serpelloni, “Wireless Instrumented Cane for Walking Monitoring in Parkinson Patients,” in *IEEE International Symposium on Medical Measurements and Applications (MeMeA)*, 2017, pp. 414–419. doi: 10.1109/MeMeA.2017.7985912.

[34] F. Khan, P. Vijesh, S. Rahool, A. Radha, S. Sukumaran, and R. Kurupath, “Physiotherapy practice in stroke rehabilitation: A cross-sectional survey of physiotherapists in the state of Kerala, India,” *Top Stroke Rehabil*, vol. 19, no. 5, pp. 405–410, Jan. 2012, doi: 10.1310/tsr1905-405.

[35] F. Coutts, “Gait analysis in the therapeutic environment,” 1999.

[36] B. Toro, C. Nester, and P. Farren, “A review of observational gait assessment in clinical practice”, doi: 10.1080/0959398039221901.

[37] F. Routhier *et al.*, “Clinicians’ perspectives on inertial measurement units in clinical practice,” *PLoS One*, vol. 15, no. 11 November, Nov. 2020, doi: 10.1371/journal.pone.0241922.

[38] R. M. Viglialoro, S. Condino, G. Turini, M. Carbone, V. Ferrari, and M. Gesi, "Review of the augmented reality systems for shoulder rehabilitation," *Information (Switzerland)*, vol. 10, no. 5. MDPI AG, 2019. doi: 10.3390/info10050154.

[39] Y. M. Aung and A. Al-Jumaily, "Augmented reality-based RehaBio system for shoulder rehabilitation," 2014.

[40] C. Gorman and L. Gustafsson, "The use of augmented reality for rehabilitation after stroke: a narrative review," *Disability and Rehabilitation: Assistive Technology*. Taylor and Francis Ltd, pp. 1–9, 2020. doi: 10.1080/17483107.2020.1791264.

[41] J. P. O. Held *et al.*, "Augmented reality-based rehabilitation of gait impairments: Case report," *JMIR Mhealth Uhealth*, vol. 8, no. 5, May 2020, doi: 10.2196/17804.

[42] C. L. Toledo-Peral *et al.*, "Virtual/Augmented Reality for Rehabilitation Applications Using Electromyography as Control/Biofeedback: Systematic Literature Review," *Electronics (Switzerland)*, vol. 11, no. 14. MDPI, Jul. 01, 2022. doi: 10.3390/electronics11142271.

[43] C. Kirner and T. G. kirner, "Development of an Interactive Artifact for Cognitive Rehabilitation based on Augmented Reality," in *International Conference on Virtual Rehabilitation (Rehab Week Zurich)*, IEEE, 2011.

[44] E. Mantovani *et al.*, "Telemedicine and Virtual Reality for Cognitive Rehabilitation: A Roadmap for the COVID-19 Pandemic," *Front Neurol*, vol. 11, Sep. 2020, doi: 10.3389/fneur.2020.00926.

[45] G. Albakri *et al.*, "Phobia Exposure Therapy Using Virtual and Augmented Reality: A Systematic Review," *Applied Sciences (Switzerland)*, vol. 12, no. 3. MDPI, Feb. 01, 2022. doi: 10.3390/app12031672.

[46] C. Suso-Ribera *et al.*, "Virtual Reality, Augmented Reality, and in Vivo Exposure Therapy: A Preliminary Comparison of Treatment Efficacy in Small Animal Phobia," *Cyberpsychol Behav Soc Netw*, vol. 22, no. 1, pp. 31–38, Jan. 2019, doi: 10.1089/cyber.2017.0672.

[47] M. De Cecco *et al.*, "Sharing Augmented Reality between a Patient and a Clinician for Assessment and Rehabilitation in Daily Living Activities †," *Information (Switzerland)*, vol. 14, no. 4, Apr. 2023, doi: 10.3390/info14040204.

[48] T. Pisoni *et al.*, "AUSILIA: Assisted Unit for Simulating Independent LIving Activities," in *IEEE International Smart Cities Conference (ISC2)*, 2016. doi: 10.1109/ISC2.2016.7580802.

[49] M. De Cecco *et al.*, "Augmented reality to enhance the clinician's observation during assessment of daily living activities," in *Lecture Notes in Computer Science (including subseries Lecture Notes in Artificial Intelligence and Lecture Notes in Bioinformatics)*, Springer Verlag, 2017, pp. 3–21. doi: 10.1007/978-3-319-60928-7_1.

[50] A. Fornaser *et al.*, "Augmented virtualized observation of hidden physical quantities in occupational therapy," in *Proceedings - 2018 International Conference on Cyberworlds, CW 2018*, Institute of Electrical and Electronics Engineers Inc., Dec. 2018, pp. 423–426. doi: 10.1109/CW.2018.00082.

[51] S. K. Ong, Y. Shen, J. Zhang, and A. Y. C. Nee, "Augmented Reality in Assistive Technology and Rehabilitation Engineering," in *Handbook of Augmented Reality*, Springer New York, 2011. doi: 10.1007/978-1-4614-0064-6.

[52] D. Krause *et al.*, "Biodynamic Feedback Training to Assure Learning Partial Load Bearing on Forearm Crutches," *Arch Phys Med Rehabil*, vol. 88, no. 7, pp. 901–906, Jul. 2007, doi: 10.1016/j.apmr.2007.03.022.

[53] B. Peres, P. F. Campos, and A. Azadegan, "A Persuasive approach in using Visual Cues to Facilitate Mobility Using Forearm Crutches."

[54] O. M. Giggins, U. M. Persson, and B. Caulfield, "Biofeedback in rehabilitation," p. 11.

[55] M. Quigley *et al.*, "ROS: an open-source Robot Operating System." [Online]. Available: http://stair.stanford.edu

[56] M. Lancini *et al.*, “Upper limb loads during robotic assisted gait: A measuring system to guide training,” pp. 613–620. doi: 10.1142/9789813231047_0074.

[57] I. Sesar, A. Zubizarreta, I. Cabanes, E. Portillo, J. Torres-Unda, and A. Rodriguez-Larrad, “Instrumented crutch tip for monitoring force and crutch pitch angle,” *Sensors (Switzerland)*, vol. 19, no. 13, Jul. 2019, doi: 10.3390/s19132944.

[58] N. B. McLaughlin and Y. Chen, “Effect of strain gage misalignment on cross sensitivity of extended ring (ER) transducers,” *Canadian Biosystems Engineering*, vol. 54, pp. 2.23-2.31, 2012, doi: 10.7451/CBE.2012.54.2.23.

[59] P. Devita, “The selection of a standard convention for analyzing gait data based on the analysis of relevant biomechanical factors,” 1994.

[60] S. Pasinetti, A. Fornaser, M. Lancini, M. De Cecco, and G. Sansoni, “Assisted Gait Phase Estimation through an Embedded Depth Camera Using Modified Random Forest Algorithm Classification,” *IEEE Sens J*, vol. 20, no. 6, pp. 3343–3355, 2020, doi: 10.1109/JSEN.2019.2957667.

[61] H. Zhao, Z. Wang, S. Qiu, Y. Shen, and J. Wang, “IMU-based Gait Analysis for Rehabilitation Assessment of Patients with Gait Disorders,” in *4th Int. Conf. Syst. Informatics, ICSAI 2017*, 2017, pp. 622–626. doi: 10.1109/ICSAI.2017.8248364.

[62] T. T. Wong and P. Y. Yeh, “Reliable Accuracy Estimates from k-Fold Cross Validation,” *IEEE Trans Knowl Data Eng*, vol. 32, no. 8, pp. 1586–1594, Aug. 2020, doi: 10.1109/TKDE.2019.2912815.

[63] D. Grimaldi and F. Lamonaca, “Techniques to Assess the Time Synchronization in Distributed Systems,” in *6 th IMEKO TC4 Symposium - Exploring New Frontiers of Instrumentation and Methods for Electrical and Electronic Measurements Measurement* , Florence, Sep. 2008. [Online]. Available: http://www.deis.unical.it/html/leim.htm

[64] N. Mikael M., K. Wojciech E., and V. Olavi, “A Method for Synchronizing Low Cost Energy Aware Sensors used in Industrial Process Monitoring,” in

The 27th Annual Conference of the IEEE Industrial Electronics Society, IEEE, 2001. doi: 10.1109/IECON.2001.976462.

[65] Z. Zhang, H. Ochiai, and H. Esaki, "An IoT Application-Layer Protocol Modem: A Case Study on Interfacing IEEE 1888 with at Commands," in *Proceedings - 2017 International Conference on Cyber-Enabled Distributed Computing and Knowledge Discovery, CyberC 2017*, Institute of Electrical and Electronics Engineers Inc., Jul. 2017, pp. 346–349. doi: 10.1109/CyberC.2017.65.

[66] H. J. Kim, U. Lee, M. Kim, and S. Lee, "Time-synchronization method for can–ethernet networks with gateways," *Applied Sciences (Switzerland)*, vol. 10, no. 24, pp. 1–11, Dec. 2020, doi: 10.3390/app10248873.

[67] H. Fu, B. Tang, Y. Huang, and L. Deng, "Path Perception Synchronization Trigger Method for Dual Mode Multiplexing Mechanical Vibration Wireless Sensor Networks," *IEEE Access*, 2021, doi: 10.1109/ACCESS.2021.3064697.

[68] P. Ottanelli *et al.*, "The Florence Trigger-Box (FTB) project: an FPGA-based configurable and scalable trigger system," Aug. 2021, doi: 10.1016/j.nima.2021.165745.

[69] B. Nalepa and A. Gwiazda, "Synchronization of Measurement Data with the Reference System," *IOP Conf Ser Mater Sci Eng*, vol. 1182, no. 1, p. 012052, Oct. 2021, doi: 10.1088/1757-899X/1182/1/012052.

[70] W. Lewandowski, J. Azoubib, and W. J. Klepczynski, "GPS: Primary Tool for Time Transfer," 1999.

[71] D. L. Mills, "Internet Time Synchronization: The Network Time Protocol," 1991.

[72] "Information technology-Ubiquitous green community control network protocol," 2015. [Online]. Available: www.iso.org

[73] J. M. O'Kane, *A gentle introduction to ROS*. Jason M. O'Kane, 2014.

[74] M. Ghidelli, S. Massardi, L. Foletti, A. C. Gonzalez, and M. Lancini, "Validation of a ROS-Based Synchronization System for Biomechanics Gait

Labs," in *2022 IEEE International Symposium on Measurements and Networking, M and N 2022 - Proceedings*, Institute of Electrical and Electronics Engineers Inc., 2022. doi: 10.1109/MN55117.2022.9887745.

[75] M. Ghidelli, C. Nuzzi, F. Crenna, and M. Lancini, "Validation of Estimators for Weight-Bearing and Shoulder Joint Loads Using Instrumented Crutches," 2023, doi: 10.3390/s23136213.

[76] T. Youm, S. G. Maurer, and S. A. Stuchin, "Postoperative management after total hip and knee arthroplasty," *Journal of Arthroplasty*, vol. 20, no. 3, pp. 322–324, 2005, doi: 10.1016/j.arth.2004.04.015.

[77] S. A. Abdalbary, "Partial weight bearing in hip fracture rehabilitation," *Future Science OA*, vol. 4, no. 1. Future Medicine Ltd., Jan. 01, 2018. doi: 10.4155/fsoa-2017-0068.

[78] Y. Laufer, "The use of walking aids in the rehabilitation of stroke patients," *Reviews in Clinical Gerontology*, vol. 14, no. 2. pp. 137–144, May 2004. doi: 10.1017/S0959259805001449.

[79] M. Raaben, H. R. Holtslag, L. P. H. Leenen, R. Augustine, and T. J. Blokhuis, "Real-time visual biofeedback during weight bearing improves therapy compliance in patients following lower extremity fractures," *Gait Posture*, vol. 59, pp. 206–210, Jan. 2018, doi: 10.1016/j.gaitpost.2017.10.022.

[80] A. M. Eickhoff, R. Cintean, C. Fiedler, F. Gebhard, K. Schütze, and P. H. Richter, "Analysis of partial weight bearing after surgical treatment in patients with injuries of the lower extremity," *Arch Orthop Trauma Surg*, vol. 142, no. 1, pp. 77–81, Jan. 2022, doi: 10.1007/s00402-020-03588-z.

[81] M. Tveit, J. Ka, and J. Kä, "LOW EFFECTIVENESS OF PRESCRIBED PARTIAL WEIGHT BEARING Continuous recording of vertical loads using a new pressure-sensitive insole."

[82] A. Vasarhelyi, T. Baumert, C. Fritsch, W. Hopfenmüller, G. Gradl, and T. Mittlmeier, "Partial weight bearing after surgery for fractures of the lower extremity - Is it achievable?," *Gait Posture*, vol. 23, no. 1, pp. 99–105, Jan. 2006, doi: 10.1016/j.gaitpost.2004.12.005.

[83] N. B. Jain, L. D. Higgins, J. N. Katz, and E. Garshick, “Association of Shoulder Pain With the Use of Mobility Devices in Persons With Chronic Spinal Cord Injury,” *PM&R*, vol. 2, no. 10, pp. 896–900, Oct. 2010, doi: 10.1016/J.PMRJ.2010.05.004.

[84] P. S. Requejo *et al.*, “Upper extremity kinetics during Lofstrand crutch-assisted gait,” *Med Eng Phys*, vol. 27, no. 1, pp. 19–29, Jan. 2005, doi: 10.1016/j.medengphy.2004.08.008.

[85] F. Crenna, M. Lancini, M. Ghidelli, G. B. Rossi, and M. Berardengo, “Biomechanics in crutch assisted walking,” *Acta IMEKO*, vol. 11, no. 4, pp. 1–5, Dec. 2022, doi: 10.21014/ACTAIMEKO.V11I4.1328.

[86] P. Westerhoff *et al.*, “In vivo measurement of shoulder joint loads during walking with crutches,” *Clinical Biomechanics*, vol. 27, no. 7, pp. 711–718, Aug. 2012, doi: 10.1016/j.clinbiomech.2012.03.004.

[87] F. Crenna, G. B. Rossi, and A. Palazzo, “Measurement of human movement under metrological controlled conditions,” *Acta IMEKO*, vol. 4, no. 4, pp. 48–56, Dec. 2015, doi: 10.21014/ACTA_IMEKO.V4I4.281.

[88] A. M. Howell, T. Kobayashi, H. A. Hayes, K. B. Foreman, and S. J. M. Bamberg, “Kinetic gait analysis using a low-cost insole,” *IEEE Trans Biomed Eng*, vol. 60, no. 12, pp. 3284–3290, 2013, doi: 10.1109/TBME.2013.2250972.

[89] V. V. Shah *et al.*, “Laboratory versus daily life gait characteristics in patients with multiple sclerosis, Parkinson’s disease, and matched controls,” *J Neuroeng Rehabil*, vol. 17, no. 1, Dec. 2020, doi: 10.1186/s12984-020-00781-4.

[90] *A Plantar Pressure Biofeedback M-Health System for Stroke Patients*. IEEE, 2020.

[91] J. L. Chen *et al.*, “Plantar Pressure-Based Insole Gait Monitoring Techniques for Diseases Monitoring and Analysis: A Review,” *Advanced Materials Technologies*, vol. 7, no. 1. John Wiley and Sons Inc, Jan. 01, 2022. doi: 10.1002/admt.202100566.

[92] M. Ghidelli, C. Nuzzi, S. Pasinetti, and M. Lancini, "Onboard gait detection crutches for gait rehabilitation," in *International Conference for Virtual Reality 2022*, Rotterdam, Jul. 2022. doi: https://doi.org/10.17605/OSF.IO/B85X9.

[93] F. Tamburella *et al.*, "Load Auditory Feedback Boosts Crutch Usage in Subjects With Central Nervous System Lesions: A Pilot Study," *Front Neurol*, vol. 12, 2021, doi: 10.3389/fneur.2021.700472.

[94] "Biomechanic of Gait and Treatment of Abnormal Gait Patterns | PM&R KnowledgeNow." Accessed: Jul. 04, 2023. [Online]. Available: https://now.aapmr.org/biomechanic-of-gait-and-treatment-of-abnormal-gait-patterns/

[95] H. Kainz *et al.*, "Reliability of four models for clinical gait analysis," *Gait Posture*, vol. 54, pp. 325–331, May 2017, doi: 10.1016/j.gaitpost.2017.04.001.

[96] L. Noreau, C. L. Richards, F. Comeau, and D. Tardif, "BIOMECHANICAL ANALYSIS OF SWING-THROUGH GAIT IN PARAPLEGIC AND NON-DISABLED INDIVIDUALS."

[97] F. Crenna, G. B. Rossi, and M. Berardengo, "A global approach to assessing uncertainty in biomechanical inverse dynamic analysis: Mathematical model and experimental validation," *IEEE Trans Instrum Meas*, vol. 70, 2021, doi: 10.1109/TIM.2021.3072113.

[98] G. B. Rossi, F. Crenna, and A. Palazzo, "A Proposal for a More User-Oriented GUM," *IEEE Trans Instrum Meas*, vol. 68, no. 5, pp. 1343–1352, 2019, doi: 10.1109/TIM.2019.2899183.

[99] M. Kumprou, P. Amatachaya, T. Sooknuan, T. Thaweewannakij, L. Mato, and S. Amatachaya, "Do ambulatory patients with spinal cord injury walk symmetrically?," *Spinal Cord*, vol. 55, no. 2, pp. 204–207, Feb. 2017, doi: 10.1038/sc.2016.149.

[100] C. Pais-Vieira *et al.*, "Method for positioning and rehabilitation training with the ExoAtlet ® powered exoskeleton," *MethodsX*, vol. 7, Jan. 2020, doi: 10.1016/j.mex.2020.100849.

[101] D. Torricelli and J. L. Pons, “EUROBENCH: Preparing robots for the real world,” *Biosystems and Biorobotics*, vol. 22, pp. 375–378, 2019, doi: 10.1007/978-3-030-01887-0_72/COVER.

[102] J. Simonsen and T. Robertson, *Routledge International Handbook of Participatory Design*, 1st ed. 2013.

[103] C. Ridao-Fernández, E. Pinero-Pinto, and G. Chamorro-Moriana, “Observational Gait Assessment Scales in Patients with Walking Disorders: Systematic Review,” *BioMed Research International*, vol. 2019. Hindawi Limited, 2019. doi: 10.1155/2019/2085039.

[104] C. D. Wickens, “Multiple resources and mental workload,” *Human Factors*, vol. 50, no. 3. pp. 449–455, Jun. 2008. doi: 10.1518/001872008X288394.

[105] S. Kulkarni, S. Deshmukh, F. Fernandes, A. Patil, and V. Jabade, “PoseAnalyser: A Survey on Human Pose Estimation,” *SN Comput Sci*, vol. 4, no. 2, p. 136, 2023, doi: 10.1007/s42979-022-01567-2.

[106] S. Haque, Z. Eberhart, A. Bansal, and C. McMillan, “Comparing Performance Between Different Implementations of ROS for Unity,” in *IEEE International Conference on Program Comprehension*, IEEE Computer Society, 2022, pp. 36–47. doi: 10.1145/nnnnnnn.nnnnnnn.

[107] I. Soares, R. B. Sousa, M. Petry, and A. P. Moreira, “Accuracy and repeatability tests on hololens 2 and htc vive,” *Multimodal Technologies and Interaction*, vol. 5, no. 8, Aug. 2021, doi: 10.3390/mti5080047.

[108] S. Kapp, M. Barz, S. Mukhametov, D. Sonntag, and J. Kuhn, “Arett: Augmented reality eye tracking toolkit for head mounted displays,” *Sensors*, vol. 21, no. 6, Mar. 2021, doi: 10.3390/s21062234.

[109] X. Luo, T. Kline, H. C. Fischer, K. A. Stubblefield, R. V Kenyon, and D. G. Kamper, “Integration of Augmented Reality and Assistive Devices for Post-Stroke Hand Opening Rehabilitation,” in *2005 IEEE Engineering in Medicine and Biology 27th Annual Conference*, pp. 6855–6858. doi: 10.1109/IEMBS.2005.1616080.

[110] G. A. de Assis, A. G. D. Corrêa, M. B. R. Martins, W. G. Pedrozo, and R. de D. Lopes, "An augmented reality system for upper-limb post-stroke motor rehabilitation: a feasibility study," *Disabil Rehabil Assist Technol*, vol. 11, no. 6, pp. 521–528, Aug. 2016, doi: 10.3109/17483107.2014.979330.

[111] C. H. Lee, Y. Kim, and B. H. Lee, "Augmented reality-based postural control training improves gait function in patients with stroke: Randomized controlled trial," *Hong Kong Physiotherapy Journal*, vol. 32, no. 2, pp. 51–57, Dec. 2014, doi: 10.1016/j.hkpj.2014.04.002.

[112] Y.-H. Cha *et al.*, "Motion sickness diagnostic criteria: Consensus Document of the Classification Committee of the Bárány Society," *Journal of Vestibular Research*, vol. 31, pp. 327–344, 2021, doi: 10.3233/VES-200005.

[113] A. Vovk, F. Wild, W. Guest, and T. Kuula, "Simulator Sickness in Augmented Reality Training Using the Microsoft HoloLens," 2018, doi: 10.1145/3173574.3173783.

[114] M. Kaufeld, M. Mundt, S. Forst, and H. Hecht, "Optical see-through augmented reality can induce severe motion sickness," 2022, doi: 10.1016/j.displa.2022.102283.

[115] M. E. Sloane and J. R. Roenker, "Noninvasive Assessment of the Visual System," 1992.

[116] C. H. Chu, Y. A. Chen, Y. Y. Huang, and Y. J. Lee, "A Comparative Study of Virtual Footwear Try-On Applications in Virtual and Augmented Reality," *J Comput Inf Sci Eng*, vol. 22, no. 4, Aug. 2022, doi: 10.1115/1.4053328.

[117] J. R. Lewis, "Psychometric Evaluation of the PSSUQ Using Data from Five Years of Usability Studies," *http://dx.doi.org/10.1080/10447318.2002.9669130*, vol. 14, no. 3–4, pp. 463–488, Sep. 2011, doi: 10.1080/10447318.2002.9669130.

[118] K. M. Stanney, K. S. Hale, I. Nahmens, and R. S. Kennedy, "What to Expect from Immersive Virtual Environment Exposure: Influences of Gender, Body Mass Index, and Past Experience,"

https://doi.org/10.1518/hfes.45.3.504.27254, vol. 45, no. 3, pp. 504–520, Aug. 2016, doi: 10.1518/HFES.45.3.504.27254.

[119] S. G. Hart and L. E. Staveland, "Development of NASA-TLX (Task Load Index): Results of Empirical and Theoretical Research," *Advances in Psychology*, vol. 52, no. C, pp. 139–183, Jan. 1988, doi: 10.1016/S0166-4115(08)62386-9.

[120] W. Macdonald, "Australian Psychologist The impact of job demands and workload on stress and fatigue", doi: 10.1080/00050060310001707107.

[121] K. M. Stanney, D. A. Graeber, and R. S. Kennedy, "Virtual environment usage protocols," *Handbook of standards and guidelines in ergonomics and human factors*, pp. 381–397, 2006.

[122] J. Sauro and J. R. Lewis, "Standardized usability questionnaires," in *Quantifying the User Experience*, Elsevier, 2016, pp. 185–248. doi: 10.1016/b978-0-12-802308-2.00008-4.

[123] D. D. Salvucci and J. H. Goldberg, "Identifying Fixations and Saccades in Eye-Tracking Protocols," 2000.

[124] A. Leykin and M. Tuceryan, "Automatic determination of text readability over textured backgrounds for augmented reality systems," 2004.

[125] J. Falk, S. Eksvard, B. Schenkman, B. Andren, and K. Brunnstrom, "Legibility and readability in Augmented Reality," in *2021 13th International Conference on Quality of Multimedia Experience, QoMEX 2021*, Institute of Electrical and Electronics Engineers Inc., Jun. 2021, pp. 231–236. doi: 10.1109/QoMEX51781.2021.9465455.

[126] J. Yu and G. J. Kim, "Eye strain from switching focus in optical see-through displays," in *Lecture Notes in Computer Science (including subseries Lecture Notes in Artificial Intelligence and Lecture Notes in Bioinformatics)*, Springer Verlag, 2015, pp. 550–554. doi: 10.1007/978-3-319-22723-8_59.

[127] M. Hussain, J. Park, and H. K. Kim, "Augmented reality sickness questionnaire (ARSQ): A refined questionnaire for augmented reality

environment," *Int J Ind Ergon*, vol. 97, Sep. 2023, doi: 10.1016/j.ergon.2023.103495.

[128] M. Hussain, J. Park, H. K. Kim, Y. Lee, and S. Park, "Motion sickness indexes in augmented reality environment," *ICIC Express Letters, Part B: Applications*, vol. 12, no. 12, pp. 1155–1160, Dec. 2021, doi: 10.24507/icicelb.12.12.1155.

[129] R. A. Grier, "How high is high? A meta-analysis of NASA-TLX global workload scores," in *Proceedings of the Human Factors and Ergonomics Society*, Human Factors and Ergonomics Society Inc., 2015, pp. 1727–1731. doi: 10.1177/1541931215591373.

[130] K. Hayashi, S. Aono, M. Fujiwara, Y. Shiro, and T. Ushida, "Difference in eye movements during gait analysis between professionals and trainees," *PLoS One*, vol. 15, no. 4, Apr. 2020, doi: 10.1371/journal.pone.0232246.

[131] K. McDuff *et al.*, "Analyzing the Eye Gaze Behaviour of Students and Experienced Physiotherapists during Observational Movement Analysis," *https://doi.org/10.3138/ptc-2019-0047*, vol. 73, no. 2, pp. 129–135, Aug. 2020, doi: 10.3138/PTC-2019-0047.

[132] B. Mahanama *et al.*, "Eye Movement and Pupil Measures: A Review," *Frontiers in Computer Science*, vol. 3. Frontiers Media S.A., Jan. 11, 2022. doi: 10.3389/fcomp.2021.733531.

Author's pubblications

M. Ghidelli et al., "Instrumented crutches with audio feedback to alter assisted gait," in 2021 IEEE International Workshop on Metrology for Industry 4.0 and IoT, MetroInd 4.0 and IoT 2021 - Proceedings, 2021. doi: 10.1109/MetroInd4.0IoT51437.2021.9488501.

M. Ghidelli, S. Massardi, L. Foletti, A. C. Gonzalez, and M. Lancini, "Validation of a ROS-Based Synchronization System for Biomechanics Gait Labs," in 2022 IEEE International Symposium on Measurements and Networking, M and N 2022 - Proceedings, Institute of Electrical and Electronics Engineers Inc., 2022. doi: 10.1109/MN55117.2022.9887745.

M. Ghidelli, C. Nuzzi, F. Crenna, and M. Lancini, "Validation of Estimators for Weight-Bearing and Shoulder Joint Loads Using Instrumented Crutches," 2023, doi: 10.3390/s23136213.

F. Tamburella et al., "Load Auditory Feedback Boosts Crutch Usage in Subjects With Central Nervous System Lesions: A Pilot Study," Front Neurol, vol. 12, 2021, doi: 10.3389/fneur.2021.700472.

R. Pagani, C. Nuzzi, M. Ghidelli, A. Borboni, M. Lancini, and G. Legnani, "Cobot user frame calibration: Evaluation and comparison between positioning repeatability performances achieved by traditional and vision-based methods," Robotics, vol. 10, no. 1, Mar. 2021, doi: 10.3390/ROBOTICS10010045.

F. Crenna, M. Lancini, M. Ghidelli, G. B. Rossi, and M. Berardengo, "Biomechanics in crutch assisted walking," Acta IMEKO, vol. 11, no. 4, pp. 1–5, Dec. 2022, doi: 10.21014/ACTAIMEKO.V11I4.1328.

M. Lancini et al., A Workaround for Recruitment Issues in Preliminary WR Studies: Audio Feedback and Instrumented Crutches to Train Test Subjects, vol. 27. 2022. doi: 10.1007/978-3-030-69547-7_101.

E. Ferlinghetti, I. Salzmann, M. Ghidelli, T. Rietveld, R. Vegter, and M. Lancini, "Algorithm Development for Contact Identification during Wheelchair Tennis Propulsion using Marker-less Vision System," in 2023 IEEE International Symposium on Medical Measurements and Applications, MeMeA 2023 - Conference Proceedings, 2023. doi: 10.1109/MeMeA57477.2023.10171886.

C. Nuzzi, M. Ghidelli, A. Luchetti, M. Zanetti, F. Crenna, and M. Lancini, "Body measurement estimations using 3D scanner for individuals with severe motor impairments," in 2023 IEEE International Symposium on Medical Measurements and Applications, MeMeA 2023 - Conference Proceedings, 2023. doi: 10.1109/MeMeA57477.2023.10171946.

E. Ferlinghetti, I. Salzmann, M. Ghidelli, T. Rietveld, R. Vegter, and M. Lancini, "Validation of Contact Measurement System for Wheelchair Tennis Propulsion using Marker-less Vision System," IEEE Trans Instrum Meas, pp. 1–1, Dec. 2023, doi: 10.1109/tim.2023.3347811.